STUDY OF SUBSTITUTION REACTION ON RING A OF ESTRADIOL

Miss Chanoknun Boonyaratsewee

A Thesis Submitted in Partial Fulfillment of the Requirements
for the Degree of Master of Science in Chemistry
Department of Chemistry
Faculty of Science
Chulalongkorn University
Academic Year 2018

การศึกษาปฏิกิริยาการแทนที่บนวงเอของเอสตราไดออล

น.ส.ชนกนันท์ บุณยรัตนเสวี

วิทยานิพนธ์นี้เป็นส่วนหนึ่งของการศึกษาตามหลักสูตรปริญญาวิทยาศาสตรมหาบัณฑิต
สาขาวิชาเคมี ภาควิชาเคมี
คณะวิทยาศาสตร์ จุฬาลงกรณ์มหาวิทยาลัย
ปีการศึกษา 2561

Thesis Title	STUDY OF SUBSTITUTION REACTION ON RING A OF ESTRADIOL
By	Miss Chanoknun Boonyaratsewee
Field of Study	Chemistry
Thesis Advisor	Assistant Professor YONGSAK SRITANA-ANANT, Ph.D.

Accepted by the Faculty of Science, Chulalongkorn University in Partial Fulfillment of the Requirement for the Master of Science

..... Dean of the Faculty of Science
(Professor POLKIT SANGVANICH, Ph.D.)

THESIS COMMITTEE

..... Chairman
(Associate Professor VUDHICHAI PARASUK, Ph.D.)

..... Thesis Advisor
(Assistant Professor YONGSAK SRITANA-ANANT, Ph.D.)

..... Examiner
(Tanatorn Khotavivattana, Ph.D.)

..... External Examiner
(Jutatip Boonsombat, Ph.D.)

ชนกนันท์ บุณยรัตนเสวี : การศึกษาปฏิกิริยาการแทนที่บนวงเอของเอสตราไดออล. (STUDY OF SUBSTITUTION REACTION ON RING A OF ESTRADIOL) อ.ที่ปรึกษาหลัก : ผศ. ดร.ยงศักดิ์ ศรีธนาอนันต์

การเชื่อมต่อเอสตราไดออลกับยาต้านมะเร็งจัดเป็นวิธีที่มีประสิทธิภาพในการต่อสู้กับเซลล์มะเร็งเต้านมได้อย่างจำเพาะและลดความเป็นพิษต่อเซลล์ปกติ จากงานวิจัยที่ผ่านมาส่วนใหญ่เป็นการเชื่อมต่อยาลงบนวงบี, ซีและดีของเอสตราไดออล ในงานวิจัยนี้จึงสนใจที่จะศึกษาการเติมหมู่ฟังก์ชันบนวงเอของเอสตราไดออล เพื่อนำไปสู่การเชื่อมต่อยาแบบใหม่ที่อาจมีความจำเพาะและประสิทธิภาพในการจับเอสโตรเจนรีเซพเตอร์ของเซล์มะเร็งที่ดีขึ้น จากการศึกษาบน 4-ครีซอลเป็นแม่แบบปฏิกิริยาไนเตรชั่นที่ตำแหน่งเมตา สามารถทำได้แต่ได้ผลร้อยละของสารผลิตภัณฑ์เพียงร้อยละ 6 ผลลัพธ์ที่ดีกว่าได้จากปฏิกิริยาไดเอโซคับปลิงบนตำแหย่งออร์โทของ 4-ครีซอล ซึ่งนำไปสู่การเติมหมู่แทนที่ที่ตำแหน่ง 2 และ 4 ของเอสตราไดออล ไดเอโซเอสตราไดออลจะถูกรีดิวซ์แล้วเชื่อมต่อกับอนุพันธ์คาร์บอกซิล ซึ่งจะเปลี่ยนให้มีหมู่ของกรดไฮดรอกซามิก ที่คล้ายกับโครงสร้างของยาต้านมะเร็งกรดซูเบอร์แอนนิโลไฮดรอกซามิก

สาขาวิชา เคมี ลายมือชื่อนิสิต .....

ปีการศึกษา 2561 ลายมือชื่อ อ.ที่ปรึกษาหลัก .....

5971932823 : MAJOR CHEMISTRY

KEYWORD: anticancer, estradiol, estrogen recepter, suberanilohydroxamic acid, breast cancer

Chanoknun Boonyaratsewee : STUDY OF SUBSTITUTION REACTION ON RING A OF ESTRADIOL. Advisor: Asst. Prof. YONGSAK SRITANA-ANANT, Ph.D.

Estradiol-conjugated anticancer drugs are the effective strategy that could specifically combat breast cancer cells, while minimizing the toxicity of the drug toward normal cells. Estradiol has been previously conjugated with drugs mostly at rings B, C and D. Functionalizations at ring A of estradiol introduce new types of conjugated drugs that could improve both the selectivity and efficiency in binding with estrogen receptor (ER). Using 4-cresol as the model, the nitration at *meta*-position was achieved, although with unsatisfied result of only 6% overall yield of the product. The practical results derived from diazo coupling on *ortho*-position of 4-cresol, which led to successful functionalizations at 2- or 4-positions of estradiol. The diazo estradiol was reduced, conjugated with dicarbonyl derivatives, which was a conjugated anticancer drug converted to a conjugated hydroxamic acid that dovely resembles suberanilohydroxamic acid (SAHA).

Field of Study: Chemistry Student's Signature .....

Academic Year: 2018 Advisor's Signature .....

ACKNOWLEDGEMENTS

Firstly, I would like to express my sincere thanks of gratitude to my advisor, Assist. Prof. Yongsak Sritana-anant for his kindness and patience for supporting my studies and thesis research, I have learnt many new things from his knowledge and suggestion, including helping me in finish this thesis.

I am sincerely grateful to the member of the thesis committee, Assoc Prof. Dr. Vudhichai Parasuk, Dr. Tanatorn Khotavivattana and Dr. Jutatip Boonsombat for their valuable comments and suggestion.

I would like to acknowledge the member of the YS research group on fourteenth floor, Mahamakut building for their friendship and always helping me a lot, especially Vasin Thummasorn for always be the kind brother and friend of mine.

Finally, I would like to acknowledge the most important things in my life, my lovely family for keep comforting me from behind, understand me a lot and stand by me all the time. With out them, I could not come this far, and they are my inspiration for continue work hard without giving up.

Chanoknun Boonyaratsewee

TABLE OF CONTENTS

LIST OF FIGURES

LIST OF TABLES

LIST OF ABBREVIATIONS

ACN	: acetonitrile
AcOH	: acetic acid
$AlCl_3$	: aluminium chloride
cm^{-1}	: unit of wavenumber (IR)
$CDCl_3$	: deuterated chloroform
°C	: degree Celsius
^{13}C NMR	: carbon-13 nuclear magnetic resonance spectroscopy
conc	: concentration
d	: doublet (NMR)
DCE	: dichloroethane
DCM	: dichloromethane
DDQ	: 2,3-dichloro-5,6-dicyano-1,4-benzoquinone
DMF	: dimethylformamide
eqv	: equivalent
$FeCl_3$	: ferric chloride
FT-IR	: fourier-transform infrared spectroscopy
g	: gram (s)
h	: hour (s)
^1H NMR	: proton nuclear magnetic resonance spectroscopy
HNO_3	: nitric acid

HRMS : high resolution mass spectrometry

H_2SO_4 : sulfuric acid

Hz : hertz (s)

KCN : potassium cyanide

K_2CO_3 : potassium carbonate

KNO_3 : potassium nitrate

Lit. : literature

M : molar (s)

m : multiplet (NMR)

MeOH : methanol

$MgSO_4$: magnesium sulfate

min : minute

mL : milliliter (s)

mmol : millimole (s)

mp : melting point

Na_2CO_3 : sodium carbonate

NaOH : sodium hydroxide

Na_2S : sodium sulfide

NEt_3 : triethylamine

$NH_2OH.HCl$: hydroxylamine hydrochloride

$NO_2^+BF_4^-$: nitronium tetrafluoroborate

NOESY : nuclear overhauser effect spectroscopy

PCC	: pyridinium chlorochromate
ppm	: parts per million (unit of chemical shift)
rf	: reflux
R_f	: retention factor
rt	: room temperature
s	: singlet (NMR)
$SnCl_2$	: tin(II) chloride
TBS	: tert-butyl dimethyl silane
TIPS	: triisopropyl silane
t	: triplet (NMR)
THF	: tetrahydrofuran
UHP	: urea hydrogen peroxide
xs	: excess
δ	: chemical shift

CHAPTER I

INTRODUCTIONS

1.1 The targeted chemotherapy

Cancer is a well-known disease that is the major cause of death worldwide. Cancer cells are abnormal cells that are uncontrollable in growth and division. At present, many treatment options for cancer have been developed such as surgery, chemotherapy and radiation therapy. Among these methods, chemotherapy is one of the most common treatments for many cancers [1]. To prevent the increase of cancer cells, certain drugs are used to kill cancer cells or stop them from spreading to other parts of the body. However, the toxicity of these drugs toward normal cells has been the serious problem that many researchers concern. To get rid of this issue, the combination between the anti-tumor drugs and target-specific carriers is one of the solutions proposed to solve this problem. The carriers that have high selectivity to receptors on target tumor cells may help delivering most of the drugs to the target cells and enhance the probability in killing them [2], together with reducing the toxic effect on normal cells [3].

1.2 Breast cancer and hormone therapy

Breast cancer is the most commonly diagnosed cancer in women [4-7]. The major reason comes from the excess in estrogen hormone in women [8, 9]. Estrogen is a sex hormone that is responsible for the development of female sexual characteristics, including the growth of breast as a girl. However, in elder females the excess production of estrogen more than need that gathers in the body could lead to breast cancer [10].

To prevent breast cancer cells to spread out all over the body, the therapeutic strategies were focused into targeting the character as hormone-

responsive breast cancer. Hormones play the role of targeting agents that can be linked with some active anti-cancer drug [11-15].

1.3 Estradiol and estrogen receptor (ER)

Estrogens are a group of steroid sex hormones **(Figure 1.1)** that involve in the development of female sex appearance [8]. The excess in these hormones could be correlated with the increasing risk of cancer. Estradiol is one of the estrogen hormones, which is the most active among 4 major types of estrogen, estrone (E1), estradiol (E2), estriol (E3), and estetrol (E4) **(Figure 1.2)**

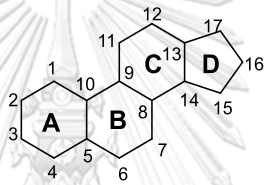

Figure 1.1 The core structure of steroids

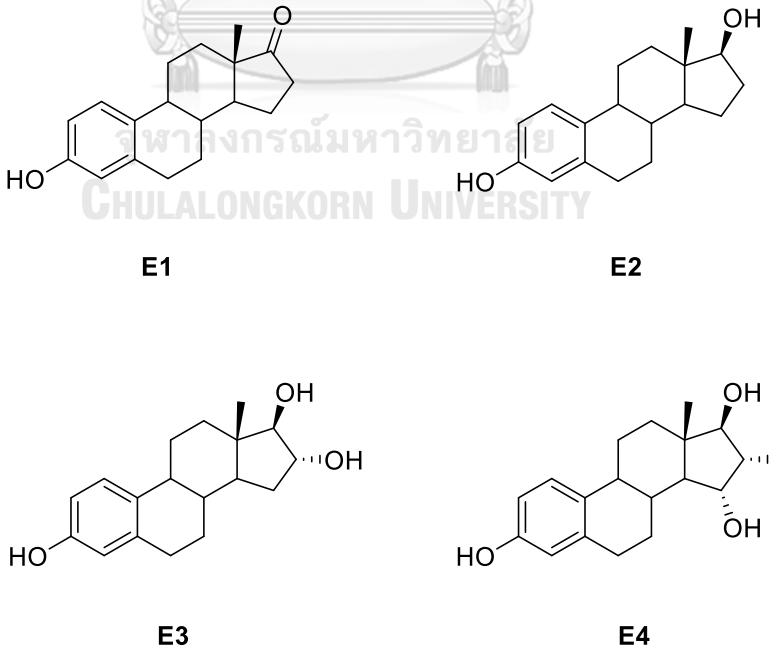

Figure 1.2 Estrogen Hormones: estrone (E1), estradiol (E2), estriol (E3), estetrol (E4)

Recently, estradiol has been introduced as a carrier for delivering anti-cancer drugs to specific cancer cells. The combination between estradiol and anti-cancer drug could increase the selectively targeting the drugs to breast cancer cell, since the existence of high level of estrogen receptor (ER) in breast cancer cells [10, 16]. With the ER excess in breast cancer cell, this will increase the probability to receive more drug to cancer cell more than normal cells and reduce the toxicity toward normal cells [17, 18].

The estrogen receptor (ER) is the protein in cells that have high efficiency binding with estrogen analogue that diffuse into the cell and bind to the ER, which located in the nucleus. The ER exists in 2 main forms, ERα and ERβ. ERα was found in endometrium, breast cancer cells, ovarian stromal cells, and the hypothalamus meanwhile ERβ were mostly found in ovarian granulosa cells, kidney, brain, bone, heart, lungs, intestinal mucosa, prostate, and endothelial cells [19].

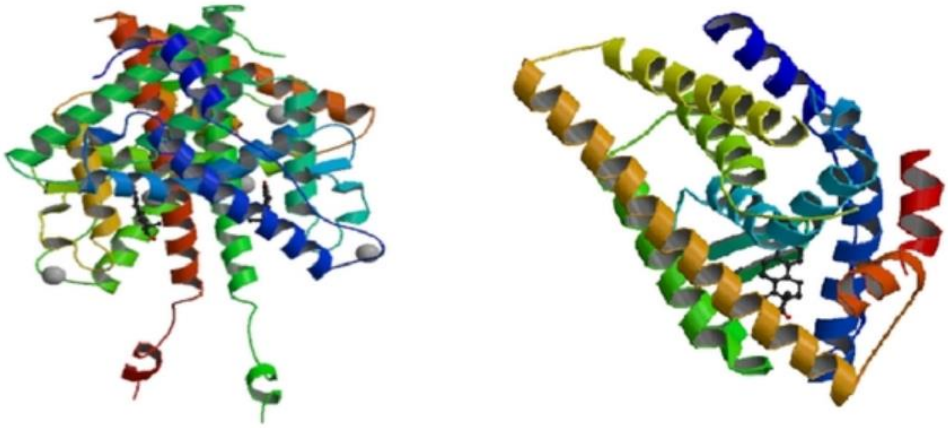

a b

Figure 1.3 two isoforms of estrogen receptors, ERα and ERβ bind with estradiol a) ERα + estradiol b) ERβ + estradiol

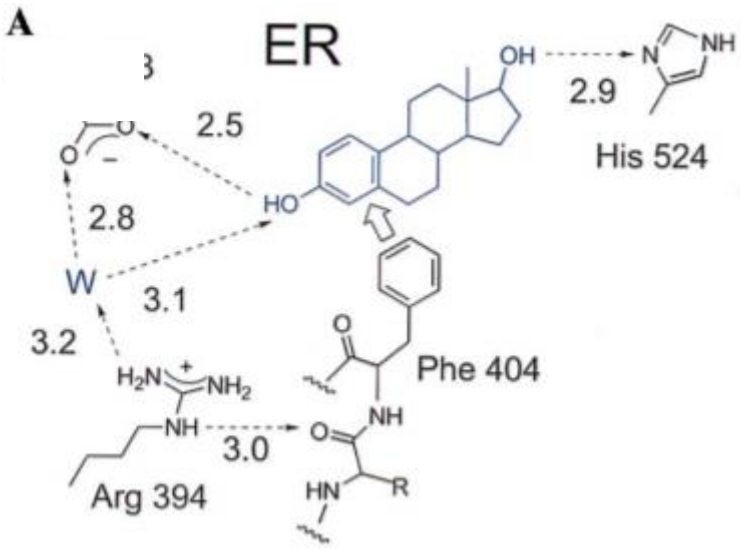

Figure 1.4 The hydrogen-bonding network between estradiol and ER

However, conjugation of the drug on estradiol may deactivate the binding affinity to the receptor. So, finding the best combination and conjugate positions on both estradiol and anticancer drug is a challenge to research in this area. **Figure 1.4** shows the existence of hydrogen bonding between ER and two hydroxy groups at 1- and 17-position of estradiol which is a specific site binding on the ERs [20, 21]. Therefore, those areas in the conjugated estradiol-drug should be free from any substitution to remain the strong binding efficiency toward ER.

1.4 Histone deacetylases (HDAC)

Histone deacetylases (HDAC) are the enzymes that catalyze the transcription in cell including the abnormal cells like cancer cells, by catalyzing the removal of acetyl groups from lysine residues on the tails of histone proteins [22]. Normally, the balance of acetylation and deacetylation of histone and nonhistone protein is an important key for normal cells. The inhibition of HDAC activities leads to nonequilibrium between these two processes and causes the problem in cell growth and division [23]. With this concept, histone deacetylase inhibitors (HDACi) are the key for study on cell proliferation in many cancers. HDACs have 18 isoforms and are classified into 4 classes. Class I, II and IV require the present in zinc ion for the activity of enzymes [24] and for class III is NAD^+ dependent enzymes [25]. The zinc-dependent enzymes active site consists of a core pocket with a zinc atom at the base of the pocket [26, 27]. HDACi inhibits the enzyme activity by chelating with Zn^{2+} in the pocket [22].

In 2004, *N*-hydroxy-*N*1-phenylactanediamide or suberanilide hydroxamic acid (SAHA) has been approved by the U.S. Food and Drug Administration (FDA) for phase II clinical trials [28].

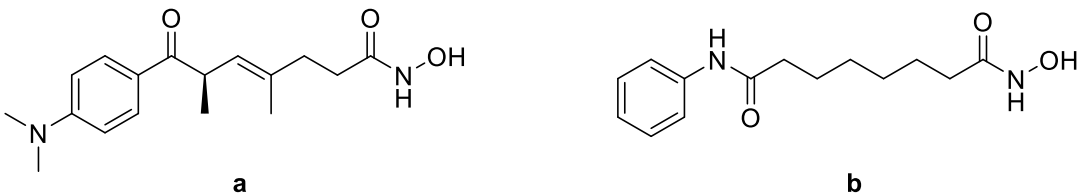

Figure 1.5 Zn^{2+} dependent-HDACi a) Trichostatin A (TSA) b) suberanilohydroxamic acid (SAHA)

Hydroxamate end chain HDACi, trichostatin A (TSA) and suberanilohydroxamic acid (SAHA) **(Figure 1.5)**, are the most common zinc binding group (ZBG) that chelate Zn^{2+} at active site [29], have a carbon linker and a hydrophobic cap that block the entrance of active site [30]. These properties of SAHA lead to the use of HDACi as cancer therapeutics in the combination with other targeting or anti-cancer agent have been developed so far.

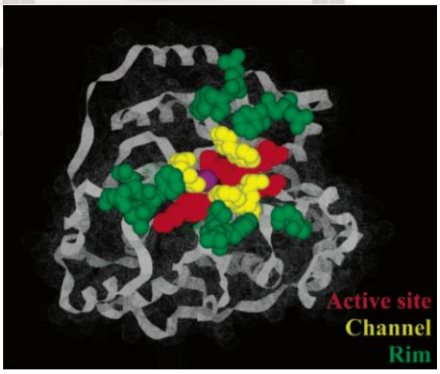

Figure 1.6 Crystal structure of HDAC, the Zn^{2+} is shown in purple [29].

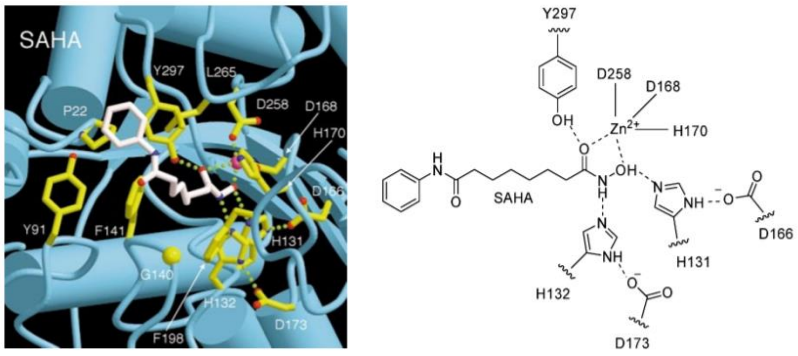

a b

Figure 1.7 SAHA chelating with Zn^{2+} a) SAHA bind with Zn^{2+} [27] b) bidentate chelation of SAHA to Zn^{2+} [29].

1.5 Literature Review

1.5.1 Substitution on estradiol structure

In 1996, Cushman and co-worker [31] synthesized the estradiol conjugated ellipticine in order to use their abilities to bind with estrogen receptor positive cell or ER+ to inhibit topoisomerase II and poisonous cancer cell in human. The three estradiol conjugations were extended from 17α-position of estradiol linked to N-2, N-6 or C-9 position of ellipticine **(Figure1.8)**.

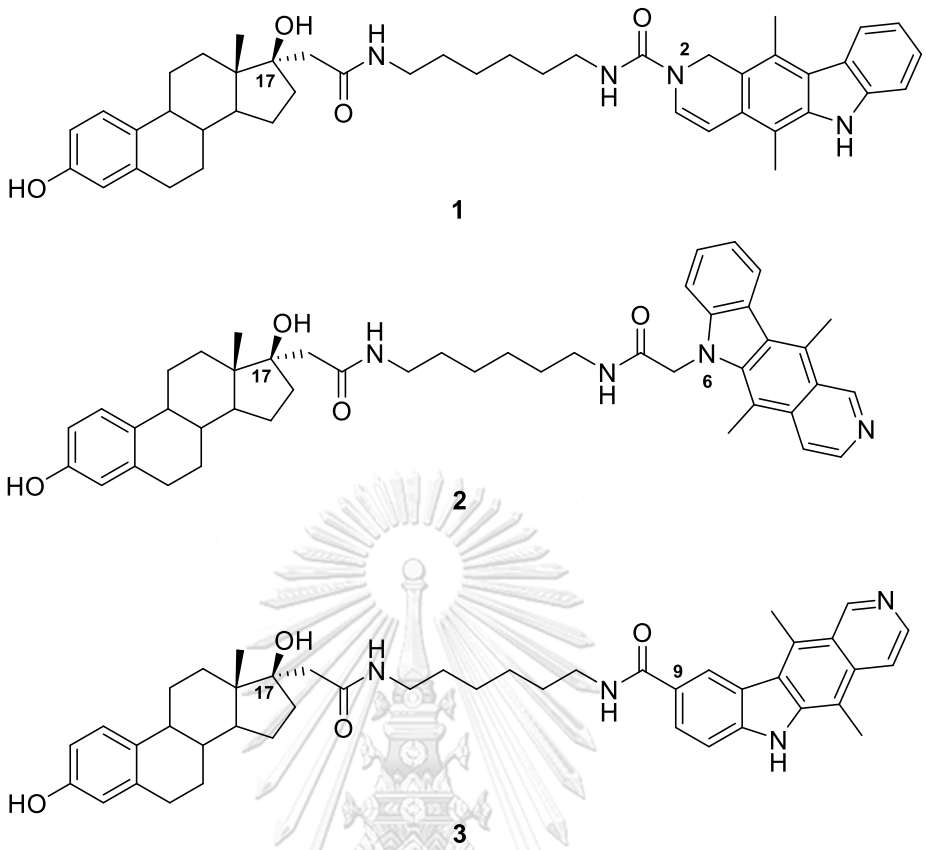

Figure 1.8 The structure of ellipticine-estradiol conjugated 1) from 17α to N-2 2) from 17α to N-6 3) from 17α to C-9

The relative binding affinities (RBAs) of conjugated compounds for ER were determined compared to unmodified estradiol (E2) (RBA=100) **(Table 1.1)**. The results showed the weak binding between three conjugated compounds with ER. The same went for the inhibitor against topoisomerase II results (**Table 1.1)**. Both studies could be inferred that the position of the conjugation of estradiol to ellipticine is an important topic related to the hinder from each piece of the conjugated compound.

Table 1.1 Relative Estrogen Receptor Binding Affinities and Topoisomerase II Inhibitory Activities of Ellipticine-Estradiol Conjugates

compound	RBA	IC_{50} (μM)
E2	100	-
1	0.132 (± 0.028)	24.1 (± 8.3)
2	-	>200
3	0.303(± 0.028)	>200

In 2001, Hochberg and co-worker [32] designed the analogue with 16α-substitution of estradiol. Various functions and the differences in length of the chain were modified at 16α-position. The protocol to substituted at 16-position was used from Katzenellenbogen group that reported in 1988 [33].

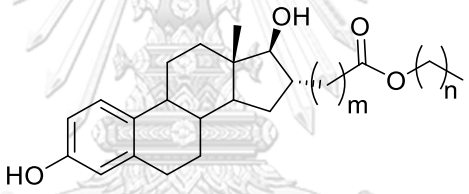

Figure 1.9 The structure analogue of 16-substituted.

Relative Estradiol Receptor Binding Affinities of 16α-substituted estradiol were measured **(Table 1.2)**. The carboxylic acid analogues (E16-1,0, E16-2,0 and E16-3,0) showed the non-binding result with ER. The increasing in chain length of an alkyl group (the number of m) decreased the binding, while the increase in alcohol portion (the number of n) didn't give any significant binding result.

Table 1.2 Relative Estrogen Receptor Binding Affinities of 16α-substituted estradiol

Compound	ER (RBA)
E2	100
E1	30 $\pm$ 11
E16-1,0	0
E16-1,1	35 $\pm$ 4
E16-1,2	40 $\pm$ 10
E16-2,0	0
E16-2,1	5 $\pm$ 2
E16-2,2	5 $\pm$ 1
E16-3,0	0.1 $\pm$ 0.1
E16-3,1	1 $\pm$ 1

The selectivity toward different types of ER was also tested with 16**α**-substituted estradiol, the selectivity preference in ER**α** over ERβ was reported **(Table 1.3)**. The preference to ER**α** is predictable due to previous work, as 16**α**-iodoestradiol [34], showed very poor binding to ERβ**.**

Table 1.3 Binding of Selected E16 to the LBD[a] of human ERα and ERβ

Compound	ERα	ERβ	ERα/ERβ
E2	100	100	1
E16-1,1	19 $\pm$ 9	0.3 $\pm$ 0.2	62 $\pm$ 10
E16-1,2	19 $\pm$ 5	0.3 $\pm$ 0.1	77 $\pm$ 12
E16-1,2F$_1$	16 $\pm$ 2	0.1 $\pm$ 0.1	89 $\pm$ 3
E16-1,F$_2$	13 $\pm$ 9	0.2 $\pm$ 0.1	67 $\pm$ 4

[a] LBD is ligand binding domain

Afterward, in 2003, the same research group [35] studied on the substitution at different rings of estradiol. The modifications were at 7, 11β and 15α-position on B, C and D-ring respectively.

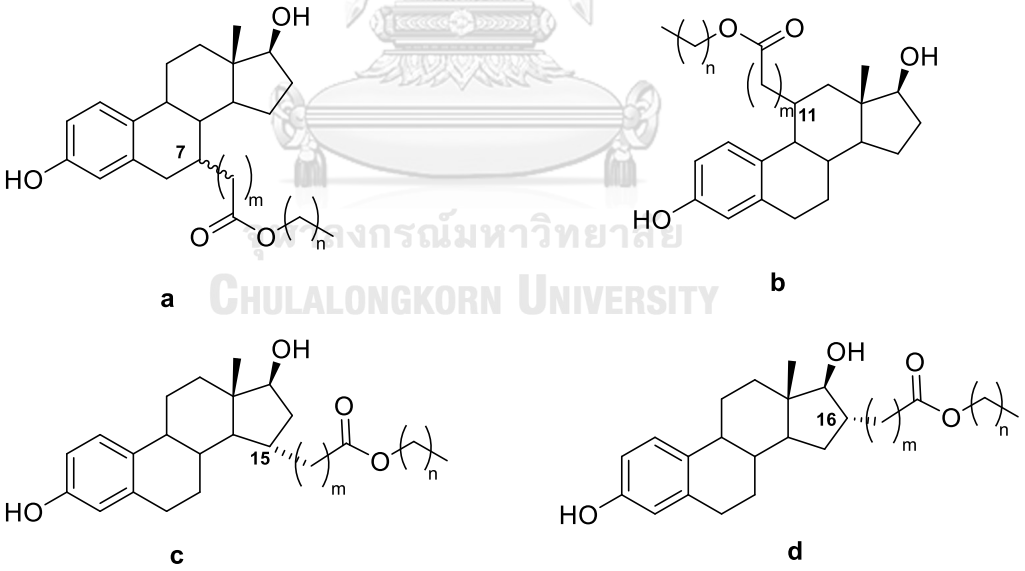

Figure 1.10 The substitution on estradiol a) 7 b) 11β c) 15α d) 16α [32]

Those synthesized products were tested for estrogen receptor binding. Like previous work [32], the carboxylic analogues of all substituted estradiol showed poorly binding with ER. The elongation in alkyl group from attached site (m number) led to decrease in binding affinity. The RBA from each substituted position still gave weakly binding with ER.

For the selectivity study, only 16α substituted estradiol showed the preference to ERα, for all the 7, 11β and 15α-substituted estradiol had no selectivity ERα and ERβ **(Table 1.4)**

Table 1.4 The selectivity of substituted estradiol to ERα and ERβ

Compound	ERα	ERβ	ERα/ERβ
E2	100	100	1
E7R-1,2	11 $\pm$ 2	9 $\pm$ 2	1 $\pm$ 0.1
E11-2,2	66 $\pm$ 11	70 $\pm$ 14	1 $\pm$ 0.04
E11-3,2	66 $\pm$ 3	64 $\pm$ 7	1 $\pm$ 0.4
E15-1,2	22 $\pm$ 5	7 $\pm$ 2	3 $\pm$ 0.6
E16-1,2 27	27 $\pm$ 6	0.3 $\pm$ 0.1	95 $\pm$ 47

1.5.2 Estradiol conjugated drug

In 1994, Nique and co-worker [36] synthesized 11β-amidoalkoxyphenyl estradiols as a new antiestrogen to compared with tamoxifen (TAM) and 4-hydroxytamoxifen (OH-TAM). Substitution at 11β-position of estradiol led to antiproliferative and antitumoral antiestrogens to compete with estrogen in binding with ER [37]. The new series of 11β-amido-alkoxyphenyl substituted estradiol derivatives were synthesized and test the activity against MCF-7 cells.

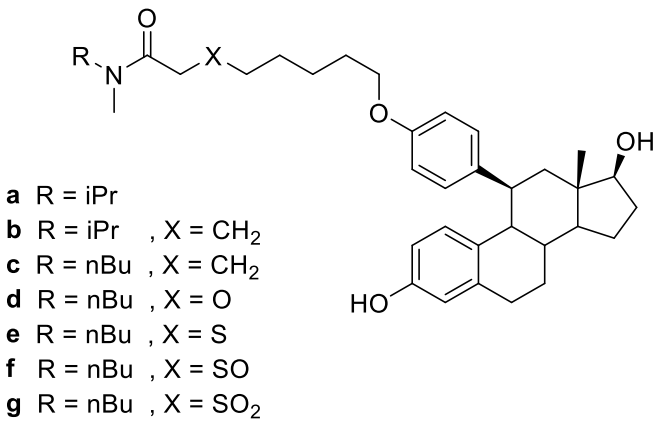

Figure 1.11 The 11β-amido-alkoxyphenyl substituted estradiol core structure

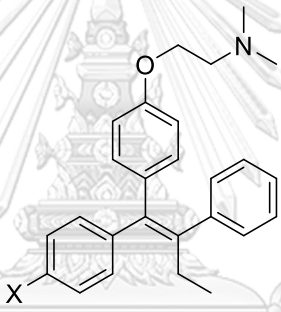

Figure 1.12 tamoxifen (TAM) and 4-hydroxytamoxifen (OH-TAM) structure

From **Table 1.5**, the activity on MCF-7 cell line under different stimulation conditions, compared to OH-TAM, synthesized 11β-amido-alkoxyphenyl substituted estradiol derivatives have the lower IC_{50} value 30 to 200 times.

Table 1.5 Pharmacological profile of ant±estrogens

	RBA ER: mice 5h, 25°C (E2=100)	**IC_{50} MCF-7 mean ± SEM (nM)**		
		E2-stimulated (0.1 nM)	Insulin Stimulated	EGF[a] PDGF[b] Stimulated
a	38 ± 13	10 ± 7	2.5 ± 1.4	0.54 ± 0.35
b	32 ± 2	0.82 ± 0.48	0.15 ± 0.09	0.21 ± 0.10
c	24 ± 3	0.53 ± 0.08	0.11 ± 0.10	0.15 ± 0.12
d	30 ± 4	0.28 ± 0.07	0.020 ± 0.015	0.012 ± 0.009
e	15 ± 2	0.43 ± 0.20	0.053 ± 0.036	0.023 ± 0.011
f	10 ± 1	0.42 ± 0.14	0.068 ± 0.036	0.021 ± 0.006
g	9.6 ± 0.8	0.32 ± 0.14	0.020 ± 0.018	0.005 ± 0.004
Tamoxifen	0.6 ± 0.1	316 ± 21	470 ± 230	580 ± 240
4-OH-TAM	40 ± 8	7.4 ± 3.4	4.2 ± 2.3	0.66 ± 0.11

[a] epidermal growth factor

[b] platelet derived growth factor

In 2012, Dao and co-worker [38] successfully synthesized estradiol-doxorubicin conjugate. Many doxorubicin derivatives had been reported for many years [39-42] mostly with tamoxifen (TAM) as the targeting carrier to ER+ on breast cancer cells. However, TAM had a weak binding ability to ER and somehow showed the binding with another site apart from ER.

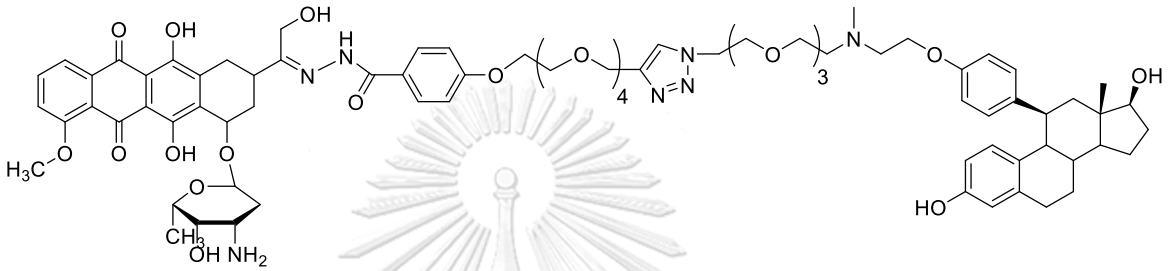

Figure 1.13 estradiol-doxorubicin conjugate

Therefore, this research group interested in combining estradiol with doxorubicin. This study not only focused on targeting and the treatment but also focused on the linker between two moieties. The linker chain should be long enough that two components of the conjugated drug not hinder each other. The elaborate design was to synthesize and link the two parts together. The new compound was tested the cytotoxicity assays against ER (+)-MCF-7 and ER (–)-MDA-MB-231 breast cancer cell lines **(Table 1.6)**.

Table 1.6 IC_{50} (nM), of Various Dox Compounds

compound	MCF-7	MDA-MB-231	MCF-7 (+ES)
Dox	602 ± 20	89 ± 7	585 ± 30
Dox-Linker	597 ± 20	86 ± 5	594 ± 20
AE-Dox	11 ± 6	90 ± 8	589 ± 3

The new conjugated compound (AE-Dox) showed the high ability in toxicity toward MCF-7 cells line with the lox IC_{50} compared to normal doxorubicin.

1.5.3 suberanilohydroxamic acid (SAHA) as histone deacetylase inhibitors (HDACi)

In 2005, Njar and co-worker [28] reported the new method to synthesize SAHA with high yield and shorter time compared to the common synthesis previously reported.

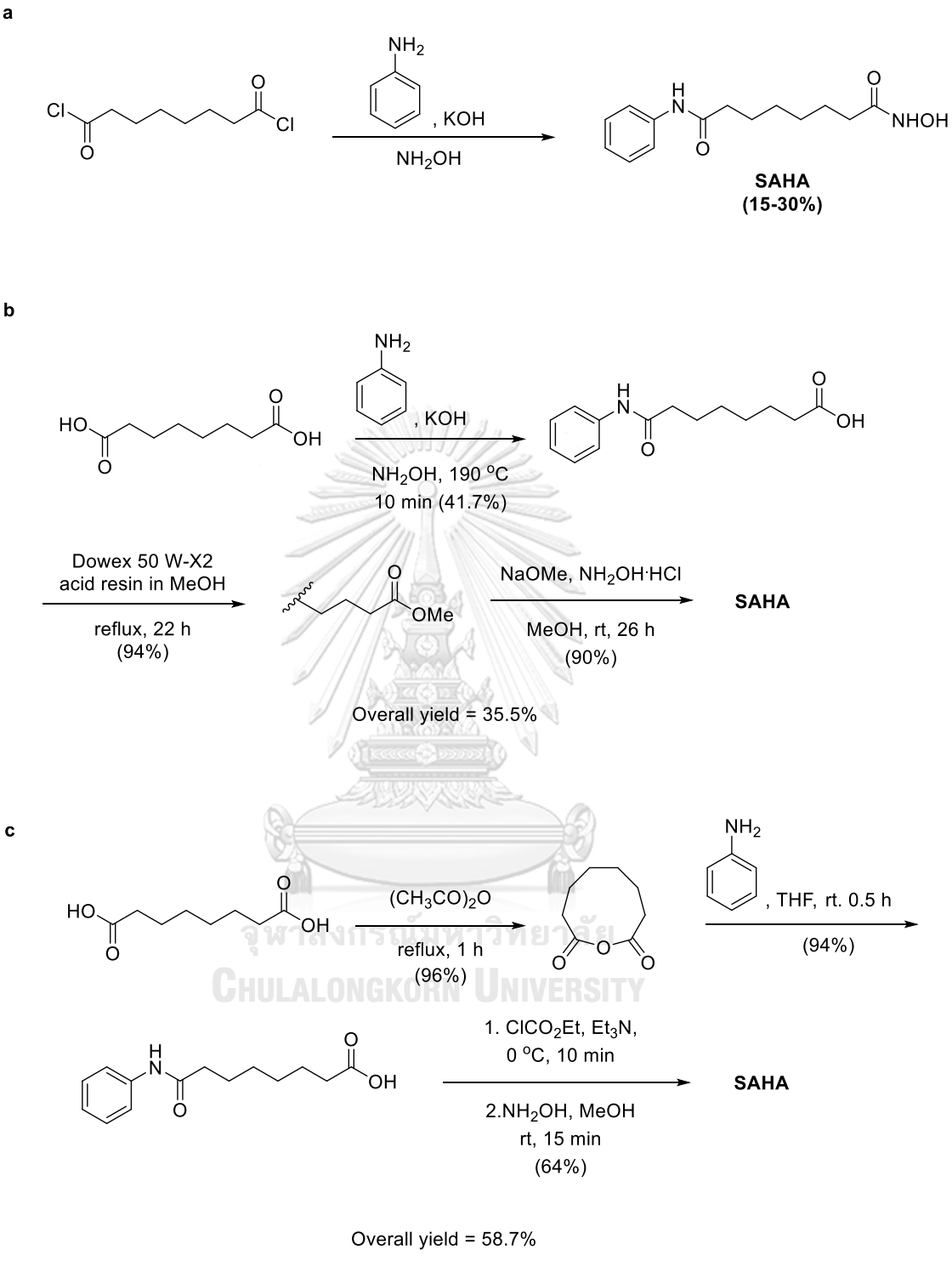

Figure 1.14 Previous procedure for the synthesis of SAHA a) Breslow et al. [43] b) Stowell et al. [44] c) Mai et al. [45]

In this research, they proposed the new way to synthesized SAHA in high yield and processing at room temperature. By using the purchase suberic acid monomethyl ester **(Figure 1.15)**, mixed with 1-hydroxybenzotriazole, aniline and DCC in DMF at room temperature to obtain suberanilic acid methyl ester in 88.7%. The methoxy group was converted to hydroxamic acid with hydroxylamine hydrochloride and potassium hydroxide in methanol. The obtained SAHA yield in 90% with an overall yield of 79.8%

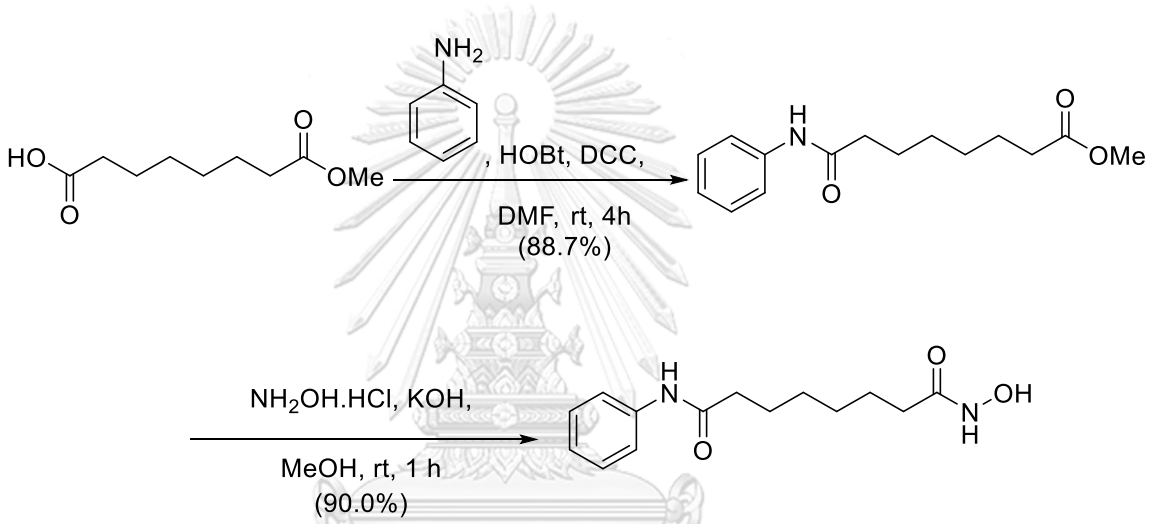

Figure 1.15 The new developed method for synthesize SAHA

In 2013, Berkley and co-worker [46] were interested in histone deacetylase inhibitors (HDACi) for inhibiting transcription of cancer cells [47, 48]. Two combinations of HDACi with other anti-cancer compound have been developed, with hormones therapy which helps in targeting HDACi to cancer cells, TAM (an antagonist and selective ER modulator) and estradiol (an ER agonist).

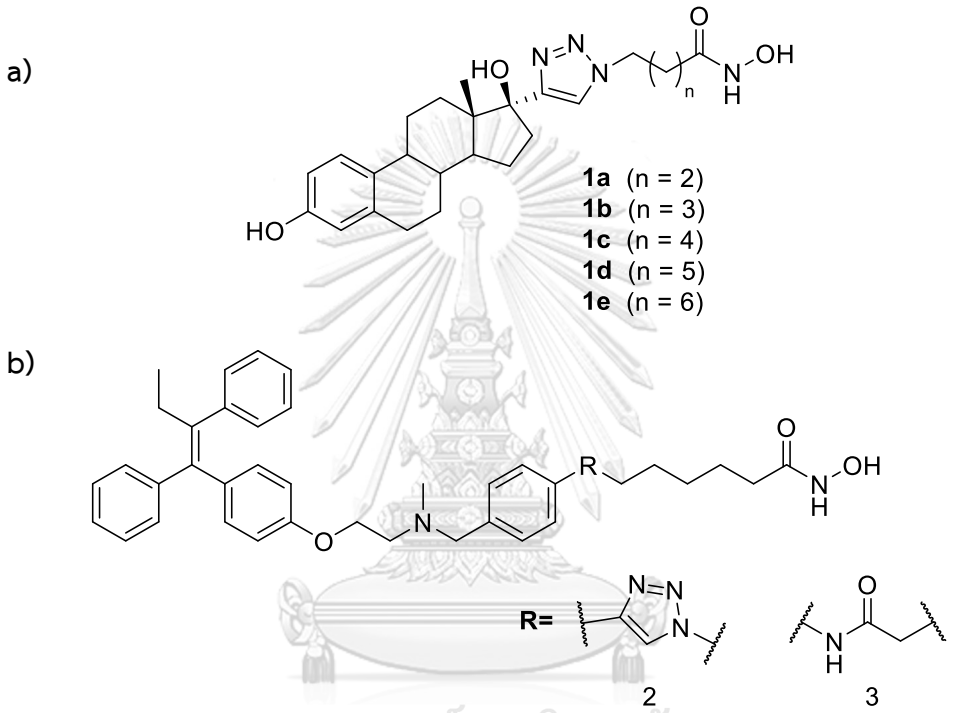

Figure 1.16 conjugated HDACi a) Ethynylestradiol–HDACi conjugates (EED-HDACi), b) tamoxifen–HDACi conjugates (TAM-HDACi)

Two types of conjugated HDACi were successfully synthesized and tested for agonist (EED-HDACi) and antagonist (TAM-HDAi) abilities. Both EED-HDACi and Tam-HDACi retain agonist or antagonist activity of their parent drugs (EED and tamoxifen, respectively). **Table 1.7**, the result showed that EED-HDACi became the weaker agonist compared to the normal estradiol as ER agonist

Table 1.7 Exhibition of ERα-agonist or antagonist activity

		Agonism (fold activation)	Antagonism IC_{50} (μM)
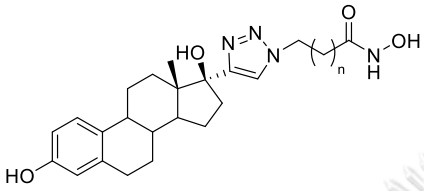 EED-HDACi	**1a** (n = 2)	1.55 ± 0.57	-
	1b (n = 3)	6.84 ± 2.05	-
	1c (n = 4)	2.00 ± 0.86	-
	1d (n = 5)	4.72 ± 2.12	-
	1e (n = 6)	1.19 ± 0.48	-
	E2	16.2 ± 2.15	-
	EED	19.9 ± 2.47	-
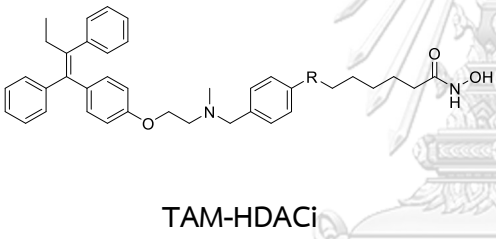 TAM-HDACi	**2** (n = 5)	-	0.248 ± 0.129
	3 (n = 5)	-	0.127 ± 0.049
	tamoxifen	-	0.039 ± 0.015

1.6 The objective of this work

The functionalization at phenolic ring A of estradiol was proposed to find the new conjugated drug which has high efficiency in binding with corresponding estrogen receptor. This may help to improve in targeting the drugs to tumor cells and reduce the toxicity toward normal cells. 4-cresol is used in the role of representation of ring A to optimize the reaction condition before applying on estradiol. Substitution at 1, 2 and 4-position of estradiol with the active functional group would lead to further conjugation with an active anti-cancer to bring the capability of the conjugated drug in the future.

.

CHAPTER II

EXPERIMENTS

2.1 Chemicals

Thin layer chromatography (TLC) was performed on aluminum sheets coated with silica gel (Merck Kieselgel 60 F_{254}, Merck KGaA, Darmstadt, Germany). Stationary phase in column chromatography was 0.040-0.060 mm or 40-60 mesh ASTM silica gel 60 (Merck Kieselgel 60 P, Merck KGaA, Darmstadt, Germany). Solvents for synthesis were reagent or analytical grades, and those for column chromatography were distilled from commercial grade. Other reagents were purchased from the following venders:

- Acros Organics (USA): hydrobromic acid 33% in glacial acetic acid, imidazole, sodium nitrite ($NaNO_2$), tin (II) chloride anhydrous, trimethylsilyl chloride,
- Carlo Erba (Italy): triethylamine
- Euriotop (USA): deuterated chloroform ($CDCl_3$), deuterated acetone (acetone-d_6)
- Merck Co. (Germany): fuming nitric acid, 4-nitrobenzyl chloride, sodium hydroxide (NaOH), sulfuric acid (H_2SO_4)
- RCI Labscan (Thailand): acetone, acetic acid, acetonitrile, 1,2-dichlroethane (DCE), dichloromethane (DCM), dimethylformamide (DMF), ethyl acetate (EtOAc), hexane, magnesium sulfate ($MgSO_4$), methanol, sodium hydrogen carbonate ($NaHCO_3$), tetrahydrofuran (THF)
- Sigma-Aldrich (USA): benzyl bromide, β-estradiol, bromine (Br_2), *tert*-butyldimethylsilyl chloride, hydroxylamine hydrochloride, *p*-toluidine
- TCI (Japan): Acetyl chloride, adepoyl chloride, aniline hydrochloride, triisopropylsilyl chloride

2.2 Instruments and Equipment

Melting points were determined with a Stuart Scientific Melting Point SMP10 (Bibby Sterlin Ltd., Staffordshire, UK). The FT-IR spectra were recorded on a Nicolet 6700 FT-IR spectrometer. ^{1}H NMR spectra were obtained from Varian Mercury NMR spectrometer operated at 400.00 MHz. ^{13}C NMR spectra were obtained from Bruker Avance 400 operated at 100.00 MHz. Mass data were measured with ESI-MS (Quattro microTM API).

2.3 Model functionalization on 4-cresol

2.3.1 2,6-dinitro-4-methylphenol (1)

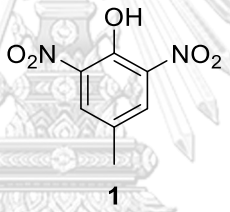

1

4-cresol (0.108 g, 1 mmol) was dissolved in glacial acetic acid (1 mL) and was added dropwise to the mixture of fuming nitric acid (0.5 mL) and conc. sulfuric acid (1.5 mL) at 0 °C in an ice bath for a period of 30 min. The reaction was warmed to room temperature and quenched by pouring into water, extracted with ethyl acetate and washed with saturated $NaHCO_3$ solution. After evaporation, the crude product was purified by column chromatography, eluted with 8:2 hexane:ethyl acetate. The yellow solid product was found to be the dinitration compound (0.123 g, 62%) [49]. mp. 74-76 °C, lit 77°C [50]. ^{1}H NMR ($CDCl_3$) δ (ppm): 11.29 (s, 1H), 8.16 (s, 2H), 2.47 (s, 3H) **(Figure A.1, Appendix)** ^{13}C NMR ($CDCl_3$) δ (ppm): 147.4, 137.3, 131.6, 129.4, 20.0. **(Figure A.2, Appendix)** FTIR (ATR, cm^{-1}): 3512, 3084, 2931, 1532, 1245. **(Figure A.3, Appendix).**

2.3.2 Phenolic *O*-silylation of 4-cresol.

General procedure: One equivalent of 4-cresol derivatives, 5 equivalent of silyl chloride and imidazole were dissolved in DMF (5-10 mL) and stirred at room temperature under nitrogen atmosphere for 30 min. The solution was then added water, extracted with ethyl acetate, washed with brine, dried over magnesium sulfate and evaporated.

2.3.2.1 tert-butyldimethyl(p-tolyloxy)silane (2)

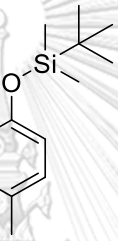

2

Following the general procedure, the mixture of 4-cresol (0.216 g, 2 mmol) and imidazole (0.68 g, 10 mmol) was added to the solution of *tert*-butyldimethylsilyl chloride (1.5 g, 10 mmol) in DMF (5 mL). The crude product was purified by passing through short column chromatography eluted with 100% hexane. The product **2** appeared as colorless liquid (0.396 g, 89%) [51, 52]. ^{1}H NMR (400 MHz, $CDCl_3$) δ (ppm): 6.97 (d, *J* = 8.4 Hz, 2H), 6.70 (d, *J* = 8.4 Hz, 2H), 2.24 (s, 3H), 0.96 (s, 9H), 0.15 (s, 6H) **(Figure A.4, Appendix)**

2.3.3 2,6-dibromo-4-methylphenol (3)

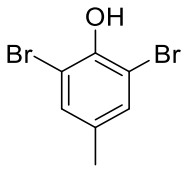

3

Bromine (1.598 g, 10 mmol) was dissolved in glacial acetic acid (8 mL) and dropped into the solution of 4-cresol (0.54 g, 5 mmol) in 1: 3 acetic acid: water at room temperature over 30 min. The mixture was then stirred for another 30 min. After the reaction completed, it was poured into distilled water (30 mL) and extracted with ethyl acetate three times. The organic layer was dried over anhydrous magnesium sulfate and the solvent was removed. The crude product **3** was purified by column chromatography using 9:1 hexane:ethyl acetate as an eluent. The product appeared as a pale-yellow solid (1.06 g, 78.3%). mp. 48-50 °C, lit 49 °C [53]. ^{1}H NMR ($CDCl_3$) δ (ppm): 7.24 (s, 2H), 5.71 (s, 1H), 2.25 (s, 3H) **(Figure A.6, Appendix).** ^{13}C NMR ($CDCl_3$) δ (ppm): 147.2, 132.4, 109.4, 20.0. **(Figure A.7, Appendix) FTIR** (ATR, cm^{-1}): 3411, 2921, 1559, 1474 **(Figure A.8, Appendix).** MS: 265.74 m/z [M^+] **(Figure A.9, Appendix)**

2.3.4 2-bromo-6-nitro-4-methylphenol (4)

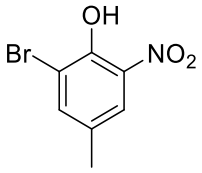

4

The solution of **3** (0.265 g, 1 mmol) in acetic acid (1 mL) was added conc. nitric acid (3 mL) and conc. sulfuric acid (1 mL) and stirred at room temperature for 30 min. The reaction was worked up by pouring into water (30 mL) and extracted with ethyl acetate. The combined organic layer was dried over anhydrous

magnesium sulfate and removed solvent by evaporation. The crude product was purified by column chromatography using 8:2 hexane:ethyl acetate as an eluent. Two products were obtained. Compound **4** (0.099g, 43%) [54, 55] was isolated as yellow solid product (R_f = 0.51, mp. 68-70°C, lit. 69°C [56, 57]). ^{1}H NMR ($CDCl_3$) δ (ppm): 10.97 (s, 1H), 7.93 (s, 1H), 7.71 (s, 1H), 2.35 (s, 3H) **(Figure A.10, Appendix)**. ^{13}C NMR ($CDCl_3$) δ (ppm): 150.2, 141.8, 132.4, 130.6, 124.1, 112.4, 20.1. **(Figure A.11, Appendix) FTIR** (ATR, cm^{-1}): 3166, 3065, 2927, 1536, 1309 **(Figure A.12, Appendix)** The second product (R_f = 0.26) was compound **1** (0.063g, 31.7%)

2.3.5 Phenolic *O*-silylation of 2,6-dibromo-4-methylphenol

2.3.5.1 (2,6-bromo-4-methylphenoxy)(tert-butyl)dimethylsilane (5)

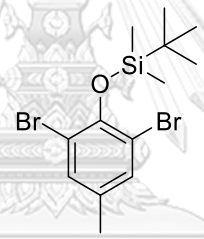

5

From the general procedure above (section 2.3.2), compound **3** (1.329 g, 5 mmol) was dissolved in DMF (10 mL) and added *tert*-butyldimethylsilyl chloride (3.75 g, 25 mmol) and imidazole (1.72 g, 25 mmol). The crude product was purified by column chromatography, eluted with 100% hexane to obtain the product **5** as colorless liquid (1.59 g, 84%) [58]. ^{1}H NMR (400 MHz, $CDCl_3$) δ (ppm): 6.93 (s, 2H), 1.89 (s, 3H), 0.71 (s, 9H), 0.00 (s, 6H) **(Figure A.13, Appendix)** FTIR (ATR, cm^{-1}): 2948, 2925, 2855, 1462, 1276, 1250 **(Figure A.14, Appendix).**

2.3.5.2 (2,6-dibromo-4-methylphenoxy)triisopropylsilane (6)

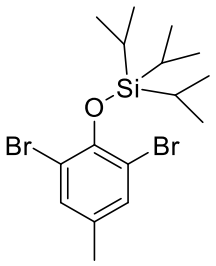

6

From the general procedure, triisopropylsilyl chloride (0.964 g, 5 mmol) was added into the solution of compound **3** (0.265 g, 1 mmol) in DMF (10 mL). The crude product was purified by column chromatography with eluent 100% hexane to get the product appear as white crystal (1.06 g, 78.3%) [59]. mp. 92-94 °C, lit 95 °C [59]. ^{1}H NMR ($CDCl_3$) δ (ppm): 7.27 (s, 2H), 2.23 (s, 3H), 1.61-1.47 (m, 3H), 1.15 (d, *J* = 7.6, 18H). **(Figure A.15, Appendix)**

2.3.6 1,3-dibromo-5-methyl-2-(4-nitrobenzyloxy)benzene (7)

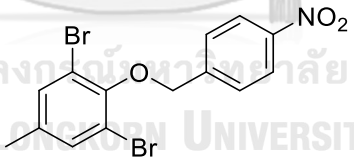

7

The mixture of **3** (0.265 g, 1 mmol), 4-nitrobenzyl chloride (0.205 g, 1.2 mmol), potassium carbonate (0.276 g, 2 mmol) were dissolved in acetonitrile (5 mL) and heated to 80 °C under nitrogen atmosphere for 8 h. After cooling to room temperature, the reaction was added 10 mL of water and extracted with ethyl acetate. The organic phase was washed three times with additional water and brine. The separated organic layer was dried over anhydrous magnesium sulfate. After removing the solvent by evaporation, the crude product was purified by column

chromatography using 8:2 hexane: ethyl acetate as an eluent to afford the product as white solid (0.312 g, 77%). mp. 117-118°C. ^{1}H NMR ($CDCl_3$) δ (ppm): 8.31 (d, *J* = 8.0 Hz, 2H), 7.91 (d, *J* = 8.0 Hz, 2H), 7.52 (s, 2H), 5.20 (s, 2H), 2.35 (s, 3H) **(Figure A.16, Appendix)** ^{13}C NMR ($CDCl_3$) δ (ppm): 155.0, 146.0, 143.7, 137.0, 133.3, 128.4, 123.7, 117.8, 73.0, 20.3. **(Figure A.17, Appendix)** FTIR (ATR, cm^{-1}): 3112, 3086, 2933, 1517, 1346. **(Figure A.18, Appendix)** HRMS: 423.8973 m/z [M+Na^+] (calculated 423.8978). **(Figure A.19, Appendix)**

2.3.7 1,3-dibromo-5-methyl-4-nitro-2-(4-nitrobenzyloxy)benzene (8a)

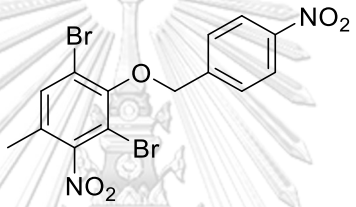

8a

Compound **9** (0.200 g, 0.5 mmol) was dissolved in dichloromethane (5 mL) in ice bath. The nitrating agent, prepared by mixing fuming HNO_3 (1.5 mL) and conc. H_2SO_4 (0.5 mL) at 0 °C, was added dropwise to the solution for 30 min. The ice bath was then removed and the reaction was stirred at room temperature for 8 h. After completion, the reaction was worked up by adding saturated $NaHCO_3$ to basic condition and extracted with ethyl acetate. The combined organic layers were dried over anhydrous magnesium sulfate. The crude mixture was purified by column chromatography using 9:1 hexane: ethyl acetate as eluent to yield product **8a** as a white solid (0.084 g, 37.8%). mp. 147-150°C. ^{1}H NMR ($CDCl_3$) δ (ppm): 8.27 (d, *J* = 8.4 Hz, 2H), 7.75 (d, *J* = 8.4 Hz), 7.56 (s, 1H), 5.15 (s, 2H), 2.33 (s, 3H) **(Figure A.21, Appendix)** ^{13}C NMR ($CDCl_3$) δ (ppm): 151.9, 151.7, 148.1, 142.8, 134.7,128.6, 128.4, 123.8, 119.8, 110.1, 73.4, 17.0. **(Figure A.22, Appendix)** FTIR (ATR, cm^{-1}): 3114, 3079, 2929, 1513, 1348. **(Figure A.23, Appendix)** HRMS: 468.8825 m/z [M+Na^+] (calculated 468.8829). **(Figure A.24, Appendix)**

2.3.8 2,6-dibromo-4-methyl-3-nitrophenol (9a)

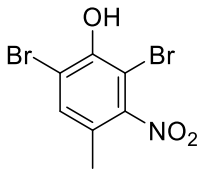

9a

Compound **8a** (0.022 g, 0.05 mmol) was dissolved in 33% hydrobromic acid in acetic acid (2 mL) and refluxed overnight. The reaction was then poured into water and extracted with ethyl acetate 3 times. The combined organic layer was dried over anhydrous magnesium sulfate, evaporated and purified by column chromatography with 8:2 hexane: ethyl acetate as eluent. The product **9a** appeared as brown liquid (0.012 g, 78.3%). ^{1}H NMR ($CDCl_3$) δ (ppm): 7.45 (s, 1H), 2.28 (s, 3H) **(Figure A.26, Appendix).**

2.3.9 2-bromo-4-methyl-5-nitrophenol (10)

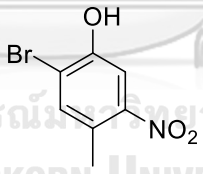

10

Compound **9a** (0.012 g, 0.038 mmol) was dissolved in 33% hydrobromic acid in acetic acid (5 mL). *p*-Toluidine (0.0163 g, 0.152 mmol) was added into the reaction as bromine scavenger. The mixture was refluxed overnight. After cooled down to room temperature, it was added water and adjusted pH to neutral with sat. $NaHCO_3$. The solution was extracted by ethyl acetate, and the organic layer was dried with anhydrous magnesium sulfate. After evaporation of the solvent, the crude product was purified by column chromatography using 8:2 hexane: ethyl acetate as eluent to

give the product **10** as brown liquid (0.0029 g, 32.4%). ^{1}H NMR ($CDCl_3$) δ (ppm): 7.60 (s, 1H), 7.41 (s, 1H), 2.45 (s, 3H) **(Figure A.29, Appendix).**

2.3.10 Diazo coupling reaction

2.3.10.1 4-methyl-2-((4'-nitrophenyl)diazenyl)phenol (11)

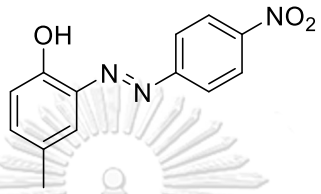

11

A cold 1 M $NaNO_2$ solution (2 mL) was added dropwise to the solution of *p*-nitroaniline (0.138 g, 1 mmol) in 3 M hydrochloric acid (1.5 mL) at 0 °C in ice bath to generate diazonium salt. Then this solution was dropped into a cooled solution of *p*-cresol (0.108 g, 1 mmol) in 1 M NaOH (2 mL). The mixture was then neutralized with 2 M Na_2CO_3, and stirred at 0 °C for another 10 min. The precipitate was filtered, washed with cold water and left to dry in a desiccator to give a brown orange solid (0.252 g, 97%) [60]. ^{1}H-NMR (acetone-d_6) δ (ppm): 11.72 (s, 1H), 8.45 (d, *J* = 8.0 Hz, 2H), 8.23 (d, *J* = 8.0 Hz, 2H), 7.80 (s, 1H), 7.35 (d, *J* = 8.4 Hz, 1H), 7.00 (d, *J* = 8.4 Hz, 1H), 2.38 (s, 3H) **(Figure A.32, Appendix)** ^{13}C-NMR ($CDCl_3$) δ (ppm): 154.2, 150.9, 137.6, 136.3, 133.6, 129.9, 125.0, 125.0, 122.7, 118.3, 20.3 **(Figure A.33, Appendix).** FTIR (ATR, cm^{-1}): 3102, 2925, 1608, 1519, 1495, 1429, 1340. **(Figure A.34, Appendix)** MS: 258.09 m/z [$M+H^+$] **(Figure A.35, Appendix).**

2.3.10.2 2-bromo-4-methyl-6-((4-nitrophenyl)diazenyl)phenol (12)

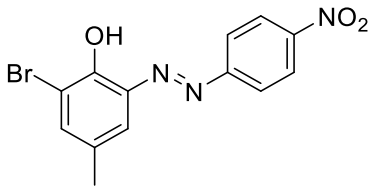

12

The cold solution of *p*-nitroaniline (0.138 g, 1 mmol) in 3 M hydrochloric acid (1.5 mL) at 0 °C was added dropwise by cold 1 M $NaNO_2$ solution (2 mL) in 5 min. Then the solution was dropped into the cold solution of **2** (0.265 g, 1 mmol) in 1 M NaOH (2 mL). The mixture was then neutralized with 2 M Na_2CO_3, and stirred at 0 °C for another 10 min. The precipitate was filtered and washed with cold water, then left to dry in a desiccator to give a brown orange solid (0.276 g, 82%). ^{1}H NMR ($CDCl_3$) δ (ppm): 13.31 (s, 1H), 8.40 (d, *J* = 8.0 Hz, 2H), 8.02 (d, *J* = 8.0 Hz, 2H), 7.79 (s, 1H), 7.55 (s, 1H), 2.41 (s, 3H) **(Figure A.36, Appendix).**

2.3.11 2-amino-4-methylphenol (13)

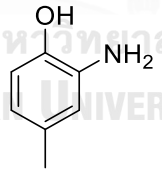

13

The solution of tin (II) chloride (0.189 g, 1 mmol) in conc. hydrochloric acid (1 mL) was added into the solution of compound **11** (0.05 g, 0.2 mmol) in ethanol (1 mL). The mixture was heated to 50 °C and stirred for 30 min. After cooling down to room temperature it was poured into water (10 mL) and was added sat. $NaHCO_3$ to adjust the pH to basic, then the solution was extracted with ethyl acetate. The organic layers were collected and dried over anhydrous magnesium sulfate. The crude product was purified by column chromatography using 2:1 hexane: ethyl

acetate to afford product **13** as brown solid (0.021 g, 90%). ^{1}H NMR ($CDCl_3$) δ (ppm): 6.99 (d, *J* = 8 Hz, 1H), 6.85 (d, *J* = 8.4 Hz, 1H), 6.80 (s, 1H), 2.30 (s, 3H) **(Figure A.37, Appendix)** ^{13}C NMR ($CDCl_3$) δ (ppm): 142.3, 139.6, 133.0, 122.2, 109.2, 108.8, 20.4. **(Figure A.38, Appendix).**

2.4 Model Synthesis for SAHA-like moiety

2.4.1 Methyl 6-oxo-6-(phenylamino)hexanoate (15)

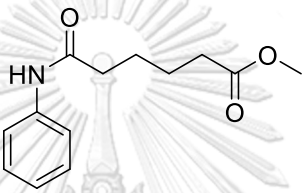

15

The mixed solution of methanol (0.20 mL, 5 mmol) and triethylamine (0.7 mL, 5 mmol) in dichloromethane (2 mL) was dropped into the solution of adipoyl chloride (0.549 g, 3 mmol) in dichloromethane (3 mL) at 0 °C in ice bath under nitrogen atmosphere. It was then added the solution of aniline (0.047 g, 0.5 mmol) and triethylamine (0.14 mL, 1 mmol) in dichloromethane (3 mL). The reaction was stirred at 0 °C for another 30 min, then quenched by adding 2 mL methanol and excess water, extracted with ethyl acetate. The organic layer was dried over anhydrous magnesium sulfate and the solvent was removed by evaporation. The crude product was purified by column chromatography with 2:1 hexane: ethyl acetate to obtain product **15** as colorless liquid (0.095 g, 80 %). ^{1}H NMR ($CDCl_3$) δ (ppm): 8.23 (s, 1H), 7.50 (d, *J* = 8 Hz, 2H), 7.25 (t, *J* = 7.6 Hz, 2H), 7.04 (t, *J* = 7.2 Hz, 1H), 3.63 (s, 3H), 2.28 (m, 4H), 1.64 (m, 4H). **(Figure A.40, Appendix)** FTIR (ATR, cm^{-1}): 3306, 2948, 2869, 2362, 1732, 1659, 1599, 1438. **(Figure A.41, Appendix)** MS: 235.87 m/z [M^+] **(Figure A.42, Appendix).**

2.4.2 N^1-hydroxy-N^6-phenyladipamide (16)

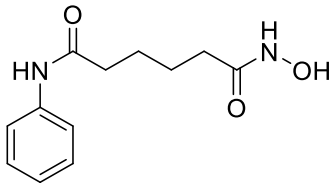

16

To a solution of compound **15** (0.023 g, 0.1 mmol) in 3 mL of 1:1 tetrahydrofuran: methanol, was added 50% aqueous solution of hydroxylamine hydrochloride (0.104 g, 1.5 mmol) and triethylamine (0.21 mL, 1.5 mmol). The reaction was stirred at room temperature for 2 days. It was then poured into water and extracted with ethyl acetate. The obtained product **16** appeared as pale-yellow solid (0.026 g, 92.5%). mp. 135-137 °C. ^{1}H NMR (CD_3OD) δ (ppm): 7.52 (d, *J* = 8.4 Hz, 2H), 7.29 (t, *J* = 7.6 Hz, 2H), 7.07 (t, *J* = 6.8 Hz, 1H), 2.37 (m, 4H), 1.69 (m, 4H). **(Figure A.44, Appendix)** FTIR (ATR, cm^{-1}): 3310, 2956, 2919, 2874, 2849, 1686, 1655, 1597, 1517. **(Figure A.45, Appendix)**

2.4.3 1-(2-(benzyloxy)-5-methylphenyl)-2-(4-nitrophenyl)diazene (17)

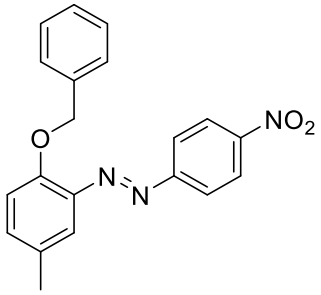

17

Compound **11** (0.026 g, 0.1 mmol), benzyl bromide (0.06 mL, 0.5 mmol) and K_2CO_3 (0.28 g, 0.5 mmol) were dissolved in acetonitrile (2 mL). The mixture was stirred overnight at room temperature, then extracted with ethyl acetate, washed with water and brine. The combined organic layer was dried over anhydrous magnesium sulfate and the solvent was removed by evaporation. The crude product was purified by column chromatography using 9:1 hexane: ethyl acetate to yield product **17** as a deep orange solid (0.028 g, 82.9%). mp. 130-131 °C. ^{1}H NMR (acetone-d_6) δ (ppm): 8.44 (d, *J* = 8.8 Hz, 2H), 8.12 (d, *J* = 8.8 Hz, 2H), 7.55-7.27 (m, 8H), 5.39 (s, 2H), 2.34 (s, 3H). **(Figure A.46, Appendix).** FTIR (ATR, cm^{-1}): 3100, 3034, 2913, 2857, 1606, 1501, 1338. **(Figure A.47, Appendix).**

2.4.4 2-(benzyloxy)-5-methylaniline (18)

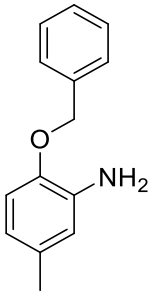

18

Tin (II) chloride (0.04 g, 0.2 mmol) was dissolved in 10% hydrochloric acid (2 mL) and transferred into the solution of compound **17** (0.014 g, 0.04 mmol) in ethanol (4 mL). The mixture was heated to 50 °C for 15 min. Then 10 mL of water was added and the resulting mixture was extracted with ethyl acetate. The organic phase was washed three times with additional water and then dried over anhydrous magnesium sulfate. After evaporation of solvent, the crude mixture was purified by column chromatography eluted by 8:2 hexane: ethyl acetate to afford product **18** as brown liquid (0.083 g, 80%). ^{1}H NMR (CD_3OD) δ (ppm): 7.44 (d, *J* = 7.6 Hz, 2H), 7.36 (t, *J* = 7.2 Hz, 2H), 7.29 (t, *J* = 6.8 Hz, 1H), 5.05 (s, 2H), 2.17 (s, 3H). **(Figure A.48, Appendix)** FTIR (ATR, cm^{-1}): 3468, 3372, 2917, 2849, 1614, 1513, 1451. **(Figure A.49, Appendix).**

2.4.5 methyl 6-((2-(benzyloxy)-5-methylphenyl)amino)-6-oxohexanoate (19)

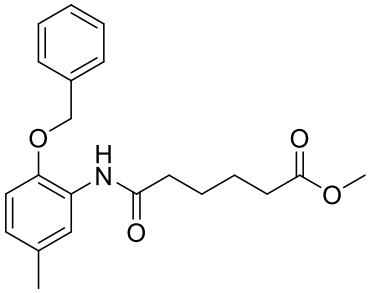

19

Methanol (0.05 mL, 1 mmol), triethylamine (0.15 mL, 1 mmol) was mixed in dichloromethane (2 mL) and dropped into the solution of adipoyl chloride (0.11 g, 0.6 mmol) in dichloromethane (3 mL) at 0 °C in ice bath under nitrogen atmosphere. Then the solution of compound **18** (0.021 g, 0.1 mmol) and triethylamine (0.07 mL, 0.5 mmol) in dichloromethane (3 mL) was added to the mixture and continue stirring at 0 °C for 30 min. Methanol 1 mL was added to work up the reaction and ethyl acetate and water were added for extractions. The organic layer was collected and the solvent was removed. The crude product was purified by column chromatography using 6:4 hexane: ethyl acetate as eluent to obtain product **19** as colorless liquid (0.034 g, 97.2%). ^{1}H NMR ($CDCl_3$) δ (ppm): 8.22 (s, 1H), 7.74 (s, 1H), 7.40 (m, 5H), 6.81 (m, 2H), 5.08 (s, 2H), 3.66 (s, 3H), 2.34 (m, 4H), 2.29 (s, 3H), 1.71 (m, 4H). **(Figure A.50, Appendix)** FTIR (ATR, cm^{-1}): 3422, 3333, 2948, 2863, 1729, 1676, 1593, 1532. **(Figure A.51, Appendix)**

2.4.6 Conversion of methoxy to hydroxamic acid

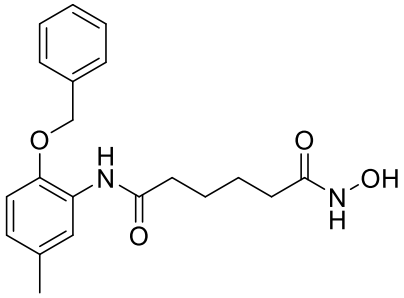

20

The aqueous solution of hydroxylamine hydrochloride (0.024 g, 0.35 mmol) was added into the solution of compound **19** (0.008 g, 0.023 mmol) and triethylamine (0.05 mL, 0.35 mmol) in 3 mL of 1:1 tetrahydrofuran: methanol. The solution was refluxed for 3 Days. After cooled down to room temperature, the water was added into the solution and extracted with ethyl acetate. The combined organic layers was dried over anhydrous magnesium sulfate and the solvent was removed by evaporator to obtain product **20** as pale yellow liquid (0.006 g, 74.8%) ^{1}H NMR ($CDCl_3$) δ (ppm): 8.21 (s, 1H), 7.76 (2, 1H), 7.40 (m, 5H), 6.82 (m, 2H), 5.08 (s, 2H), 2.36 (m, 4H), 2.29 (s, 3H), 1.72 (m, 4H). **(Figure A.52, Appendix)**

2.5 Functionalization on *β*-estradiol.

2.5.1 Diazo coupling on *β*-estradiol

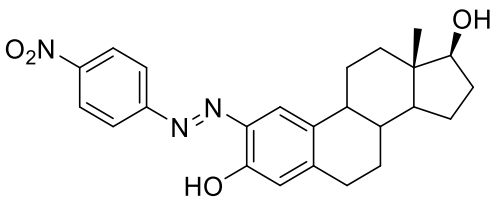

21a

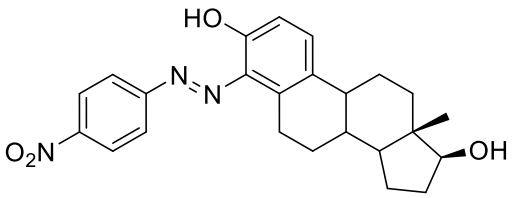

21b

Similar to the diazo coupling protocol in section 2.3.10, diazonium salts was generated by dropping cold 1 M $NaNO_2$ (0.2 mL) to solution of *p*-nitroaniline (0.014 g, 0.1 mmol) in 3 M hydrochloric acid (1.5 mL) in ice bath. After 5 min, the mixture was added dropwise to the cold solution of estradiol (0.027 g, 0.1 mmol) in 1 M NaOH (5 mL) at 0 ℃. After 10 min, the reaction was adjusted to neutral by adding 2 M Na_2CO_3 and stirred at 0 ℃ for another 2 h. The crude product was filtered and left to dry in desiccator. Two isomers of diazo products were obtained after purification by column chromatography using 2:1 dichloromethane: ethyl acetate as eluent. The first product (R_f = 0.71) was compound **21a** appeared as a yellow solid (0.014 g, 34%). mp. 231-234°C. ^{1}H NMR ($CDCl_3$) δ (ppm): 12.50 (s, 1H), 8.38 (d, *J* = 8.8 Hz, 2H), 7.97 (d, *J* = 8.8 Hz, 2H), 7.86 (s, 1H), 6.77 (s, 1H), 3.77 (t, *J* = 8.4 Hz, 1H), 2.93 (m, 2H), 2.44 (d, *J* = 13.4 Hz, 1H), 2.32-2.20 (m, 1H), 2.19-2.08 (m, 1H), 2.08-1.85 (m, 3H), 1.46-1.11 (m, 6H), 0.82 (s, 3H). **(Figure A.53, Appendix).** The second product **21b** appear as an orange solid (0.012 g, 29%). ^{1}H NMR ($CDCl_3$) δ (ppm): 13.46 (s, 1H), 8.37 (d, *J* = 9.2 Hz, 2H), 7.95 (d, *J* = 9.2 Hz, 2H), 7.43 (d, *J* = 8.8 Hz, 1H), 6.85 (d, *J* = 8.8 Hz, 1H), 3.77 (t, *J* = 8.4 Hz, 1H), 3.73-3.71 (m, 2H), 3.59 (dd, *J* = 18.6, 5.6 Hz, 1H), 3.25-3.08 (m, 2H), 2.87 (d, *J* = 50.4 Hz, 1H), 2.41-1.82 (m, 6H), 1.81-1.69 (m, 2H), 0.85-0.76 (m, 3H). **(Figure A.54, Appendix).**

2.5.2 Benzylation of 2-diazo-estradiol

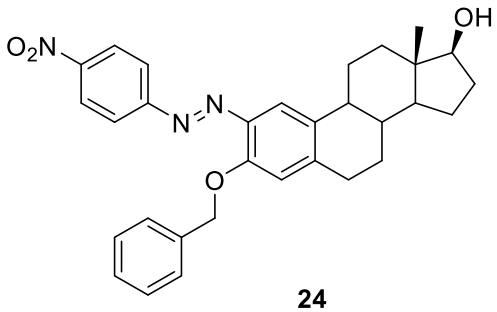

24

The mixture of compound **21a** (0.02 g, 0.05 mmol), benzyl bromide (0.05 mL, 0.4 mmol) and K_2CO_3 (0.06 g, 0.4 mmol) in acetonitrile (4 mL) was stirred at room temperature overnight. The reaction was quenched by adding water, extracted with ethyl acetate and washed with brine. After drying organic layers with anhydrous magnesium sulfate, the solvent was removed using evaporator. The crude product was purified by column chromatography with 2:1 hexane: ethyl acetate as eluent to afford product **24** as an orange solid. (0.018 g, 74.14%) ^{1}H NMR ($CDCl_3$) δ (ppm): 8.33 (d, *J* = 8.8 Hz, 2H), 7.97 (d, *J* = 8.8 Hz, 2H), 7.71 (s, 1H), 7.49-7.33 (m, 5H), 6.87 (s, 1H), 5.30 (s, 2H), 3.75 (m, 1H), 2.90 (m, 2H), 2.42-1.10 (m, 13H) **(Figure A.57, Appendix).** FTIR (ATR, cm^{-1}): 3370, 2923, 2869, 1606, 1521, 1338. **(Figure A.58, Appendix)**

2.5.3 Reduction of protected 2-diazo-estradiol

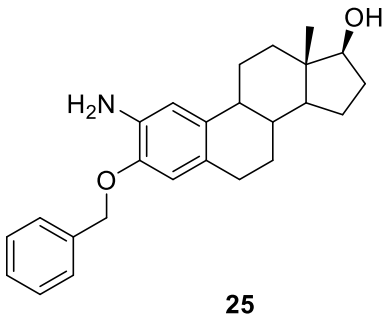

25

The solution of tin (II) chloride (0.029 g, 0.15 mmol) in 10% hydrochloric acid (2 mL) was transferred to the solution of compound **24** (0.014 g, 0.03 mmol) in ethanol (2 mL). The mixture was stirred for 15 min. Then the reaction was added 10 mL of water and extracted with ethyl acetate. The organic phase was dried over anhydrous magnesium sulfate. After removal of solvent, the crude mixture was purified by column chromatography eluted with 1:1 hexane: ethyl acetate to afford product **25** as brown liquid (0.007 g, 67.8%). ^{1}H NMR ($CDCl_3$) δ (ppm): 7.49-7.28 (m, 5H), 6.71 (s, 1H), 6.59 (s, 1H), 5.04 (s, 2H), 3.72 (m, 1H), 2.75 (m, 2H), 2.28-1.03 (m, 13H), 0.77 (s, 3H). **(Figure A.59, Appendix)** FTIR (ATR, cm^{-1}): 3355, 2921, 2851, 1595, 1511, 1307. **(Figure A.60, Appendix)**

2.5.4 Conjugation with SAHA-like moiety

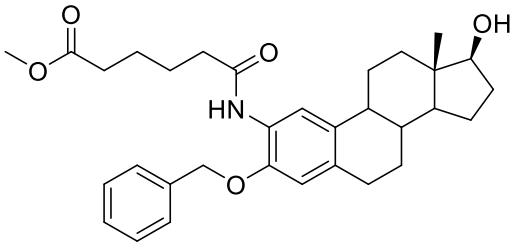

26

Mixture of methanol (0.01 mL, 0.2 mmol), triethylamine (0.03 mL, 0.2 mmol) and dichloromethane (2 mL) was dropped into the solution of adipoyl chloride (0.022 g, 0.12 mmol) in dichloromethane (3 mL) at 0 °C under nitrogen atmosphere. The mixture of compound **25** (0.007 g, 0.02 mmol) and triethylamine (0.01 mL, 0.04 mmol) in dichloromethane (3 mL) and added into the previous solution and stirred at 0 °C for 30 min. Methanol 2 mL and excess water were added to the reaction and the mixture was then extracted with ethyl acetate. The organic layer was collected and the solvent was removed. The crude product was purified by column chromatography using 1:1 hexane: ethyl acetate as eluent to obtain product **26** as colorless liquid (0.003 g, 31%). ^{1}H NMR ($CDCl_3$) δ (ppm): 8.36 (s, 1H), 7.67 (s, 1H), 7.41 (s, 5H), 6.66 (s, 1H), 5.07 (s, 2H), 3.74 (m, 1H), 3.66 (s, 3H), 2.79 (m, 2H), 2.68-0.94 (m, 13H), 0.77 (s, 3H). **(Figure A.61, Appendix)** FTIR (ATR, cm^{-1}): 3415, 2925, 2857, 1733, 1521. **(Figure A.62, Appendix)**

2.5.5 Conversion to hydroxamic acid

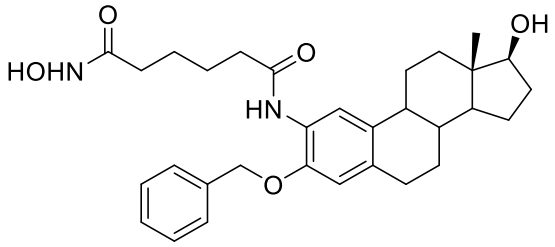

27

Hydroxylamine hydrochloride (0.008 g, 0.12 mmol) in aqueous solution was added into the solution of compound **26** (0.004 g, 0.008 mmol) and triethylamine (0.02 mL, 0.12 mmol) in 2 mL of 1:1 tetrahydrofuran: methanol. The solution was refluxed for 5 days. After cooled down to room temperature, the water was added into the solution and extracted with ethyl acetate. The combined organic layer was dried over anhydrous magnesium sulfate and the solvent was removed by evaporator. The crude product was purified by column chromatography using gradient eluent from 1:1 hexane: ethyl acetate to 100% ethyl acetate to obtain product **27** as pale yellow liquid (0.002 g, 49.9%) ^{1}H NMR ($CDCl_3$) δ (ppm):) 8.35 (s, 1H), 7.68 (s, 1H), 7.41 (s, 5H), 6.66 (s, 1H), 5.07 (s, 2H), 3.73 (m, 1H) **(Figure A.63, Appendix).**

CHAPTER III

RESULTS AND DISCUSSION

3.1 Model Synthesis

3.1.1 Nitration of 4-methylphenol

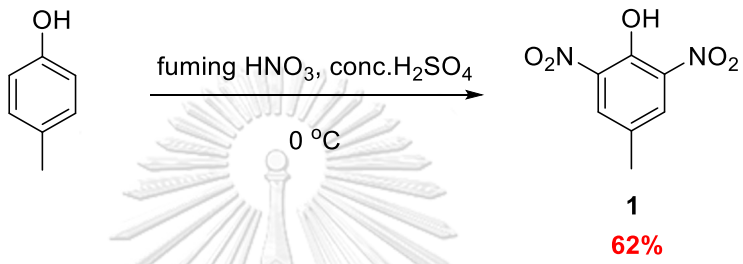

2,6-Dinitro-4-methylphenol was synthesized through nitration reaction of 4-methylphenol[61]. The conditions of the reaction were varied to see whether partial nitration on the substrate is possible, as shown in **Table 3.1**.

Table 0.1The synthesis condition for 2,6-dinitro-4-methylphenol

Entry	Type of HNO_3 (mL)	Conc. H_2SO_4 (mL)	solvent	Time (h)	Temperature (°C)	Yield (%)
1	fuming (0.5)	1.5	AcOH	0.5	0	62
2	conc. (1)	0	AcOH	1	0	70
3	20% (1)	0	DCE	overnight	rt	56

Following **Table 3.1,** the typical nitrating agent (entry 1) gave the 2 times nitrated product in high yield. Even milder conditions as simple concentrated HNO_3

or just 20% solution without sulfuric acid, (entries 2 and 3) all gave only dinitrated compound as the major product with no sign of mononitration. This result indicated that the reaction was too facile and difficult to control.

3.1.2 Nitration of protected 4-methylphenol

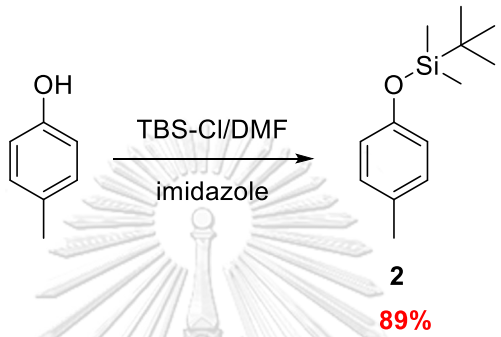

2

89%

To deactivate 4-methylphenol toward the nitrating agent, the hydroxy group was protected using the highly steric TBS as the protecting group. The structure of the product was confirmed with ^{1}H NMR spectrum [51, 52] **(Figure A.9, Appendix)**.

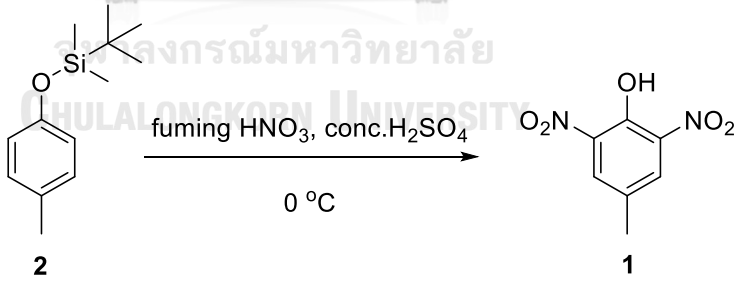

2 **1**

TBS-protected 4-methylphenol was nitrated using the ordinary method of fuming HNO_3 and conc. H_2SO_4, expecting the single substitution at one of the *ortho*-positions. Unfortunately, the O-Si bond was too labile in such a harsh condition and was removed during the process. Therefore, the deprotected 4-methylphenol reacted with the reagent and gave the same dinitrated product as in section 3.1.1.

3.1.3 Oxidation/addition of 4-methylphenol

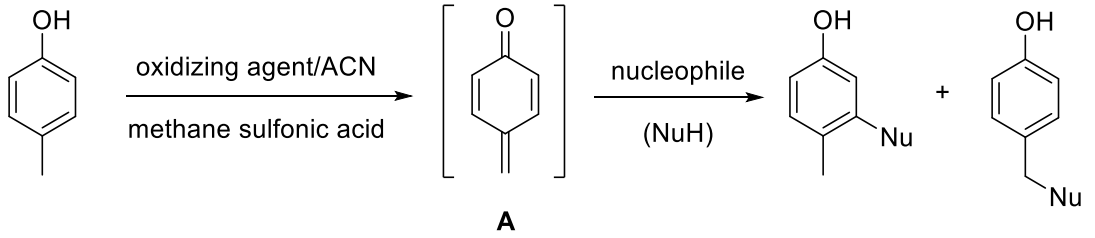

One of our challenging goals on estradiol functionalization is to put the conjugation point at its 1-position, which is meta to the hydroxy group that is generally much less preferred for typical nucleophilic aromatic substitutions Therefore, a sequence of oxidation to quinoid followed by nucleophilic addition was attempted. As the model, 4-methylphenol was presumably oxidized to the quinoid intermediate **A**, then a nucleophile was added, preferably at either *meta*-position of the formerly hydroxy group just like a Michael addition or even further addition at δ-position of the carbonyl group **(Figure 3.1)**. Many oxidizing agents were screened for obtaining **A** as shown in **Table 3.2**.

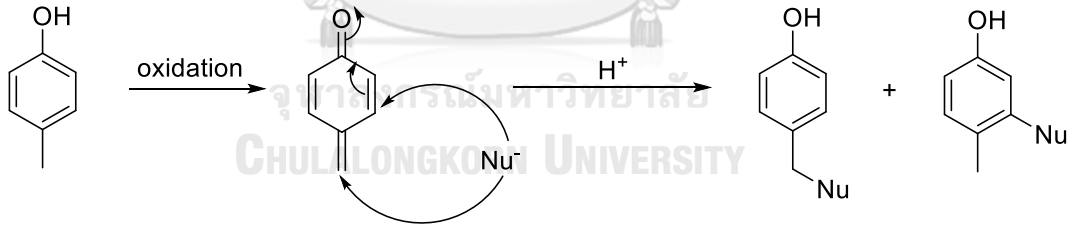

Figure 3.1 Propose mechanism from oxidation/nucleophilic substitution on 4-methylphenol

Table 3.2 Oxidations of 4-methylphenol

Entry	Oxidizing agent	solvent	Oxidation progress
1	DDQ	ACN	✖
2	$NaOCO_3$	ACN/H_2O	✖
3	PCC	ACN	✖
4	$NaIO_4$/MSA	ACN/H_2O	✓
5	UHP	ACN	✖
6	Pd/C	ACN	✖
7	2-methyl pyridine oxide	ACN	✖

According to **Table 3.2**, various oxidizing agent were used to oxidize 4-methylphenol such as 2,3-dichloro-5,6-dicyano-1,4-benzoquinone (DDQ), $NaOCO_3$, pyridinium chlorochromate (PCC), $NaIO_4$, urea hydrogen peroxide (UHP), Pd/C and 2-methyl pyridine oxide, only $NaIO_4$ with 1 drop of methane sulfonic acid (MSA) as the oxidizing agent gave the progress of oxidation (entry 4). When diethylamine was added into the mixture, a spot of a new product was observed on TLC within 5 min. However, the characterization of this product after purification by ^1H NMR showed no signal that corresponded to ethyl groups from the added nucleophile **(Figure A.5, Appendix)**.

It's possible that the reaction stopped at the intermediate **A**, which was isolated. Other nucleophiles such as morpholine, KCN, Na_2S or pyrrolidine were added in place of diethylamine to the reaction above. No evidence of nucleophile incorporation was observed.

Blocking the *ortho*-positions of 4-methylphenol may divert the electrophile to react at its *meta*-positions instead. Bromine has been reported to be used as the blocking groups, or protecting groups, that could be removed or deprotected later [62].

3.1.4 Brominations of 4-methylphenol

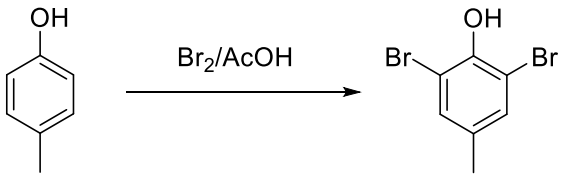

3

78.3%

2,6-Dibromo-4-methylphenol was successfully synthesized from brominations on both *ortho*-positions of the substrate, giving good yield (78.3%) of the product. The ^{1}H NMR spectrum **(Figure A.6, appendix)** showed the signals that matched with those previously report [53].

3.1.5 Nitration of 2,6-dibromo-4-methylphenol

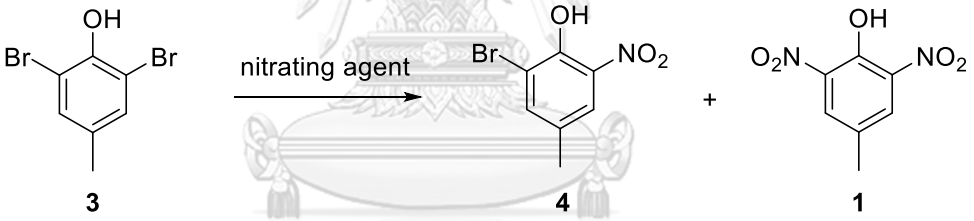

3 **4** **1**

43% **32%**

The bromine blocked 4-methylphenol was nitrated via the general procedure, fuming HNO_3 and conc.H_2SO_4, expected the nitro group would be substituted at the free *meta*-positions relate to hydroxy group of the substrate. However, the reaction gave almost equal yields of 2-bromo-6-nitro-4-methylphenol [54, 55] **(Figure A.10, Appendix)** and 2,6-dinitro-4-methylphenol [63]. Turning the reagent to milder conditions or even changing the reagent altogether were attempted in order to control the nitration. The changes in these conditions are shown in **Table 3.3**.

Table 3.3 The condition for nitration of 2,6-dibromo-4-methylphenol

Entry	Nitrating agent	Solvent	Temperature
1	fuming HNO_3/H_2SO_4	AcOH	rt
2	fuming HNO_3	AcOH	0°C
3	conc. HNO_3	AcOH	0°C
4[a]	5-20% HNO_3	AcOH	0°C
5	20% $HNO_3/KNO_3/AlCl_3$	DCM	0°C
6	20% HNO_3	DCM	rt
7	1 eqv.$NO_2^+BF_4^-$	DCM	rt
8	1.5 eqv.$NO_2^+BF_4^-$	DCM	rt

[a] used 4 concentrations: 5%, 10%, 15% and 20%.

Following **Table 3.3**, all conditions gave the two products, 2-bromo-6-nitro-4-methylphenol and 2,6-dinitro-4-methylphenol, as the major product mixture, even without H_2SO_4 or lower HNO_3 concentrations. It is noted that no reaction occurred when only 5% HNO_3 was used.

To avoid the acidic polar condition that might be the reason for bromine removal, KNO_3 was used with 20%HNO_3 and $AlCl_3$ in DCM under two-phase condition. The reaction gave spot of a new product on TLC (R_f = 0.15) **(Figure A.64, Appendix)**. Unfortunately, this new product was not the desired one and might occur from $AlCl_3$ reacted with dichloromethane, generating chloromethyl electrophile that substituted onto the substrate.

When nitration salt was used as the nitrating agent, the removal of bromine still occurred, even in the non-protonic, neutral condition. The issue learned from this reaction is that the Br groups could not block the nitration. The bromo groups at *ortho*-positions were still preferably substituted over the unsubstituted (or protonated) *meta*-positions. Therefore, substitution at *meta*-position of phenols was not yet achieved.

3.1.6 Protections of 2,6-dibromo-4-methylphenol

3.1.6.1 Silyl protection

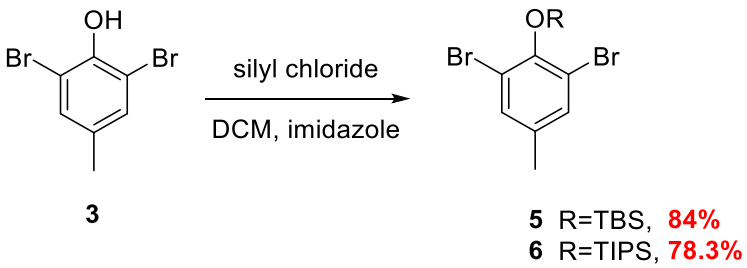

3

5 R=TBS, **84%**
6 R=TIPS, **78.3%**

TBS-Cl and TIPS-Cl were chosen to protect the hydroxy group of 2,6-dibromo-4-methylphenol [58]. Both protected products were successfully synthesized in good yields (84%, 78% respectively). ^{1}H NMR spectra confirmed their structures with previous works [58, 59].

3.1.6.2 nitro benzyl groups protection

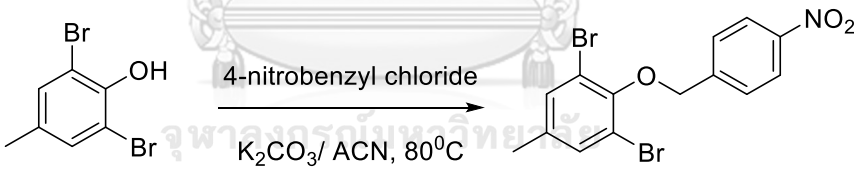

2

7
77%

4-Nitrobenzyl protection was obtained from the reaction between 2,6-dibromo-4-methylphenol and 4-nitrobenzyl chloride using K_2CO_3 as base [64]. High yield of the product was obtained, and the reaction performed well in larger scale. ^{1}H NMR spectrum showed the peaks of nitrobenzyl ring at 8.31 ppm and 7.91 ppm and the singlet peak of benzyl-group at 5.20 ppm **(Figure A.16, Appendix).**

3.1.7 nitration of protected 4-methylphenol

3.1.7.1 Silyl protection

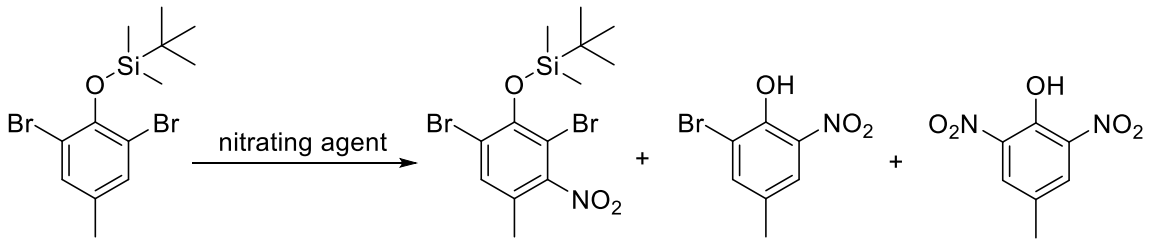

5 **4** **1**

Various nitration conditions were carried out as shown in **Table 3.4**. The *meta*-nitro substituted product was produced mostly in very low yield **(Figure A.20, Appendix)**. The silyl protecting groups could not withstand the conditions and was removed, followed by the mono- and dinitration at *ortho*-position to the typical product mixture of phenol derivatives similar to the unprotected substrate. (section 3.1.5)

Table 3.4 The condition for nitration on silyl protected 2,6-dibromo-a-methylphenol

Entry	Protecting group	Nitrating agent	Solvent	Temperature	% yield of *meta*-nitro product
1	TBS	Fuming HNO_3/H_2SO_4	-	0°C	3.6
2	TBS	Conc.HNO_3	-	0°C	-
3	TBS	50-60% HNO_3[a]	H_2O	0°C	2.6[b]
4	TBS	Conc. HNO_3/H_2SO_4	DCM	rt	1.3
5	TIPS	Conc. HNO_3/H_2SO_4	DCM	rt	-

[a] with 50%, 55% and 60% HNO_3

[b] average yield from 3 concentrations

3.1.7.2 Nitro benzyl groups protection

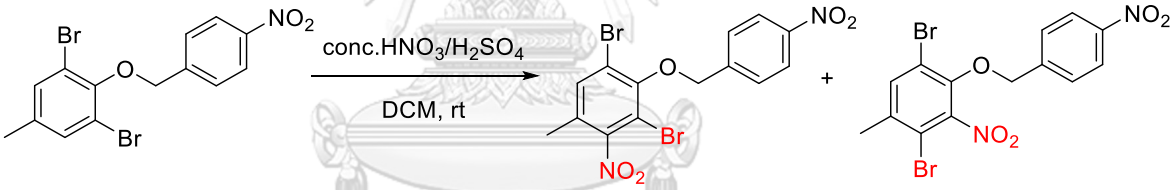

7 **8a** **28%** **8b** **16%**

Follow the general procedure, conc. HNO_3 and H_2SO_4 were used as nitrating agent in two-phase condition with dichloromethane. Two products **8a** and **8b** were obtained in 28 % and 16% yields respectively. ^{1}H NMR spectra of both products have the same number of peaks with slightly difference in chemical shifts **(Figure 3.2)**. The derived *meta*-nitro product **8a** could be increased in yield using fuming HNO_3 instead of conc. HNO_3 (% yields of **8a:8b = 38: 4)**. High resolution mass spectrometry was used to confirm that the two products were actually regioisomers. **(Figure A.24 and A.25, Appendix)**.

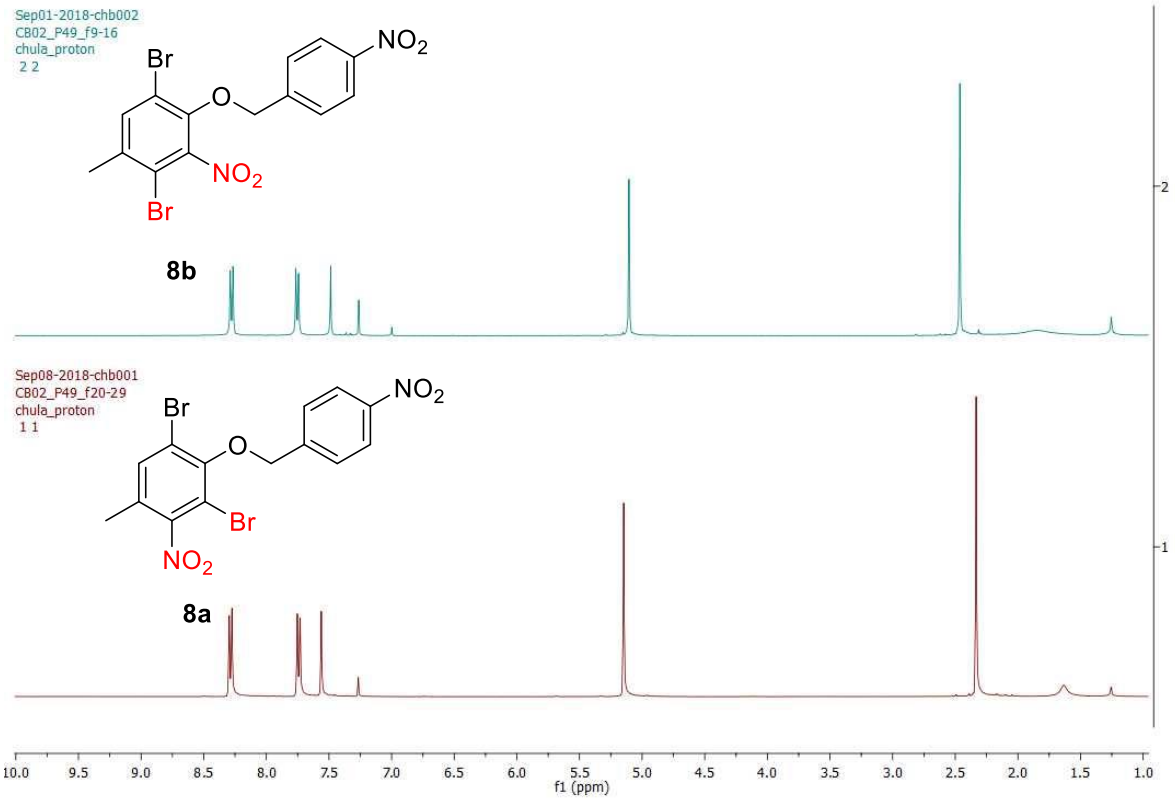

Figure 3.2 Comparison of ^{1}H NMR spectra between 8a and 8b

Compound **8b** was produced from the rearrangement of bromine from *ortho*-position to *meta*-position via bromonium bridge followed by re-aromatization. **(Figure 3.3)**

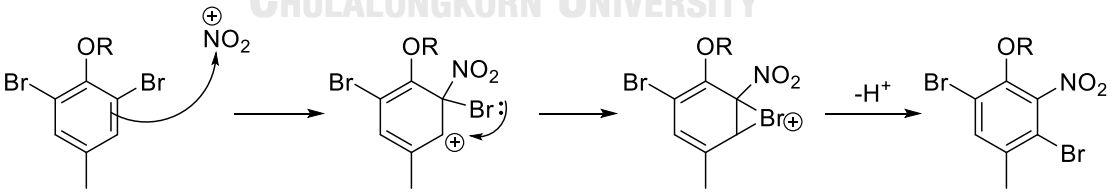

Figure 3.3 The proposed mechanism for bromine rearrangement

3.1.8 Deprotection of nitrobenzyl protected 2,6-dibromo-4-methylphenol

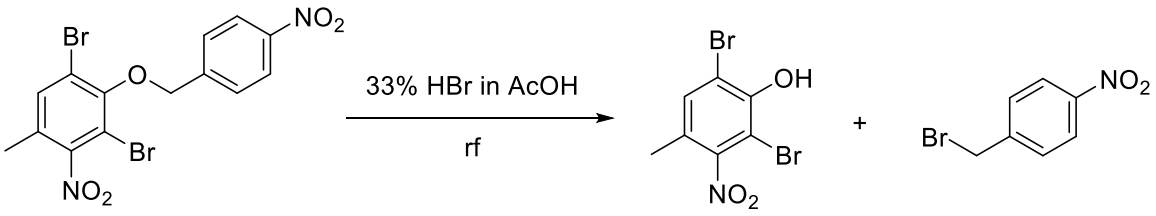

8a **9a** 78.3%

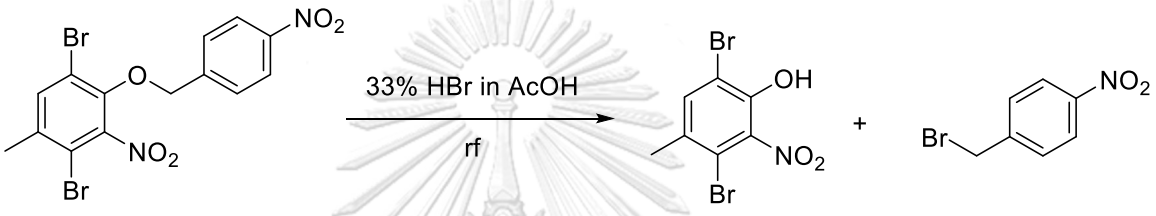

8b **9b** 67.8%

Deprotection of 4-nitrobenzyl protections of **8a** and **8b** were achieved by refluxing the substrate with 33% HBr in AcOH. Both **8a** and **8b** gave the product **9a (Figure A. 26, Appendix)** and **9b (Figure A. 27, Appendix)** together with the 4-nitrobenzyl bromide **(Figure A.28, Appendix)**

3.1.9 Debrominations of compound 9a

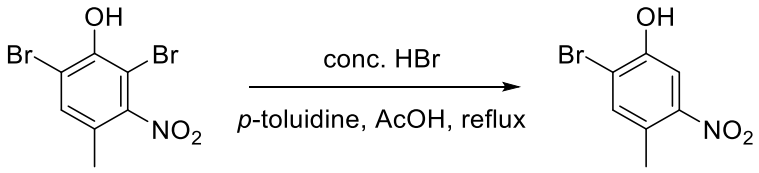

9a **10**

32.4%

Debrominations of **9** were operated using previous reported method [62]. *p*-Toluidine was added in order to act as bromine scavenger. The reaction underwent bromine transfer, cleavaged from the substrate and re-brominated on *p*-toluidine. Unluckily, only one bromine could be eliminated from the substrate. To product **10 (Figure A.29, Appendix).**

The characterization of compound **10** was also confirmed by ^{1}H-^{1}H NOESY-NMR **(Figure 3.4 and Figure A.30, Appendix)** compared to compound **3 (Figure 3.4 and Figure A.31, Appendix)** From **Figure 3.4,** the spectrum showed only one correlation between aromatic proton signal at 7.47 ppm and protons on the methyl group at 2.52 ppm. This would confirm that only one *meta*-proton to the hydroxy group was present. On the other hand, the NOESY signal from compound **3** showed the correlations between two *meta*-aromatic proton signals and those on the methyl group, supporting the presence of two protons located at *meta*-positions to the hydroxy group. From the result, it was clear that the original protected phenolic derivative was successfully nitrated at *meta*-position, although the overall yield of the process was quite low. More studies were needed for further improvement on this unprecedented substitution at *meta*-positions of electron-rich aromatic compounds [65-67]

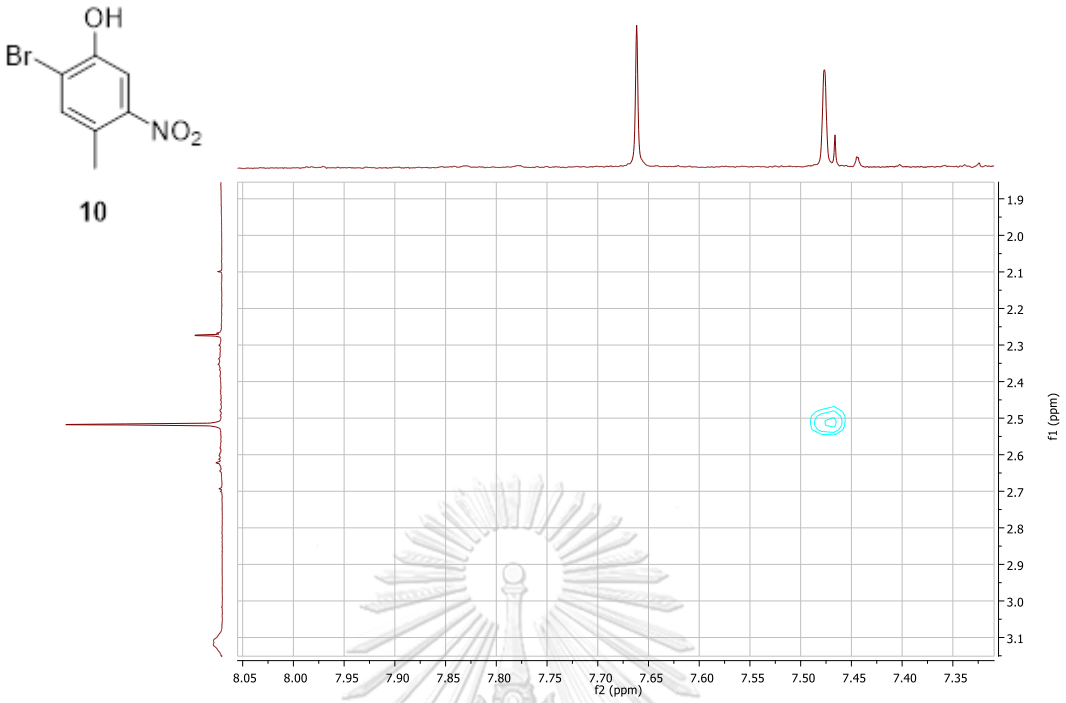

Figure 3.4 ^{1}H-^{1}H NOESY NMR spectrum ($CDCl_3$) of compound 10

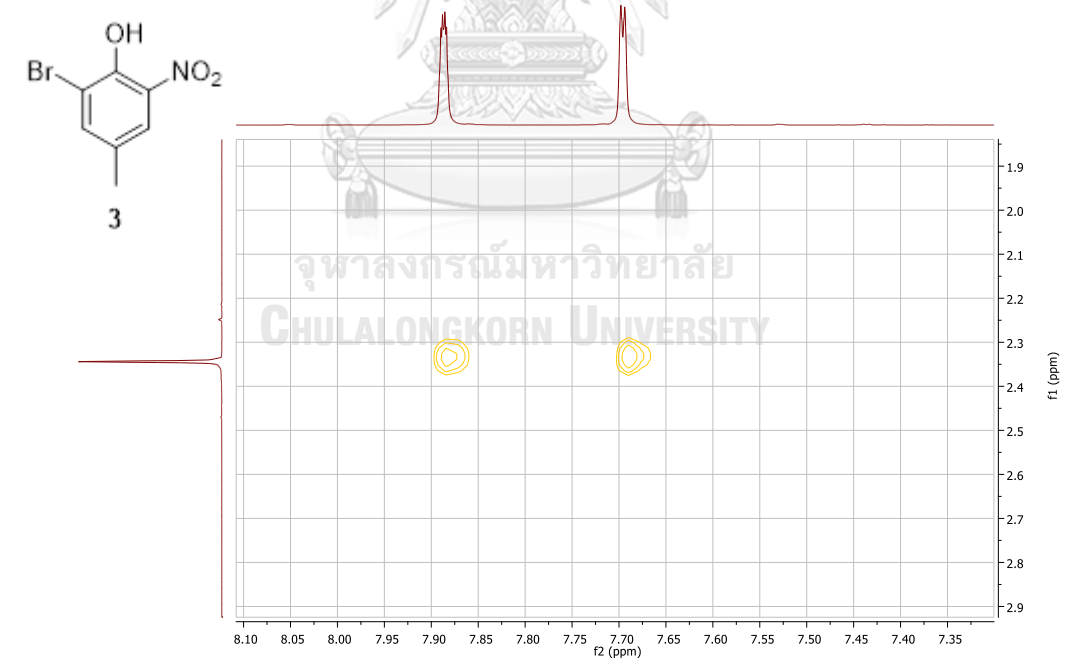

Figure 3.5 ^{1}H-^{1}H NOESY NMR spectrum ($CDCl_3$) of compound 3

3.1.10 Diazo coupling reaction

3.1.10.1 diazo coupling with 4-methylphenol

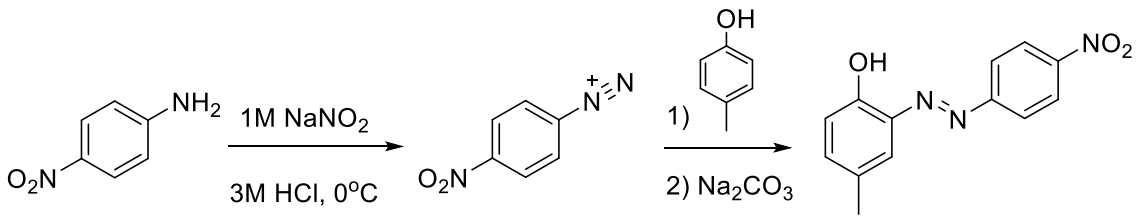

11

97%

Because nitrations on phenolic rings are difficult to control, diazo coupling reaction is the alternative method to introduce substituents onto the phenolic rings in a supposedly controllable fashion. As an example, the diazo coupled-product **11** was afforded from the coupling of 4-methylphenol in excellent yield up to (97%) as the mono-substitution at an *ortho*-position of the product [60]. The diazo group could later be reduced to an amino group by the various reducing agent [68-71]

3.1.10.2 diazo coupling with 2,6-dibromo-4-methylphenol

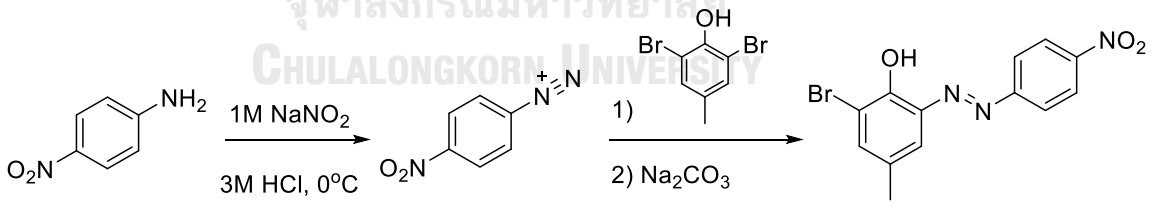

12

82%

2,6-Dibromo-4-methylphenol was coupled with a diazonium salt to examined if bromine could block the *ortho*-position and divert the diazo group to attach at *meta*-position. From ^{1}H NMR spectrum, apart from nitrophenyl signals, showed two singlet peaks at 7.79 ppm and 7.55 ppm **(Figure A.36, Appendix).** These peaks indicated that the diazo group was substituted at *ortho*-position, replacing one of the

bromine groups similar to nitration (section 3.1.5). Furthermore, the observed -OH peak was very downfield to 13.31 ppm, reflecting on the existence of strong intramolecular hydrogen bond between the hydroxy group and the adjacent N-atom of the diazo group at *ortho*-position.

3.1.11 2-amino-4-methylphenol

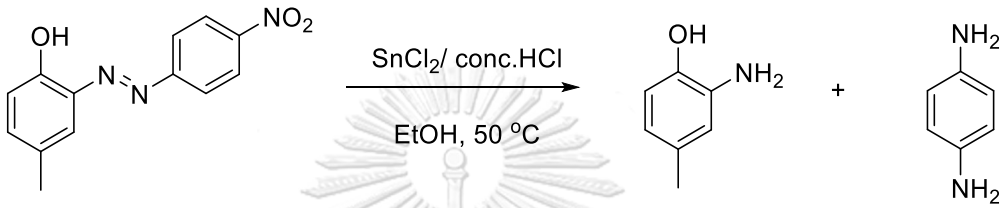

11 **13** **90%**

For further conjugation with other functional groups, the diazo group was reduced to an amino group with $SnCl_2$ in ethanol. 2-Amino-4-methylphenol was easily obtained in relatively short reaction time (5 min) and good yield. (90%)

3.1.12 Conjugation with adipoyl chloride using aniline as a model substrate

Adipoyl chloride (a C6 diacid chloride) was selected to represent the bifunctional bridge that link 2 bioactive moieties together as a conjugated drug, just like that of anticancer drug suberanilohydroxamic acid (SAHA). In condition A the diacid chloride reacted with aniline immediately and yield the diamide compound **14** as the only isolable product in high yield (91%), even with limited amount of aniline. **(Figure A.39, Appendix).** The acid chloride functional group seemed to be too active and difficult to control to limit its reaction halfway.

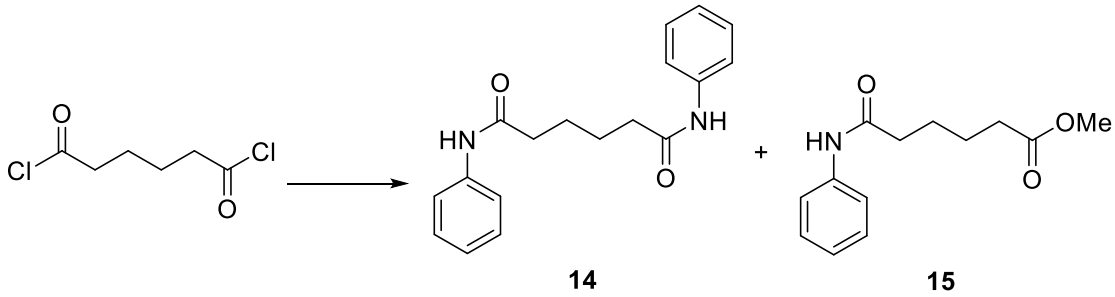

14 **15**

Condition A: 1) aniline 2) NEt_3/0 °C 3) $NH_2OH.HCl/NEt_3$ (**14:15** 91%:0%)

B: 1) NEt_3/ 0°C 2) aniline 3) MeOH/NEt_3 (**14:15** 56%:31%)

The process was changed to condition B by dissolving adipoyl chloride (1 eqv.) in DCM and NEt_3 at 0°C in an ice bath, then cold aniline (0.5 eqv.) in DCM was slowly added into the mixture. This process gave the derived product **15 (Figure A.40, Appendix)**. in moderate yield (31%), but still gave compound **14** as the major product (56%). The excess adipoyl chloride was quenched by methanol to give the corresponding diester compound (31 %) **(Figure A.43, Appendix)**.

The development in order to improve the reaction toward higher ratio of asymmetric substitution product was to switch the sequence of synthetic steps by preparing half acid chloride before reacting with aniline **(Figure 3.6)**

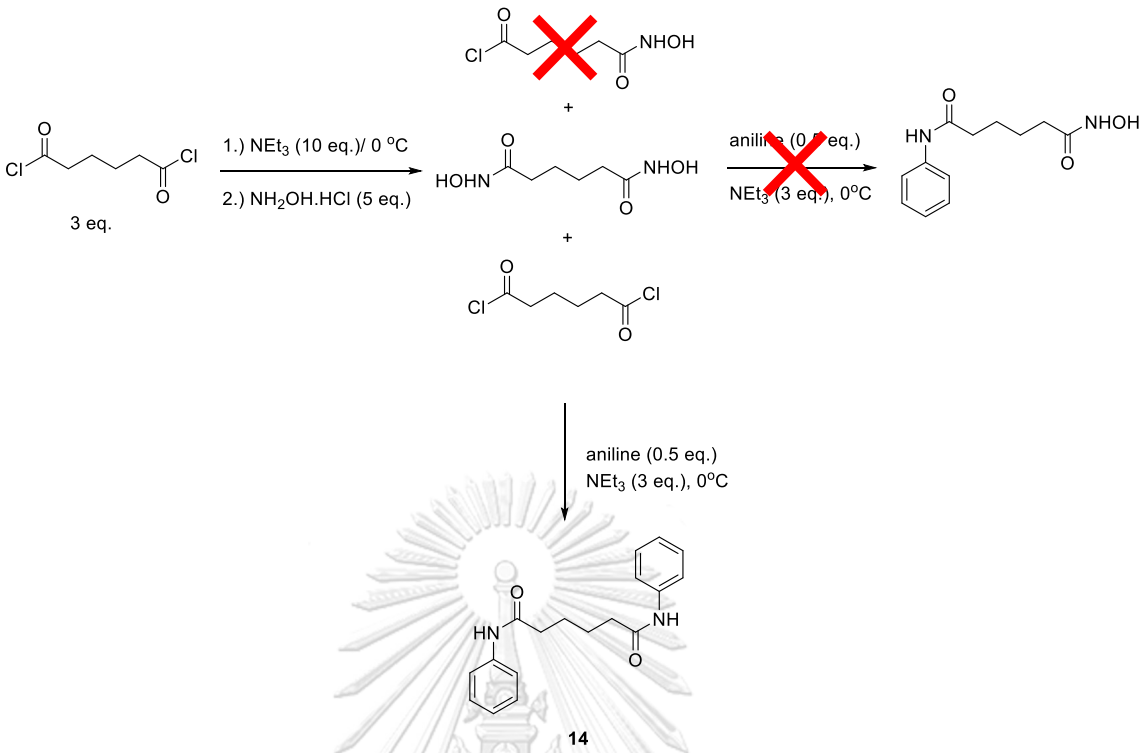

Figure 3.6 The new condition for conjugation with adipoyl chloride

From **Figure 3.6**, half acid chloride was prepared by mixing adipoyl chloride with slightly excess $NH_2OH.HCl$, expecting some of the half acid chloride would be lifted for further reaction with aniline. Unfortunately, NH_2OH was too reactive toward adipoyl chloride, and perhaps even more with the half acid chloride. It reacted twice to preferably give the dihydroxamic acid as the major product (63.5%) and leave the remaining adipoyl chloride to react with aniline to yield **14** as another main product.

The first nucleophile was then replaced with less reactive methanol to get the half ester/ acid chloride intermediates shown in **Figure 3.7.**

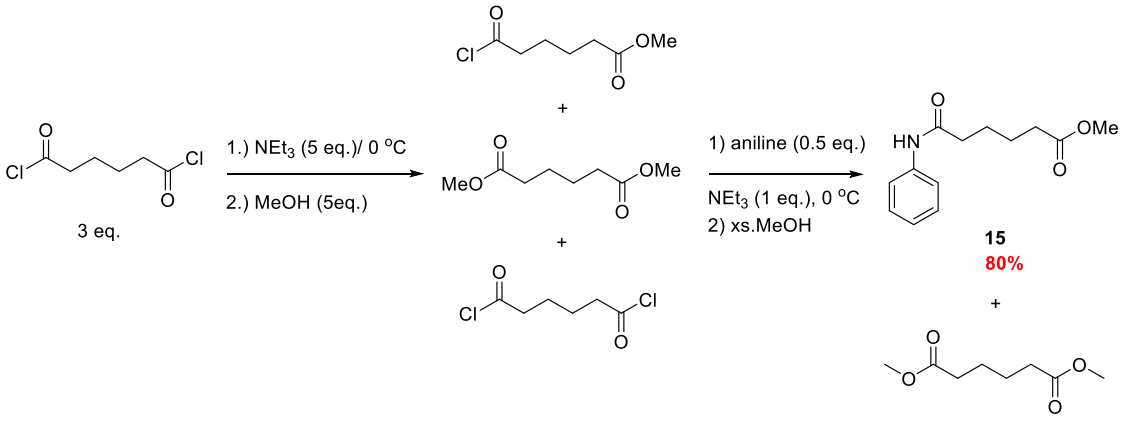

Figure 3.7 Another condition for conjugation with adipoyl chloride

According to **Figure 3.7**, half acid-ester was successfully produced. The expected, approximately 1 equivalence of unreacted acid chloride would further react with aniline (0.5 eq.). The combination of this scheme obtained the desired half amide-ester in high yield based on the starting aniline (80%) **(Figure A.40, Appendix)**. Methanol seemed to react randomly with available acid chloride. Therefore, the amount of half acid chloride intermediate was left large enough for incoming aniline as the second nucleophile to give the desired asymmetric product.

3.1.13 Conversion to hydroxamic acid

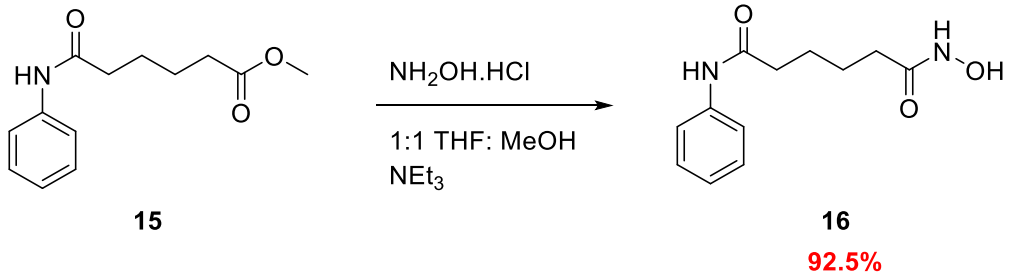

15 **16**
92.5%

The hydroxamic acid could be produced from the methyl ester using $NH_2OH{\cdot}HCl$ in mixed solvents of 1:1 THF:methanol in the presence of NEt_3. The

chemical test for the hydroxamic acid functional group was performed using 5% $FeCl_3$. [72]. The yellow solution of Fe (III) clearly turned to red-violet solution upon complexing with hydroxamic acid, supporting the structural characterizations by spectroscopic methods. **(Figure A.44-A.45, Appendix)**

3.1.14 Protection of diazo-4-methylphenol

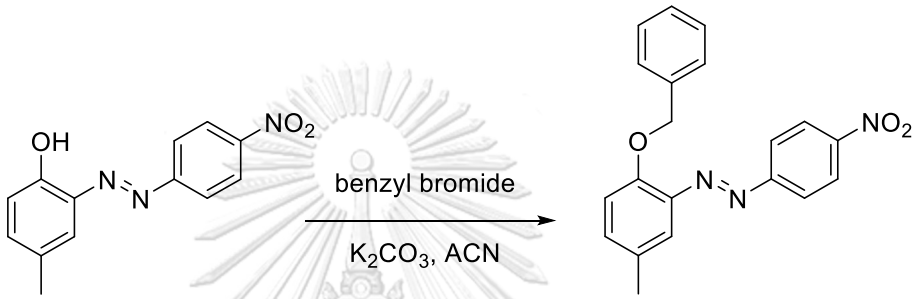

11 **17**

82.9%

All diazo groups were expected to be reduced to amino groups for conjugation with many types of compounds. Therefore, to avoid the unwanted side reactions, the hydroxy group was needed to be protected.

Table3.5 Various protections of diazo-4-methylphenol

Entry	Protecting reagent (5 eq.)	Base (5 eq.)	solvent	% yield of protected product
1[a]	TBS-Cl	imidazole	DMF	-
2	Benzyl bromide	K_2CO_3	ACN	83
3	Acetyl chloride	K_2CO_3	DCM	-

[a] *t*-BuO^-K^+ was added after 2 Days.

According to **Table 3.5**, only benzyl bromide (entry 2) was successful to protect the hydroxy group providing the benzyl protected product in good yield **(Figure A.46, Appendix).** The TBS or acetyl protections (entry 1 and 3) showed no progress on the reaction. As described in **Figure 3.8** the diazo group at the adjacent *ortho*-position might act as an internal nucleophile and initiate a facile intramolecular deprotection.

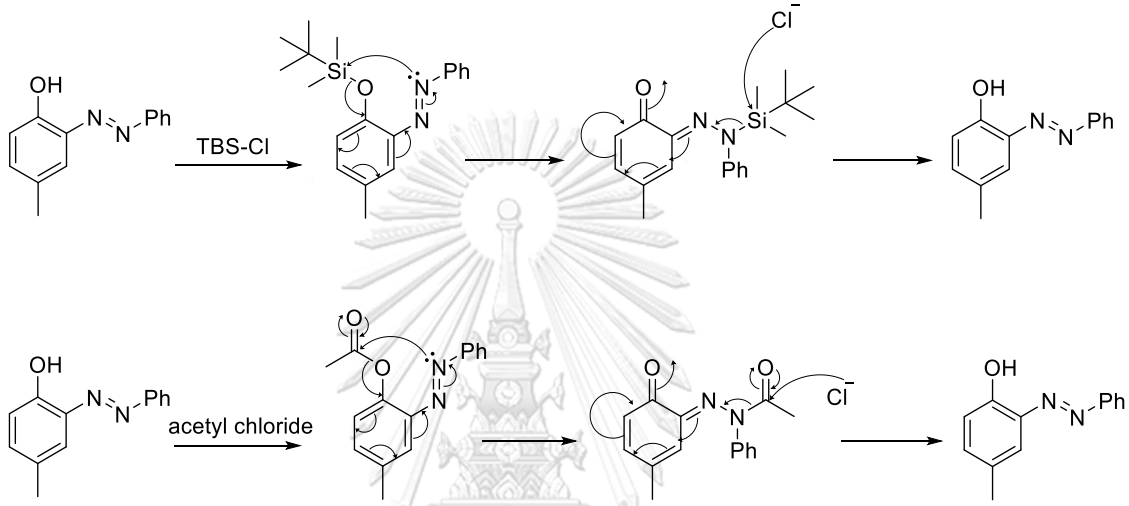

Figure 3.8 The proposed mechanism for intramolecular deprotection by diazo group

3.1.15 Diazo reduction from benzyl protected-4-methylphenol

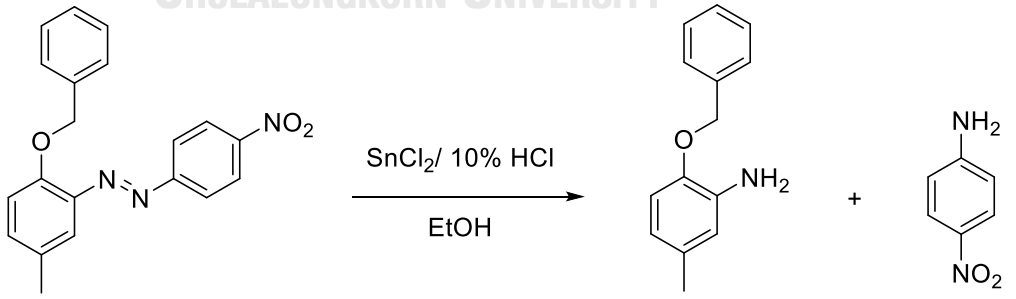

17 **18** **80%**

Following the same reduction procedure on diazo-4-methylphenol (section 3.1.11) and to decrease the risk from hazardous conc. acid, 10% HCl was used

instead. The outcome gave satisfied yield of the desired product with slightly longer reaction time. This milder also gave 4-nitroaniline as another product instead of *p*-phenylene diamine as in conc. HCl condition.

3.1.16 Conjugation of the aniline derivative with adipoyl chloride

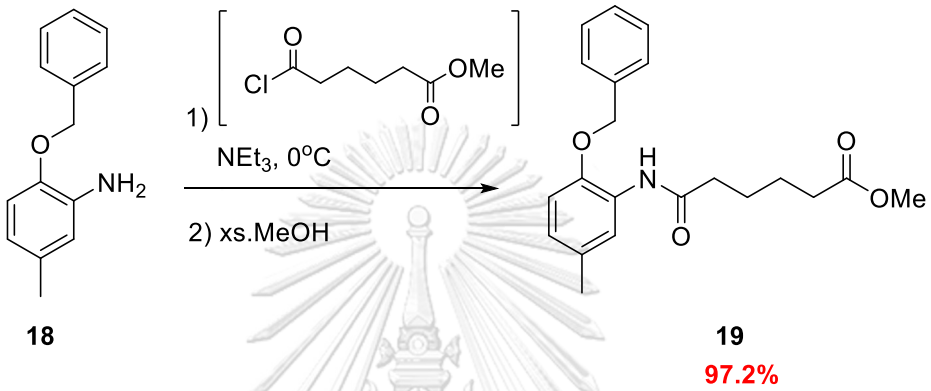

18 **19** **97.2%**

Following the protocol optimized in section 3.1.12 **(Figure 3.7),** the half amide-ester (compound **19**) was prepared in the same way in excellent yield (97%). ^{1}H NMR spectrum showed the new methoxy singlet peak at 3.66 ppm along with the benzyl protons at 5.08 ppm **(Figure A.50, Appendix).** In theory, this compound could be further converted to the corresponding half hydroxamic acid similar to compound **16** in section 3.1.13

3.1.17 Convert methyl ester to hydroxamic acid

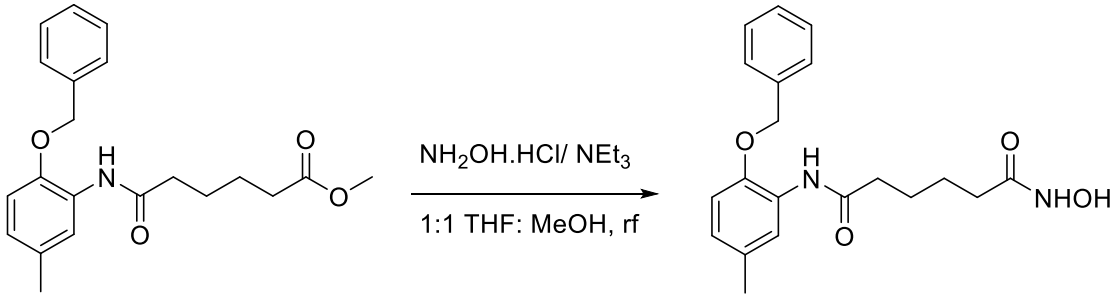

19 **20**
74.8%

From the section 3.1.13 the hydroxamic acid was produce from methyl ester using $NH_2OH{\cdot}HCl$, the reaction was completed after reflux for 3 Days. The chemical test was performed with 5% $FeCl_3$.

3.2 Functionalization at ring A of estradiol

3.2.1 diazo coupling on estradiol

Based on the successful model reactions on *p*-cresol, we continued to perform similar diazo coupling reactions on β-estradiol. In order to optimize the efficiency of the reaction and separation of the two possible regioisomers of the coupling products, the diazonium salts were generated from three different aniline derivatives (aniline, *p*-toluidine and 4-nitroaniline).

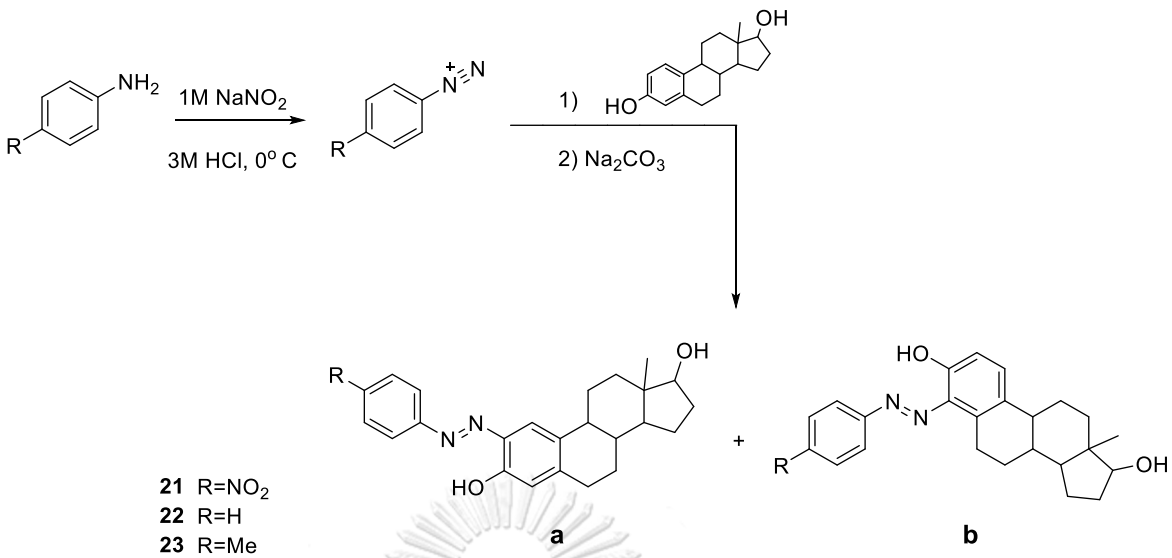

Diazonium salts from different aniline derivatives were prepared with the previously described method (section 3.1.10) and dropped into the 1M NaOH solution of estradiol. It was found that different kinds of aniline derivatives didn't affect the reaction efficiency. Although unlike the reaction on 4-methylphenol, the diazo coupling reactions on estradiol gave two possible regioisomers (**a** and **b**). It was found from TLC that mixture derived from diazonium salt of 4-nitroaniline was the easiest pair to be separated. Two pure isomers isolated from this pair were characterized to identify the products to be the slightly higher amount of 2-substituted **(21a)** and 4-substituted estradiol **(21b)**. ^{1}H NMR could clearly identify the isomers, with their unique aromatic peaks. Apart from the double of doublet of nitrophenyl signals, the 2-substituted estradiol **(21a)** gave 2 singlet peaks at 7.86 and 6.77 ppm **(Figure A.53, Appendix)**, while the 4-substituted estradiol **(21b)** showed 2 doublet peaks at 7.43 and 6.85 ppm. **(Figure A.54, Appendix).**

3.2.2 Protection on diazo coupled estradiol

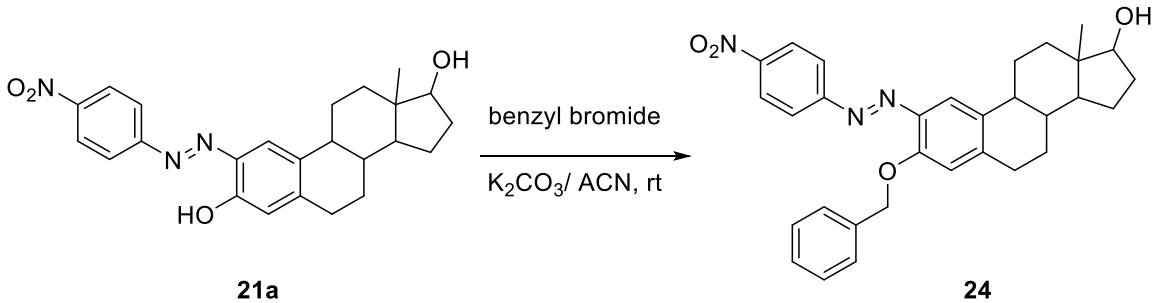

21a **24**

74.1%

Using the same protocol from protection of diazo-4-methylphenol, the benzyl protecting group was attempted on the 2-substituted estradiol **(21a)**. The phenolic hydroxy group was successfully protected as the model compound, however, the other hydroxy group at C-17 of estradiol surprisingly remained unprotected. The reason for its inactivity toward substitution could be due to the highly steric crowd from nearby tertiary alkyl group and surrounded rings that hindered the substitution. The other reason is from their acidity, the phenolic hydroxy group has lower pK_a (9.29±0.10) compare with cyclopentanol (15.33±0.40). From ^{1}H NMR spectrum of compound **24**, the integration of the benzyl protons (5.30 ppm, 2H) was only twice of the peak of the proton on C-17 of estradiol (3.75 ppm, 1H) **(Figure A.57, Appendix).**

3.2.3 Reduction of diazo estradiol

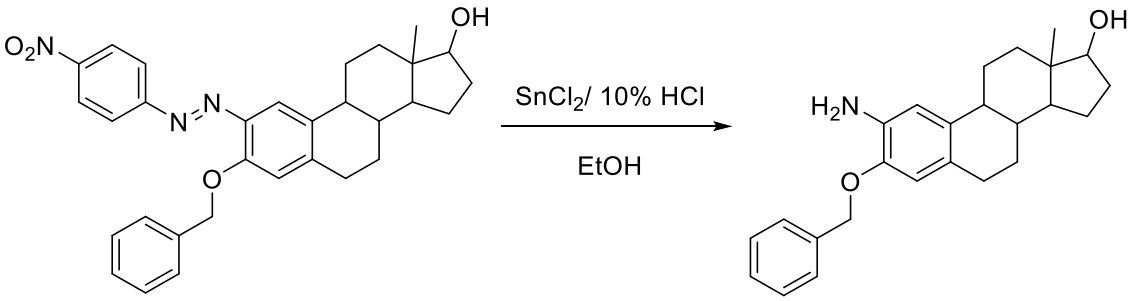

24 **25**

67.8%

The 2-amino substituted protected estradiol **25** was synthesized via the reduction protocol as that of the model (section 3.1.15). The amino product was obtained in good yield (68%). The two singlet aromatic peaks in ^{1}H NMR spectrum were shifted upfield to 6.71 and 6.59 ppm **(Figure A.59, Appendix).**

3.2.4 Conjugation of amino estradiol with adipoyl chloride

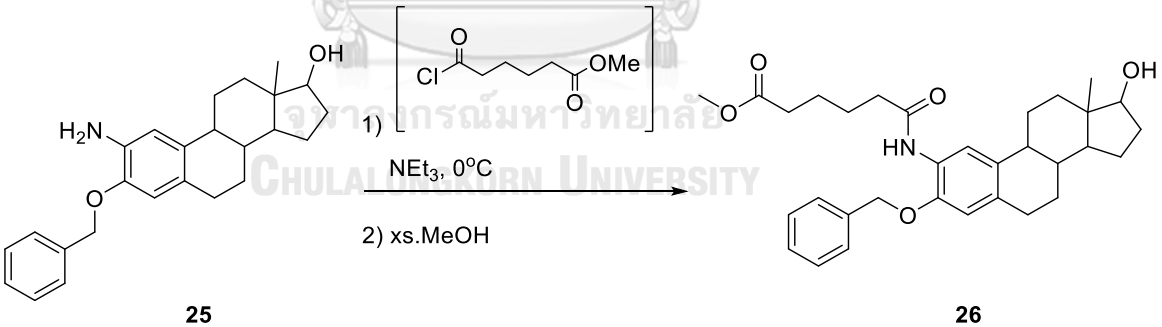

25 **26**

31%

Following the protocol in section 3.1.12 **(Figure 3.7),** the prepared half acid chloride-ester was generated in situ and reacted with amino estradiol **25** to obtain the product **26** in moderate yield (31%). Part of the ^{1}H NMR spectrum was compared with that of the model compound **19.** The pattern of the proton signals of the added dicarbonyl moieties was consistent with the model **(Figure A.61, Appendix)**.

The hydroxy group at C-17 still remained unreacted and didn't interfere with the reaction.

3.2.5 Conversion to hydroxamic acid

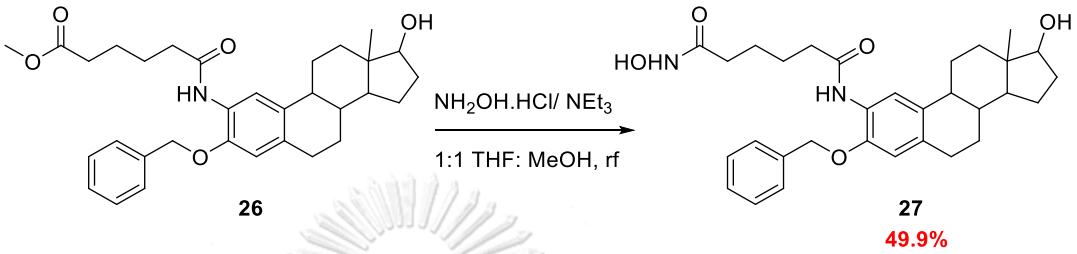

According to the protocol in section 3.1.17, the methyl ester group of **22** was converted to hydroxamic acid by $NH_2OH.HCl$ and refluxed with 1:1 THF: MeOH. Unfortunately, the reaction was rarely moved forward in a long period of time. Therefore, the reaction was worked up in halfway and purified to remove the left-over substrate. The new product was characterized by ^1H NMR and chemical test to confirmed structural and functional group. **(Figure A.63, Appendix).**

CHAPTOR IV

CONCLUSION

The functionalizations at the 1, 2 or 4-positions of estradiol were the main targets for further conjugations with anti-tumor moieties to provide target-specific antitumor drugs. The substitution reactions had been examined on 4-cresol as the model. To control the substitutions on the desired positions, two types of reactions were performed: nitration and diazo coupling reaction. The normal nitration conditions led to uncontrollable substitution mostly at *ortho*-positions even with phenolic-O-protection or *ortho*-aromatic bromo substitutions. The *meta*-substituted product was finally synthesized from 4-cresol via 5 steps **(Figure 4.1)**, although with overall yield of only 6%. Further research upon improvement of this new methodology is needed.

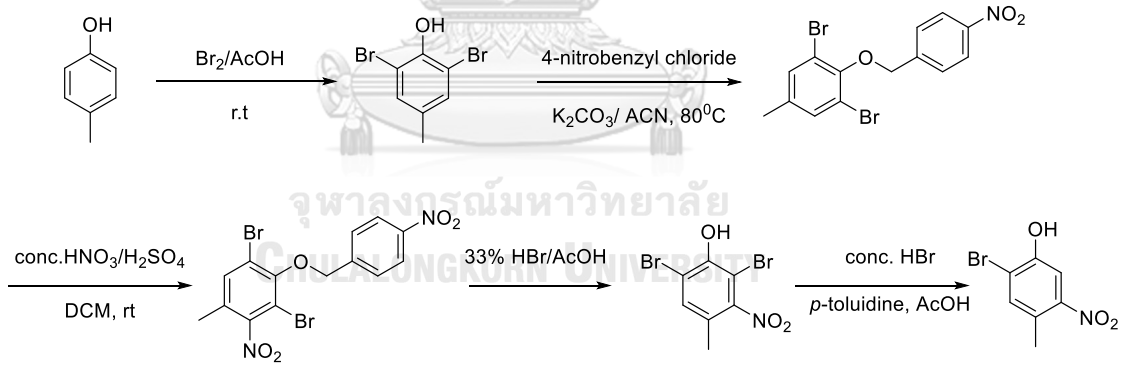

Figure 0.1 The overall reaction of meta-substitution

The diazo coupling reaction was found to be the preferred method for introducing substituents on *ortho*-positions of phenol derivatives. 2-amino-4-methylphenol was synthesized from diazo coupling, followed by reduction to yield the product in 87% from 2 steps. This model was then used as the substrate to

explore the optimized conditions to conjugate with adipoyl chloride to provide a link for further attachment of other bioactive moieties.

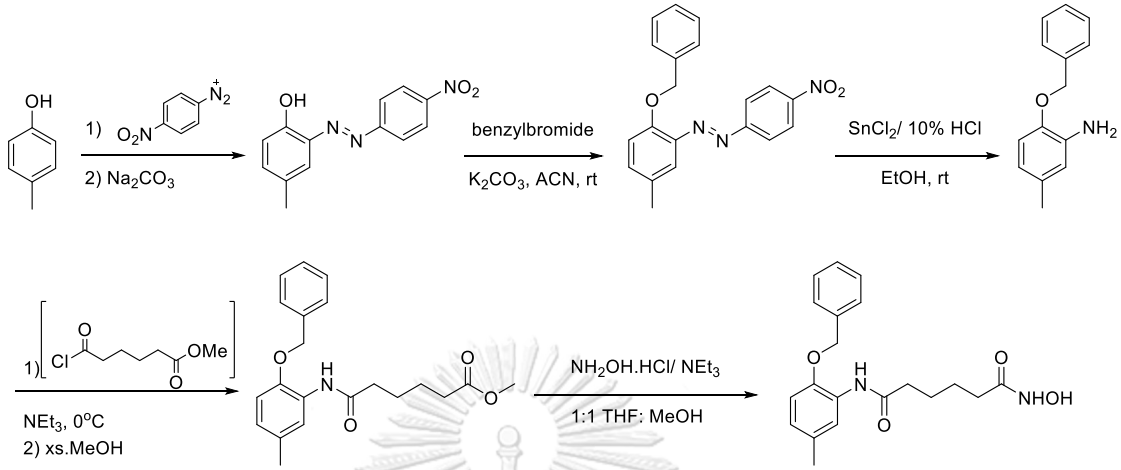

Figure 4.2 The conjugation of aniline derivative with adipoyl hydroxamic acid

The reactions on the model compound led to successful results on functionalizations of β-estradiol. The 2 and 4-positions of estradiol were easily substituted through diazo coupling reactions. The substituted estradiol could be similarly reduced and conjugated with adipoyl linker, ready for further attachment with other active compounds with anti-tumor moiety.

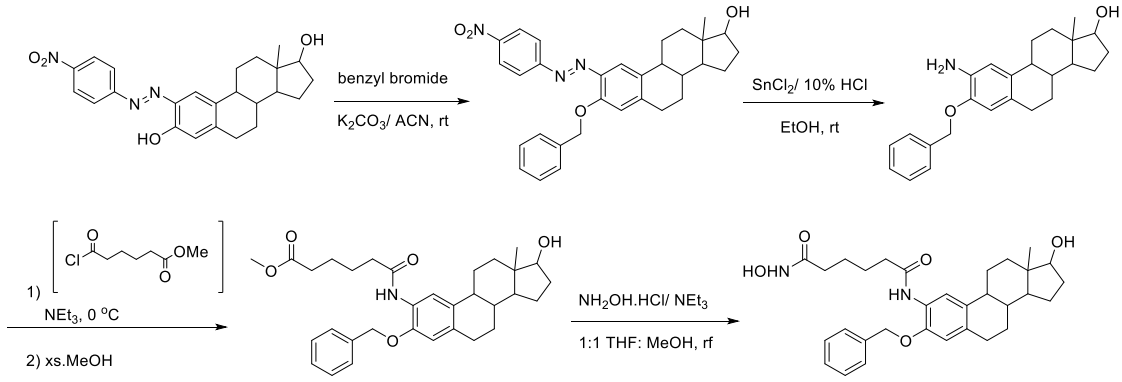

Figure 4.3 Functionalization on estradiol

REFERENCES

[1] Morphy, R. and Rankovic, Z., Designed multiple ligands. An emerging drug discovery paradigm. Journal of medicinal chemistry 48(21) (2005): 6523-6543.

[2] Fray, M. J.; Bish, G.; Brown, A. D.; Fish, P. V.; Stobie, A.; Wakenhut, F. and Whitlock, G. A., *N*-(1, 2-Diphenylethyl) piperazines: A new class of dual serotonin/noradrenaline reuptake inhibitor. Bioorganic & medicinal chemistry letters 16(16) (2006): 4345-4348.

[3] Neumeyer, J. L.; Peng, X.; Knapp, B. I.; Bidlack, J. M.; Lazarus, L. H.; Salvadori, S.; Trapella, C. and Balboni, G., New opioid designed multiple ligand from Dmt-Tic and morphinan pharmacophores. Journal of medicinal chemistry 49(18) (2006): 5640-5643.

[4] Aiyer, H. S.; Warri, A. M.; Woode, D. R.; Hilakivi-Clarke, L. and Clarke, R., Influence of berry polyphenols on receptor signaling and cell-death pathways: implications for breast cancer prevention. Journal of agricultural and food chemistry 60(23) (2012): 5693-5708.

[5] DeSantis, C. E.; Ma, J.; Goding Sauer, A.; Newman, L. A. and Jemal, A., Breast cancer statistics, 2017, racial disparity in mortality by state. CA-A Cancer Journal for Clinicians 67(6) (2017): 439-448.

[6] Xu, Y.; Wang, W.; Wang, M.; Liu, X.; Lee, M.-H.; Wang, M.; Zhang, H.; Li, H. and Chen, W., High Salt Intake Attenuates Breast Cancer Metastasis to Lung. Journal of agricultural and food chemistry 66(13) (2018): 3386-3392.

[7] Bateman, N. W.; Sun, M.; Bhargava, R.; Hood, B. L.; Darfler, M. M.; Kovatich, A. J.; Hooke, J. A.; Krizman, D. B. and Conrads, T. P., Differential proteomic analysis of late-stage and recurrent breast cancer from formalin-fixed paraffin-embedded tissues. Journal of proteome research 10(3) (2010): 1323-1332.

[8] Zahid, M.; Mondal, B.; LeVan, T. D. and Rogan, E. G., Estrogen Metabolism in African-American Women with and without Breast Cancer: A Pilot Study. Chemical research in toxicology 32(1) (2019): 190-194.

[9] Kaaks, R.; Berrino, F.; Key, T.; Rinaldi, S.; Dossus, L.; Biessy, C.; Secreto, G.;

Amiano, P.; Bingham, S.; Boeing, H.; Bueno de Mesquita, H. B.; Chang-Claude, J.; Clavel-Chapelon, F.; Fournier, A.; van Gils, C. H.; Gonzalez, C. A.; Gurrea, A. B.; Critselis, E.; Khaw, K. T.; Krogh, V.; Lahmann, P. H.; Nagel, G.; Olsen, A.; Onland-Moret, N. C.; Overvad, K.; Palli, D.; Panico, S.; Peeters, P.; Quiros, J. R.; Roddam, A.; Thiebaut, A.; Tjonneland, A.; Chirlaque, M. D.; Trichopoulou, A.; Trichopoulos, D.; Tumino, R.; Vineis, P.; Norat, T.; Ferrari, P.; Slimani, N. and Riboli, E., Serum sex steroids in premenopausal women and breast cancer risk within the European Prospective Investigation into Cancer and Nutrition (EPIC). Journal of the National Cancer Institute 97(10) (2005): 755-765.

[10] Walker, K.; Bratton, D. J. and Frost, C., Premenopausal endogenous oestrogen levels and breast cancer risk: a meta-analysis. British Journal of Cancer 105(9) (2011): 1451-1457.

[11] Swamy, N.; Purohit, A.; Fernandez-Gacio, A.; Jones, G. B. and Ray, R., Nuclear estrogen receptor targeted photodynamic therapy: Selective uptake and killing of MCF-7 breast cancer cells by a C17α-alkynylestradiol-porphyrin conjugate. Journal of cellular biochemistry 99(3) (2006): 966-977.

[12] Eisenbrand, G.; Berger, M.; Fischer, J.; Schneider, M.; Tang, W. and Zeller, W., Development of more selective anti-cancer nitrosoureas. Anti-cancer drug design 2(4) (1988): 351-359.

[13] Eisenbrand, G.; Fischer, J.; Mühlbauer, K.; Schied, G.; Schreiber, J.; Tang, W. and Zelezny, O., Synthesis and Characterization of Steroid-linked N-(2-Chloroethyl) nitrosoureas. Archiv der Pharmazie 322(12) (1989): 863-872.

[14] Ali, H.; Ahmed, N.; Tessier, G. and van Lier, J. E., Synthesis and biological activities of nucleoside–estradiol conjugates. Bioorganic & medicinal chemistry letters 16(2) (2006): 317-319.

[15] Liu, C.; Strobl, J. S.; Bane, S.; Schilling, J. K.; McCracken, M.; Chatterjee, S. K.; Rahim-Bata, R. and Kingston, D. G., Design, synthesis, and bioactivities of steroid-linked taxol analogues as potential targeted drugs for prostate and breast cancer. Journal of natural products 67(2) (2004): 152-159.

[16] Hasan, M.; Leak, R. K.; Stratford, R. E.; Zlotos, D. P. and Witt-Enderby, P. A.,

Drug conjugates—an emerging approach to treat breast cancer. Pharmacology research & perspectives 6(4) (2018): 417-434.

[17] Henderson, B. E. and Feigelson, H. S., Hormonal carcinogenesis. Carcinogenesis 21(3) (2000): 427-433.

[18] Yue, W.; Wang, J.-P.; Li, Y.; Bocchinfuso, W. P.; Korach, K. S.; Devanesan, P. D.; Rogan, E.; Cavalieri, E. and Santen, R. J., Tamoxifen versus aromatase inhibitors for breast cancer prevention. Clinical cancer research 11(2) (2005): 925-930.

[19] Deroo, B. J. and Korach, K. S., Estrogen receptors and human disease. The Journal of clinical investigation 116(3) (2006): 561-570.

[20] Tanenbaum, D. M.; Wang, Y.; Williams, S. P. and Sigler, P. B., Crystallographic comparison of the estrogen and progesterone receptor's ligand binding domains. Proceedings of the National Academy of Sciences 95(11) (1998): 5998-6003.

[21] Möcklinghoff, S.; Rose, R.; Carraz, M.; Visser, A.; Ottmann, C. and Brunsveld, L., Synthesis and crystal structure of a phosphorylated estrogen receptor ligand binding domain. Chembiochem 11(16) (2010): 2251-2254.

[22] Gryder, B. E.; Sodji, Q. H. and Oyelere, A. K., Targeted cancer therapy: giving histone deacetylase inhibitors all they need to succeed. Future Medicinal Chemistry 4(4) (2012): 505-524.

[23] Lehrmann, H.; Pritchard, L. L. and Harel-Bellan, A., Histone acetyltransferases and deacetylases in the control of cell proliferation and differentiation. Advances in Cancer Research (2002): 41-65.

[24] Verdin, E.; Dequiedt, F. and Kasler, H. G., Class II histone deacetylases: versatile regulators. TRENDS in Genetics 19(5) (2003): 286-293.

[25] Bieliauskas, A. V. and Pflum, M. K. H., Isoform-selective histone deacetylase inhibitors. Chemical Society Reviews 37(7) (2008): 1402-1413.

[26] Butler, L. M.; Agus, D. B.; Scher, H. I.; Higgins, B.; Rose, A.; Cordon-Cardo, C.; Thaler, H. T.; Rifkind, R. A.; Marks, P. A. and Richon, V. M., Suberoylanilide hydroxamic acid, an inhibitor of histone deacetylase, suppresses the growth of prostate cancer cells in vitro and in vivo. Cancer research 60(18) (2000): 5165-5170.

[27] Finnin, M. S.; Donigian, J. R.; Cohen, A.; Richon, V. M.; Rifkind, R. A.; Marks, P. A.; Breslow, R. and Pavletich, N. P., Structures of a histone deacetylase homologue bound to the TSA and SAHA inhibitors. Nature 401(6749) (1999): 188-193.

[28] Gediya, L. K.; Chopra, P.; Purushottamachar, P.; Maheshwari, N. and Njar, V. C., A new simple and high-yield synthesis of suberoylanilide hydroxamic acid and its inhibitory effect alone or in combination with retinoids on proliferation of human prostate cancer cells. Journal of medicinal chemistry 48(15) (2005): 5047-5051.

[29] Miller, T. A.; Witter, D. J. and Belvedere, S., Histone deacetylase inhibitors. Journal of medicinal chemistry 46(24) (2003): 5097-5116.

[30] Li, X.; Zhou, Q.; Hanus, J.; Anderson, C.; Zhang, H.; Dellinger, M.; Brekken, R. and Wang, S., Inhibition of multiple pathogenic pathways by histone deacetylase inhibitor SAHA in a corneal alkali-burn injury model. Molecular pharmaceutics 10(1) (2012): 307-318.

[31] Devraj, R.; Barrett, J. F.; Fernandez, J. A.; Katzenellenbogen, J. A. and Cushman, M., Design, synthesis, and biological evaluation of ellipticine–estradiol conjugates. Journal of medicinal chemistry 39(17) (1996): 3367-3374.

[32] Labaree, D. C.; Reynolds, T. Y. and Hochberg, R. B., Estradiol-16α-carboxylic acid esters as locally active estrogens. Journal of medicinal chemistry 44(11) (2001): 1802-1814.

[33] Fevig, T. L.; Mao, M. K. and Katzenellenbogen, J. A., Estrogen receptor binding tolerance of 16α-substituted estradiol derivatives. Steroids 51(5-6) (1988): 471-497.

[34] Hochberg, R. B. and Rosner, W., Interaction of 16 alpha-[125I] iodo-estradiol with estrogen receptor and other steroid-binding proteins. Proceedings of the National Academy of Sciences of the United States of America 77(1) (1980): 328-332.

[35] Labaree, D. C.; Zhang, J.-x.; Harris, H. A.; O'Connor, C.; Reynolds, T. Y. and Hochberg, R. B., Synthesis and evaluation of B-, C-, and D-ring-substituted

estradiol carboxylic acid esters as locally active estrogens. Journal of medicinal chemistry 46(10) (2003): 1886-1904.

[36] Nique, F.; Van de Velde, P.; Bremaud, J.; Hardy, M.; Philibert, D. and Teutsch, G., 11β-Amidoalkoxyphenyl estradiols, a new series of pure antiestrogens. The Journal of steroid biochemistry and molecular biology 50(1-2) (1994): 21-29.

[37] Claussner, A.; Nedelec, L.; Nique, F.; Philibert, D.; Teutsch, G. and Vandevelde, P., 11β-Amidoalkyl estradiols, a new series of pure antiestrogens. The Journal of steroid biochemistry and molecular biology 41(1992): 609-614.

[38] Dao, K.-L.; Sawant, R. R.; Hendricks, J. A.; Ronga, V.; Torchilin, V. P. and Hanson, R. N., Design, synthesis, and initial biological evaluation of a steroidal anti-estrogen–doxorubicin bioconjugate for targeting estrogen receptor-positive breast cancer cells. Bioconjugate chemistry 23(4) (2012): 785-795.

[39] Burke, P. J.; Kalet, B. T. and Koch, T. H., Antiestrogen binding site and estrogen receptor mediate uptake and distribution of 4-hydroxytamoxifen-targeted doxorubicin– formaldehyde conjugate in breast cancer cells. Journal of medicinal chemistry 47(26) (2004): 6509-6518.

[40] Burke, P. J. and Koch, T. H., Design, synthesis, and biological evaluation of doxorubicin– formaldehyde conjugates targeted to breast cancer cells. Journal of medicinal chemistry 47(5) (2004): 1193-1206.

[41] Dreaden, E. C.; Mwakwari, S. C.; Sodji, Q. H.; Oyelere, A. K. and El-Sayed, M. A., Tamoxifen– poly (ethylene glycol)– thiol gold nanoparticle conjugates: enhanced potency and selective delivery for breast cancer treatment. Bioconjugate chemistry 20(12) (2009): 2247-2253.

[42] Jordan, V. C., New insights into the metabolism of tamoxifen and its role in the treatment and prevention of breast cancer. Steroids 72(13) (2007): 829-842.

[43] Breslow, R.; Marks, P.; Rifkind, R. and Jursic, B. Novel potent inducers of terminal differentiation and methods thereof. 1993.

[44] Stowell, J. C.; Huot, R. I. and Van Voast, L., The synthesis of N-hydroxy-N'-phenyloctanediamide and its inhibitory effect on proliferation of AXC rat prostate cancer cells. Journal of medicinal chemistry 38(8) (1995): 1411-1413.

[45] Mai, A.; Esposito, M.; Sbardella, G. and Massa, S., A NEW FACILE AND

EXPEDITIOUS SYNTHESIS OF N-HYDROXY-N′-PHENYLOCTANEDIAMJDE, A POTENT INDUCER OF TERMINAL CYTODIFFERECNTIATION. Organic Preparations and Procedures International 33(4) (2001): 391-394.

[46] Gryder, B. E.; Rood, M. K.; Johnson, K. A.; Patil, V.; Raftery, E. D.; Yao, L.-P. D.; Rice, M.; Azizi, B.; Doyle, D. F. and Oyelere, A. K., Histone deacetylase inhibitors equipped with estrogen receptor modulation activity. Journal of medicinal chemistry 56(14) (2013): 5782-5796.

[47] Ring, A. and Dowsett, M., Mechanisms of tamoxifen resistance. Endocrine-related cancer 11(4) (2004): 643-658.

[48] Speirs, V.; Malone, C.; Walton, D. S.; Kerin, M. J. and Atkin, S. L., Increased expression of estrogen receptor β mRNA in tamoxifen-resistant breast cancer patients. Cancer research 59(21) (1999): 5421-5424.

[49] Yin, W.-P. and Shi, M., Nitration of phenolic compounds by metal-modified montmorillonite KSF. Tetrahedron 61(46) (2005): 10861-10867.

[50] Foroughifar, N. and FATHINEZHAD, J. H., Nitration of phenolic compounds by antimony nitrate. (2010):

[51] Matsubara, H.; Maegawa, T.; Kita, Y.; Yokoji, T. and Nomoto, A., Synthesis and properties of fluorous benzoquinones and their application in deprotection of silyl ethers. Organic & biomolecular chemistry 12(29) (2014): 5442-5447.

[52] Degner, A.; Carlsson, H.; Karlsson, I.; Eriksson, J.; Pujari, S. S.; Tretyakova, N. Y. and Tornqvist, M., Discovery of novel N-(4-Hydroxybenzyl) valine hemoglobin adducts in human blood. Chemical research in toxicology 31(12) (2018): 1305-1314.

[53] Adimurthy, S.; Ramachandraiah, G.; Bedekar, A. V.; Ghosh, S.; Ranu, B. C. and Ghosh, P. K., Eco-friendly and versatile brominating reagent prepared from a liquid bromine precursor. Green Chemistry 8(10) (2006): 916-922.

[54] Ghorpade, P. V.; Pethsangave, D. A.; Some, S. and Shankarling, G. S., Graphene oxide promoted oxidative bromination of anilines and phenols in water. The Journal of organic chemistry 83(14) (2018): 7388-7397.

[55] Ochs, C.; Hahn, F. E. and Fröhlich, R., Coordination Chemistry of Unsymmetrical Tripodal Ligands with an NNO2 Donor Set. European Journal of Inorganic

Chemistry 2001(9) (2001): 2427-2436.

[56] Raiford, L. C., MOLECULAR REARRANGEMENT IN THE ACYLATION OF CERTAIN AMINOPHENOLS. Journal of the American Chemical Society 41(12) (1919): 2068-2080.

[57] Takaaki, K.; Hiroyuki, S.; Tadashi, Y.; Tsuyoshi, O. and Shoji, K., Halogenation Using Quaternary Ammonium Polyhalides. XX. Bromination of Phenols with Polymer-Bound Benzyltrimethylammonium Tribromide. Bulletin of the Chemical Society of Japan 62(10) (1989): 3373-3375.

[58] Akai, S.; Ikawa, T.; Takayanagi, S.-i.; Morikawa, Y.; Mohri, S.; Tsubakiyama, M.; Egi, M.; Wada, Y. and Kita, Y., Synthesis of Biaryl Compounds through Three-Component Assembly: Ambidentate Effect of the tert-Butyldimethylsilyl Group for Regioselective Diels–Alder and Hiyama Coupling Reactions. Angewandte Chemie International Edition 47(40) (2008): 7673-7676.

[59] Thadani, A. N.; Huang, Y. and Rawal, V. H., Expedient, High-Yielding Synthesis of Silyl-Substituted Salen Ligands. Organic Letters 9(20) (2007): 3873-3876.

[60] Deng, Y.; Tang, B.; Zhao, H.; Xu, J.; Xiao, J.; Zhang, X.; Xu, H. and Zhang, S., Dyeing method and properties of polymaleic acid dyes on cotton. Coloration Technology 129(2) (2013): 144-149.

[61] Tanaseichuk, B. S.; Tomilin, O. B.; Pryanichnikova, M. K.; Boyarkina, O. V. and Burtasov, A. A., Relative stability of 1-(4-R-2,6-dinitrophenyl)-2,2-diphenylhydrazides. Russian Journal of Organic Chemistry 53(5) (2017): 679-685.

[62] Choi, H. Y. and Chi, D. Y., A facile debromination reaction: Can bromide now be used as a protective group in aromatic systems? Journal of the American Chemical Society 123(37) (2001): 9202-9203.

[63] Jirandehi, H. F. and Mirzaeian, M., Nitration of Phenolic Compounds by Antimony Nitrate. Synthesis and Reactivity in Inorganic, Metal-Organic, and Nano-Metal Chemistry 41(3) (2011): 284-286.

[64] Kumar, G.; Kotian, S.; U Kudva N, N.; Banerjee, D.-K.; Vicas, C. S.; Rai, K.; Vittal, R. and Byrappa, K., Synthesis of Novel Isoxazoline Derivatives and Evaluation of their Antimicrobial Activity. Journal of Chemical, Biological and Physical Sciences 6(2015): 128-137.

[65] Miller, B.; McLaughlin, M. P. and Marhevka, V. C., Meta substitution in electrophilic benzylations of 2,6-dimethylphenol and alkyl 2,6-dimethylphenyl ethers: product distributions and mechanism. The Journal of organic chemistry 47(4) (1982): 710-719.

[66] Barlow, H. L.; Teskey, C. J. and Greaney, M. F., Ruthenium-Catalyzed meta-Carboxylation. Organic Letters 19(24) (2017): 6662-6665.

[67] Hofmann, N. and Ackermann, L., meta-Selective C–H Bond Alkylation with Secondary Alkyl Halides. Journal of the American Chemical Society 135(15) (2013): 5877-5884.

[68] Abiraj, K.; Srinivasa, G. R. and Gowda, D. C., Palladium-catalyzed simple and efficient hydrogenative cleavage of azo compounds using recyclable polymer-supported formate. Canadian Journal of Chemistry 83(5) (2005): 517-520.

[69] Srinivasa, G.; Abiraj, K. and Gowda, D. C., Polymer-supported formate and magnesium: an efficient transfer hydrogenation system for the facile reduction of azo compounds. Journal of Chemical Research 2005(2) (2005): 123-125.

[70] Gejjalagere, S.; Abiraj, K. and Gowda, C., Clean and Efficient Hydrogenative Cleavage of Azo Compounds Using Polymer-Supported Formate and Zinc. Synthetic Communications 35(2005): 1161-1165.

[71] Gowda, S.; Abiraj, K. and Gowda, D. C., Reductive cleavage of azo compounds catalyzed by commercial zinc dust using ammonium formate or formic acid. Tetrahedron letters 43(7) (2002): 1329-1331.

[72] Miller, M. J., Syntheses and therapeutic potential of hydroxamic acid based siderophores and analogs. Chemical Reviews 89(7) (1989): 1563-1579.

APPENDIX

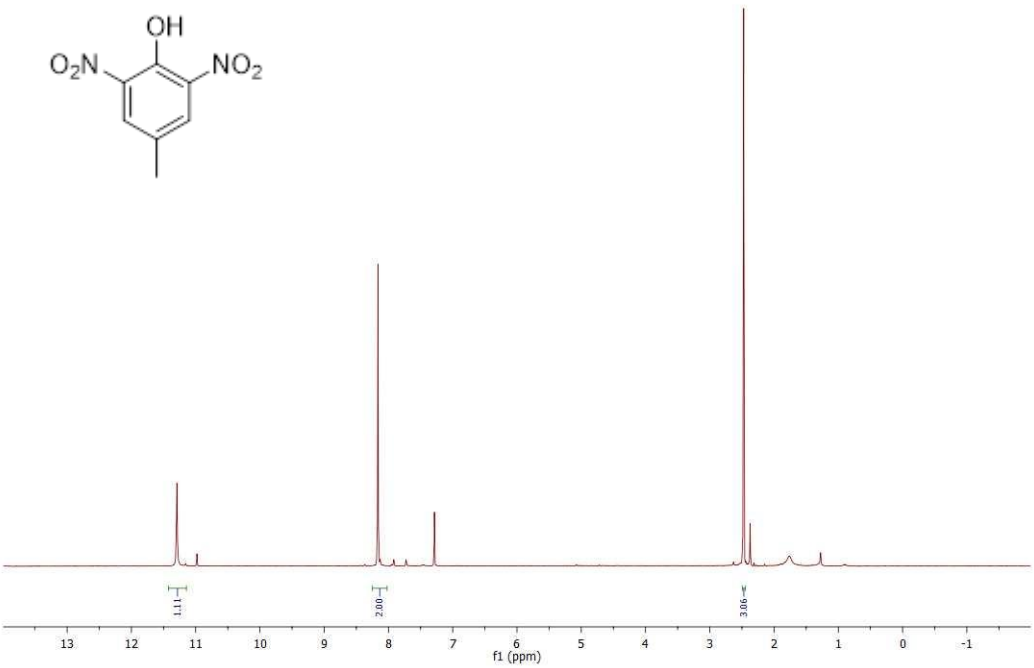

Figure A.1 ^{1}H NMR ($CDCl_3$) spectrum of **compound 1**

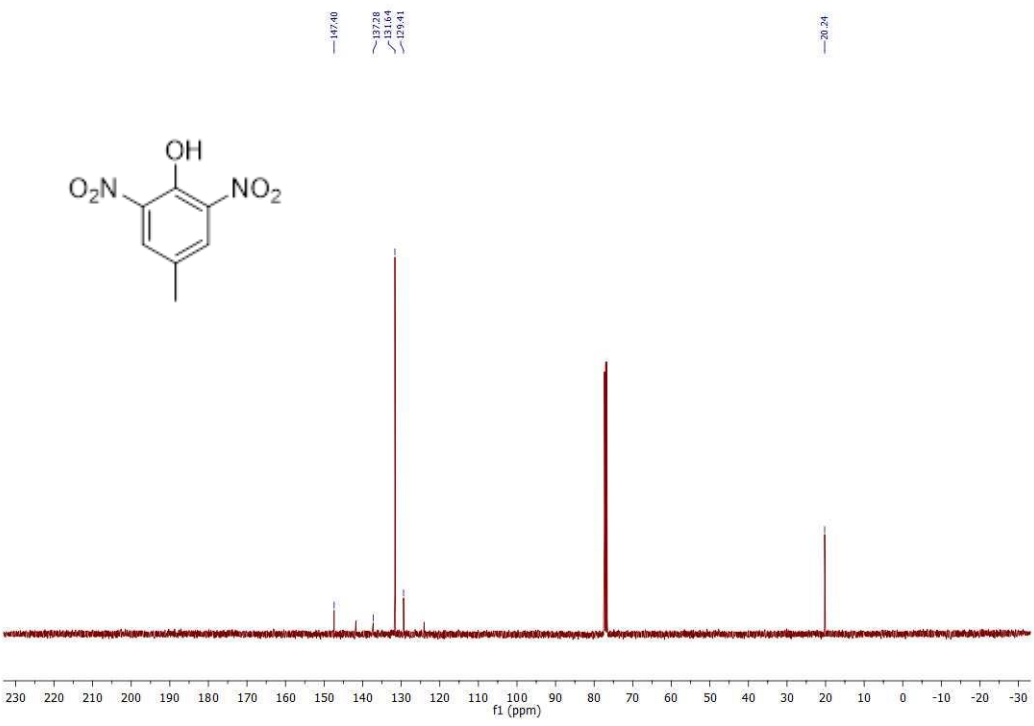

Figure A.2 ^{13}C NMR ($CDCl_3$) spectrum of **compound 1**

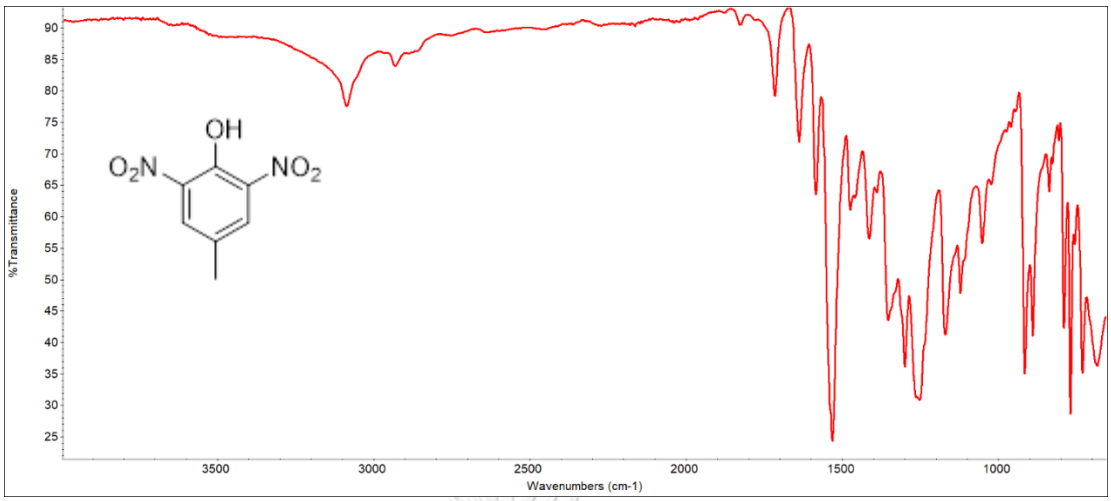

Figure A.3 IR spectrum of **compound 1**

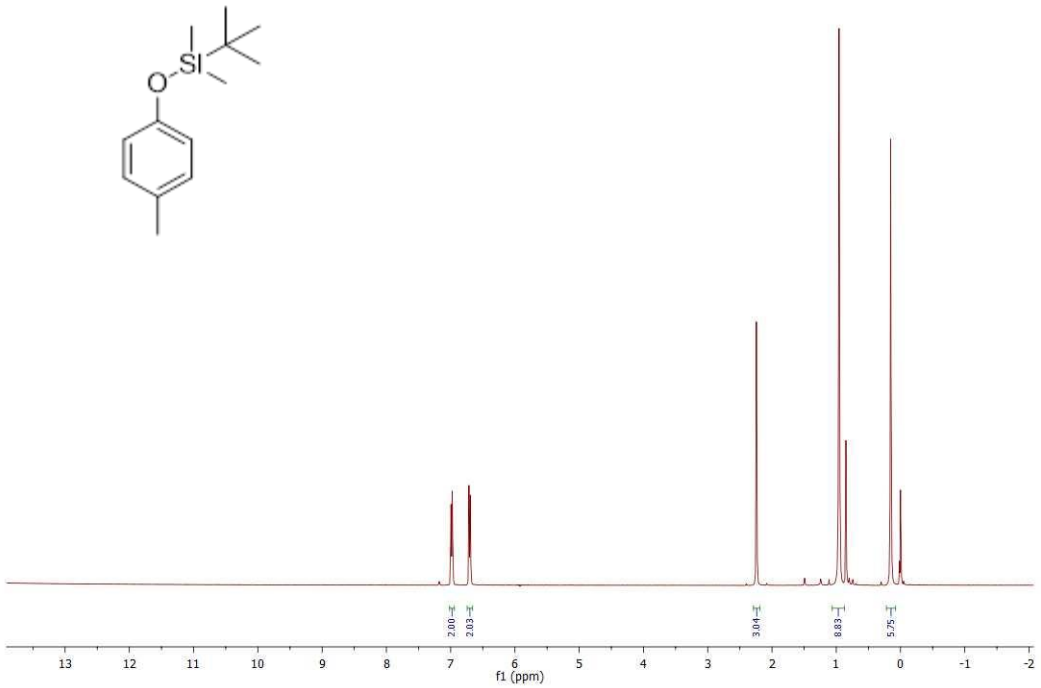

Figure A.4 ^{1}H NMR ($CDCl_3$) spectrum of **compound 2**

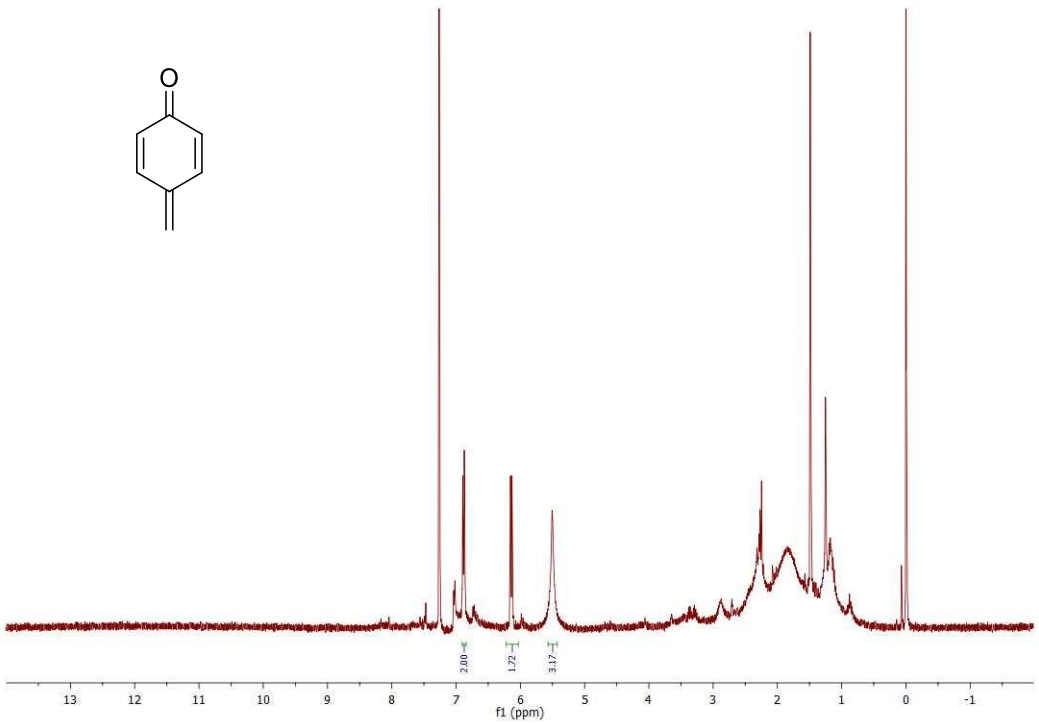

Figure A.5 ^{1}H NMR ($CDCl_3$) spectrum of **intermediate A**

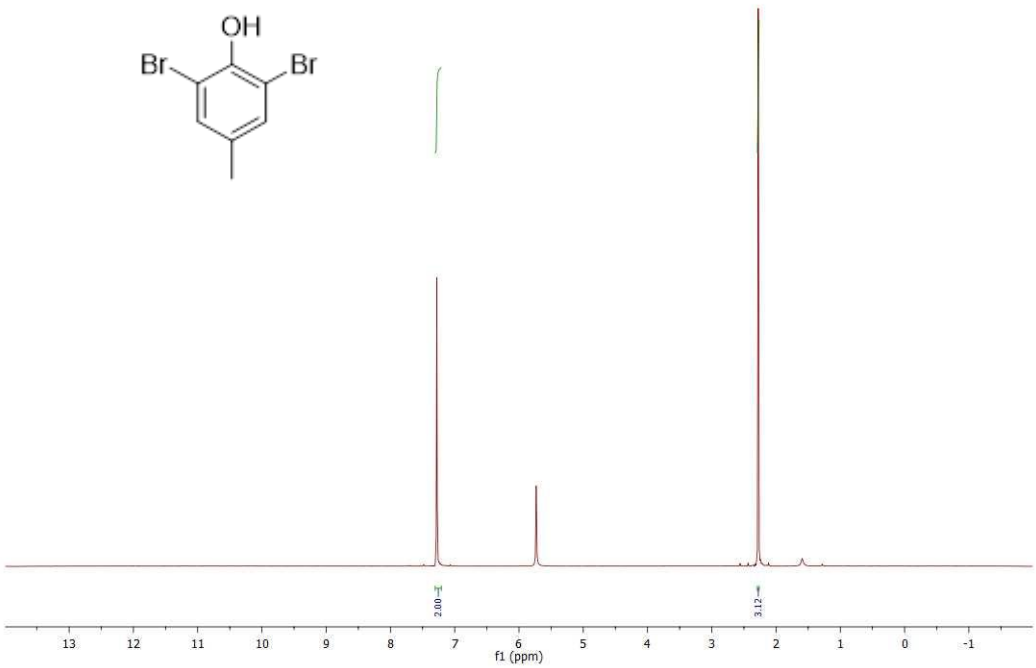

Figure A.6 ^{1}H NMR ($CDCl_3$) spectrum of **compound 3**

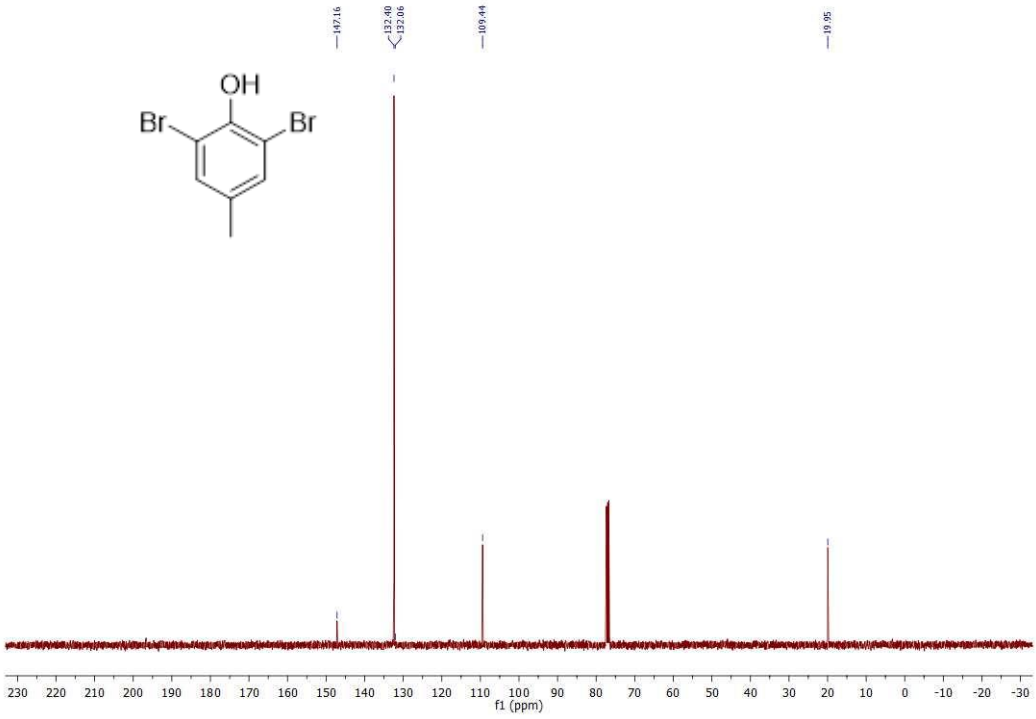

Figure A.7 ^{13}C NMR ($CDCl_3$) spectrum of **compound 3**

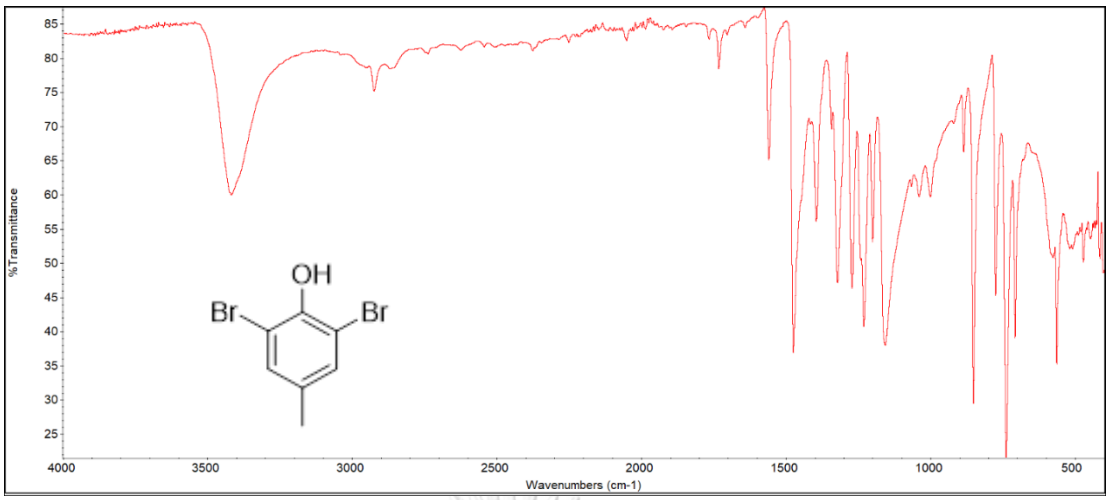

Figure A.8 IR spectrum of **compound 3**

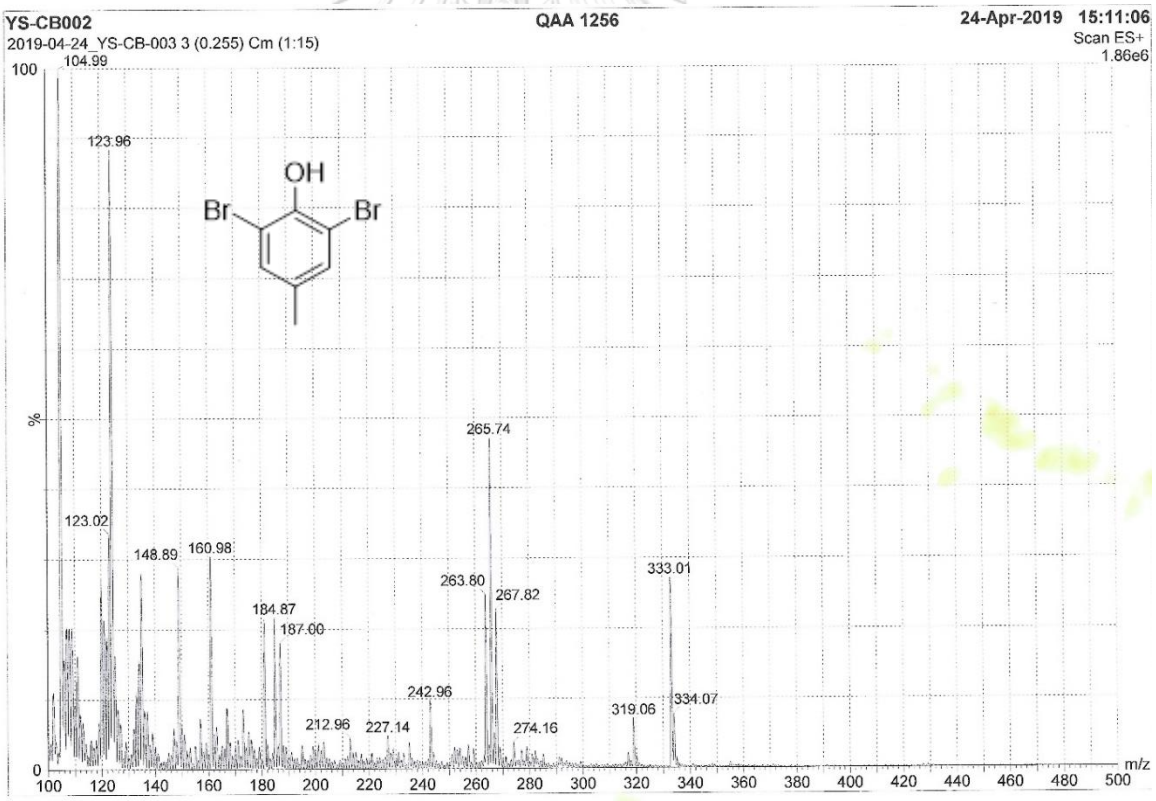

Figure A.9 Mass spectrum of **compound 3**

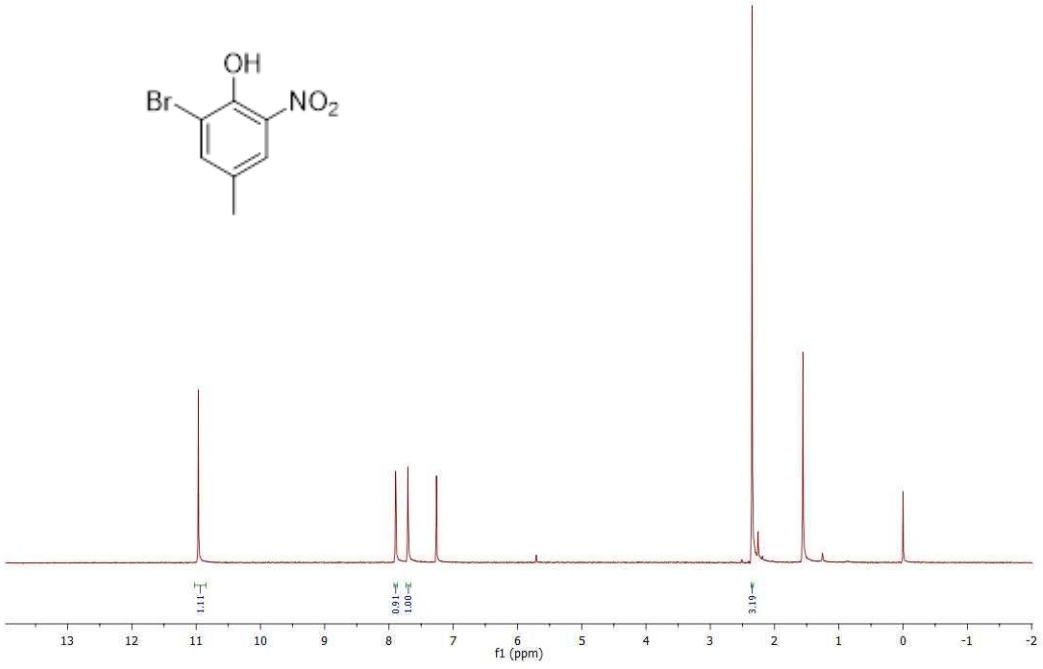

Figure A.10 ^{1}H NMR ($CDCl_3$) spectrum of **compound 4**

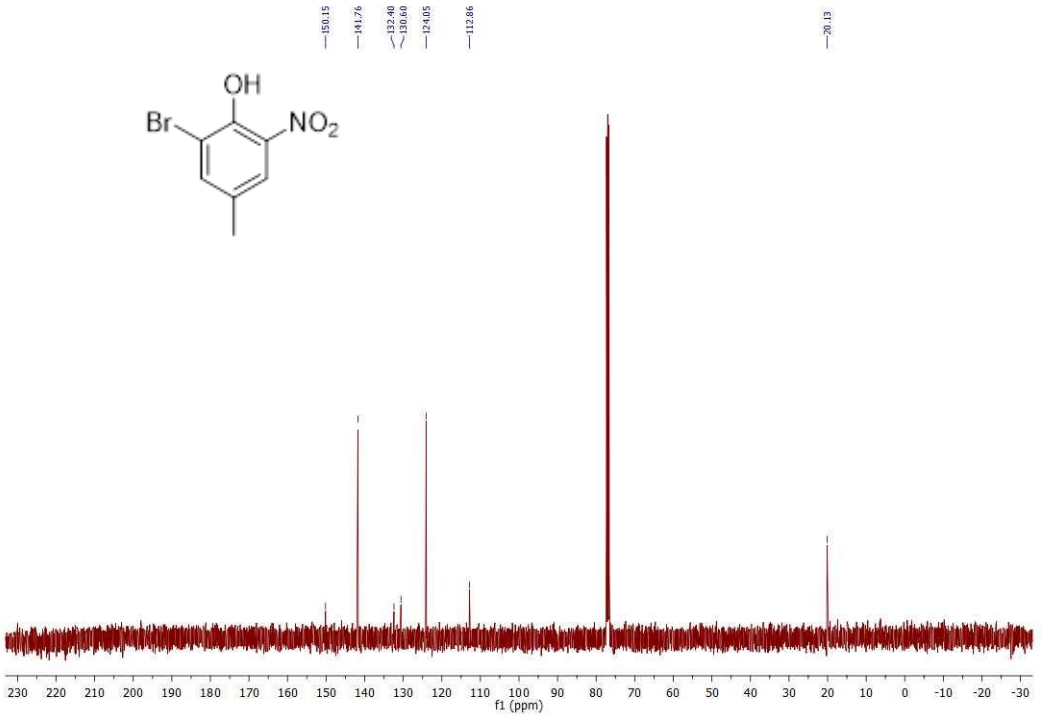

Figure A.11 ^{13}C NMR ($CDCl_3$) spectrum of **compound 4**

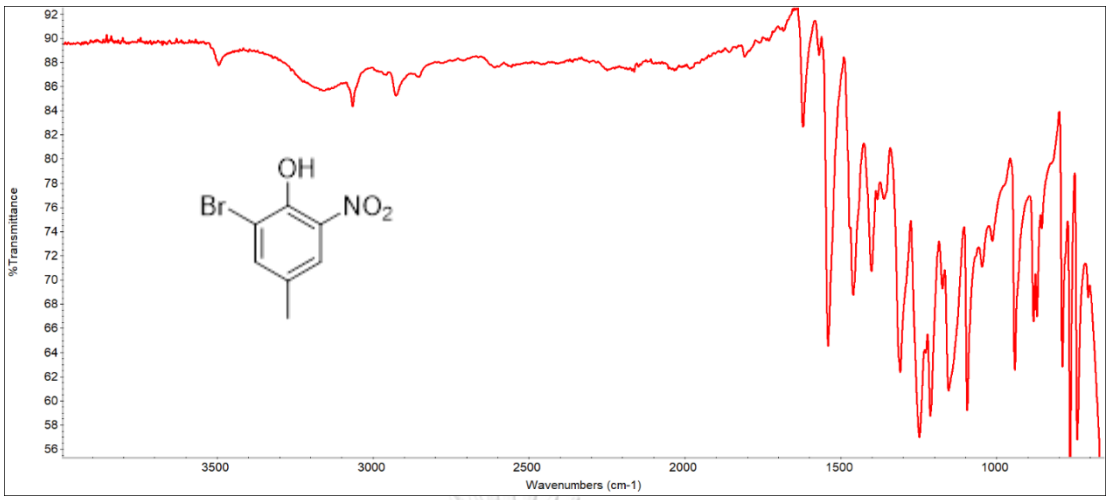

Figure A.12 IR spectrum of **compound 4**

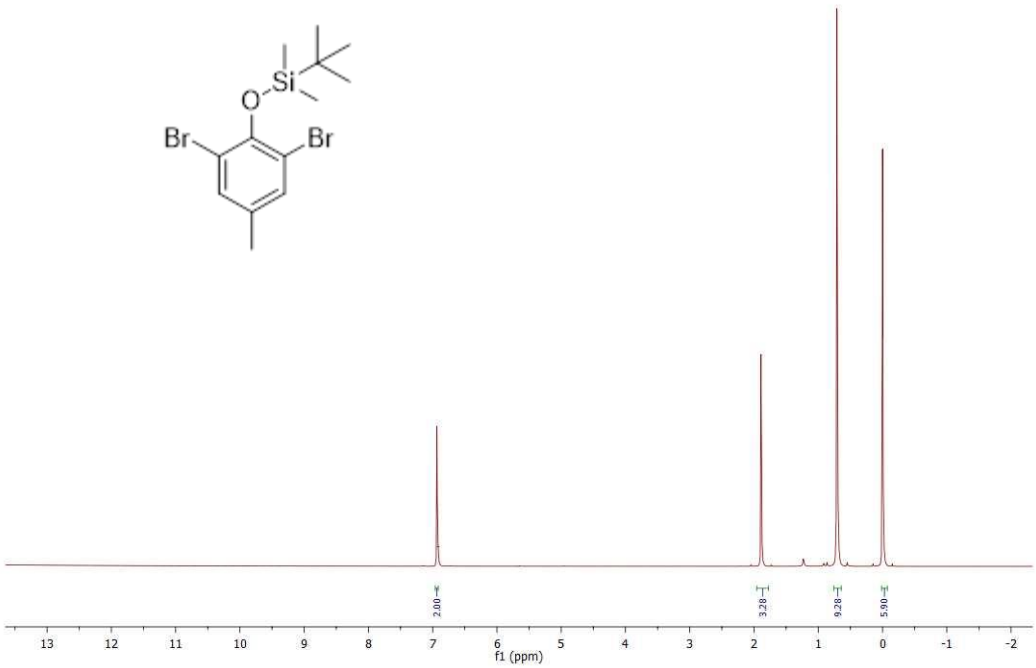

Figure A.13 ^{1}H NMR ($CDCl_3$) spectrum of **compound 5**

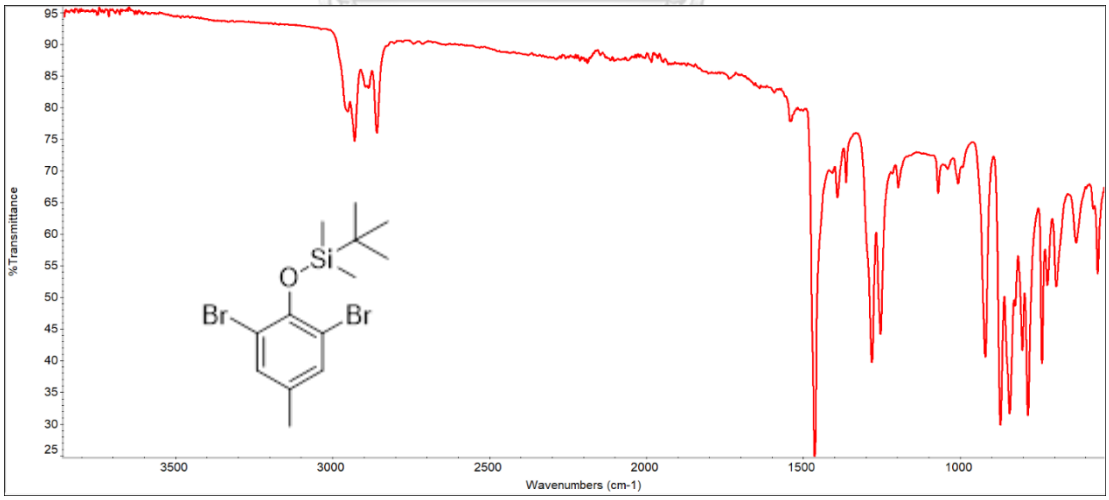

Figure A.14 IR spectrum of **compound 5**

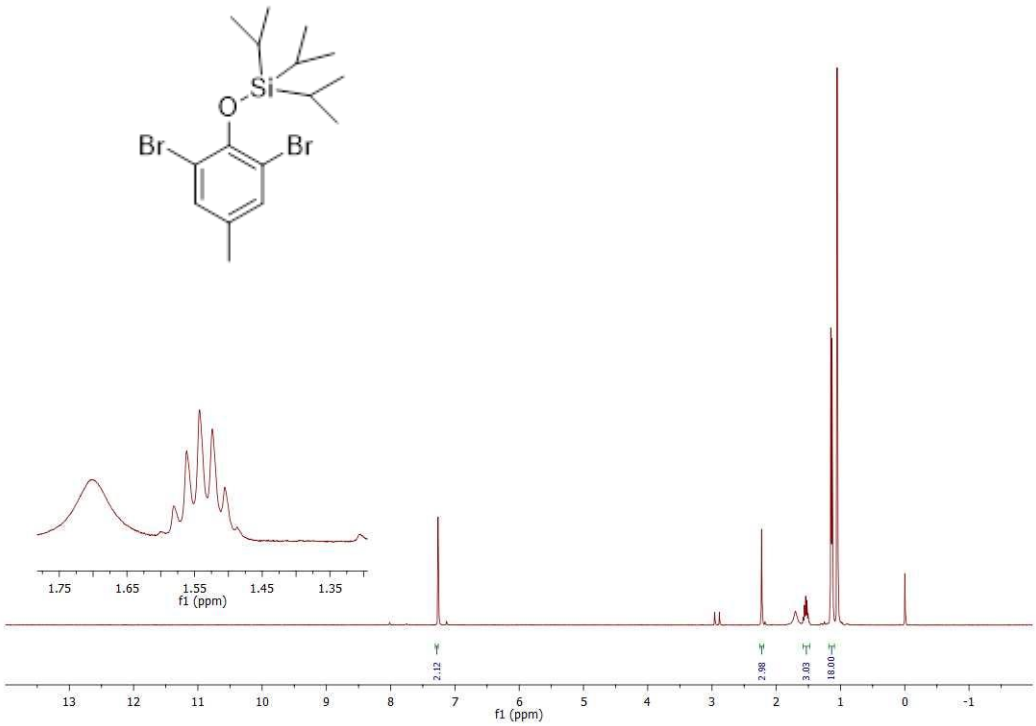

Figure A.15 ^{1}H NMR ($CDCl_3$) spectrum of **compound 6**

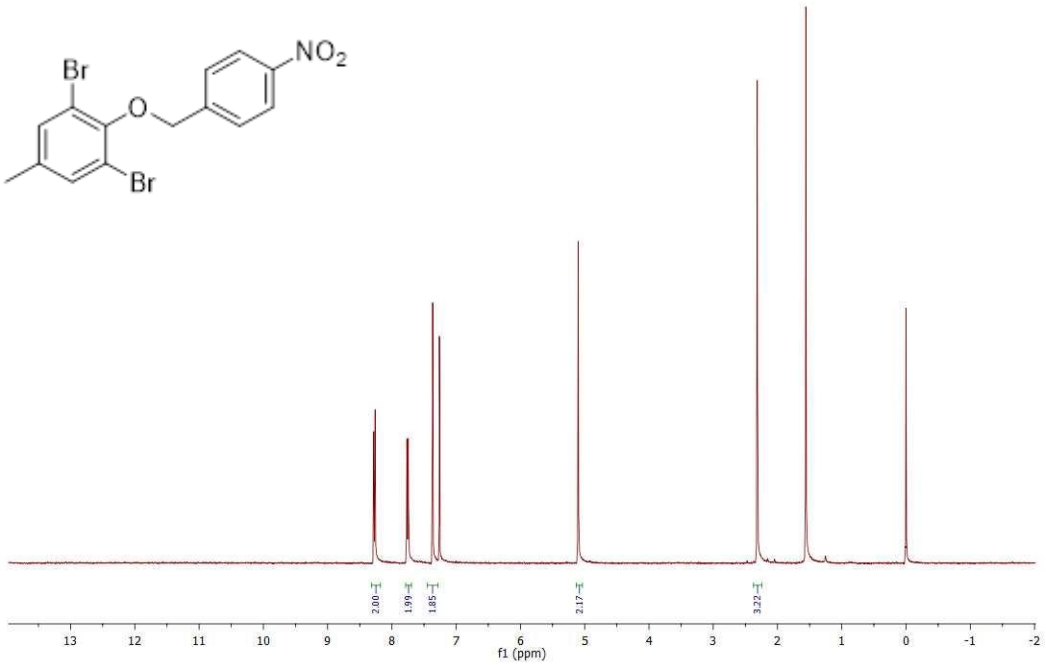

Figure A.16 ^{1}H NMR ($CDCl_3$) spectrum of **compound 7**

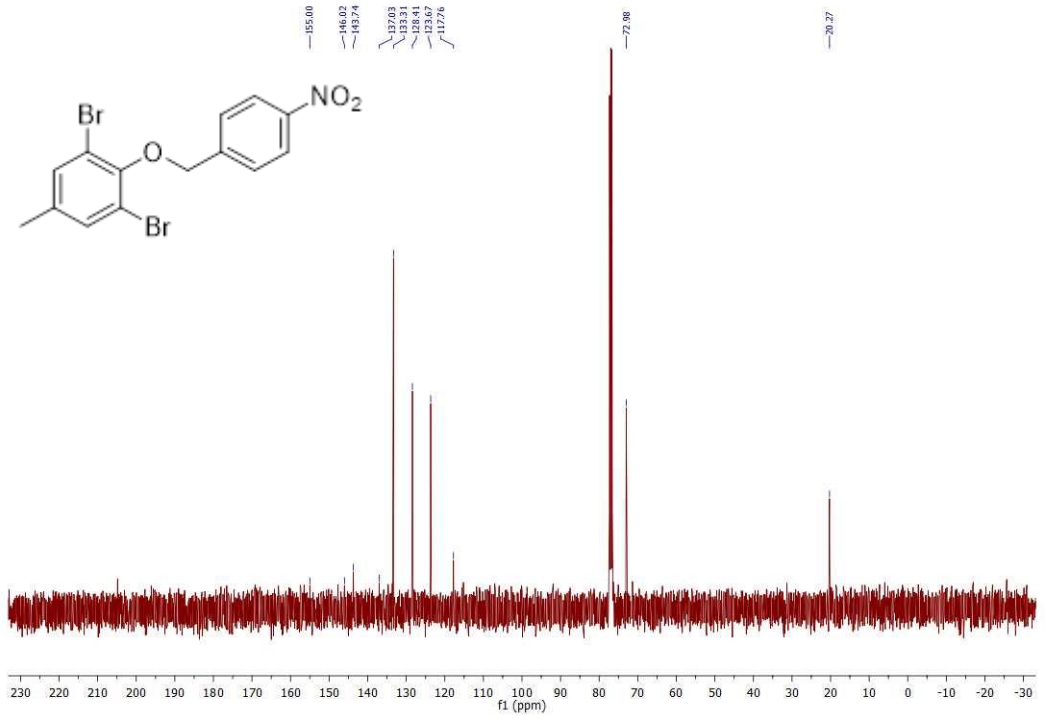

Figure A.17 ^{13}C NMR ($CDCl_3$) spectrum of **compound 7**

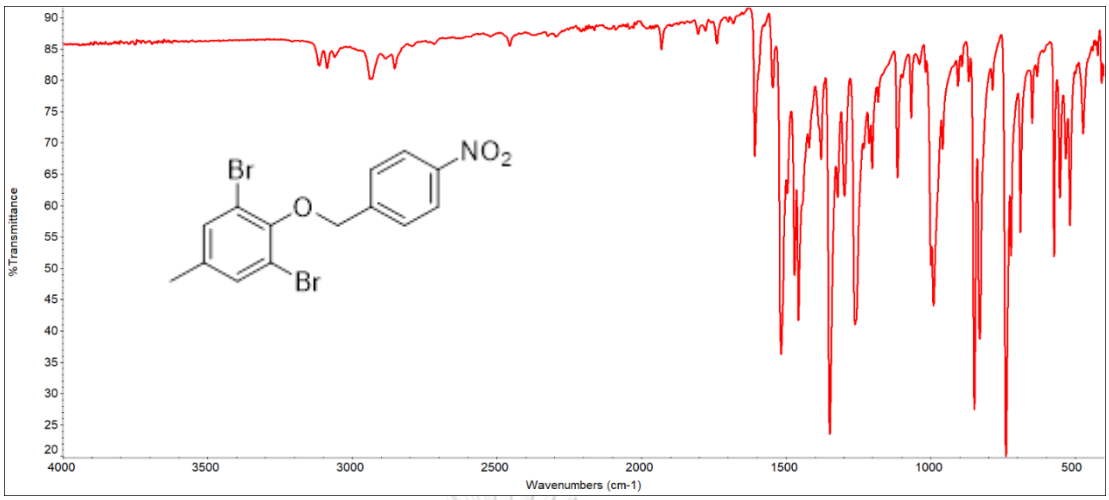

Figure A.18 IR spectrum of **compound 7**

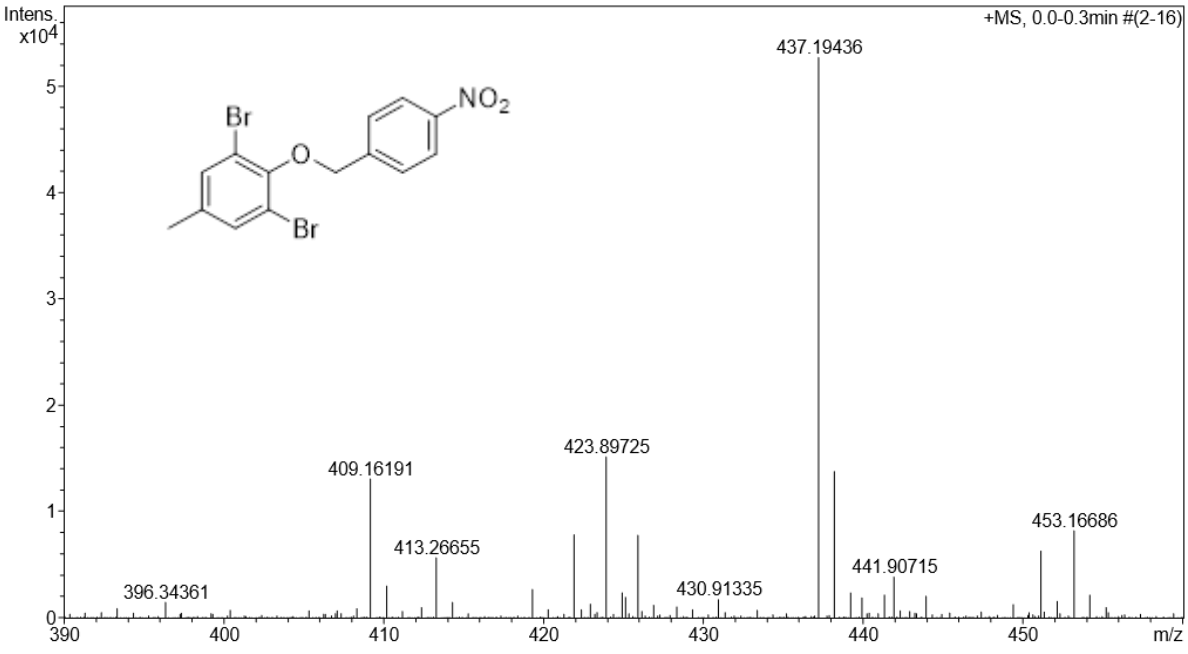

Figure A.19 Mass spectrum of **compound 7**

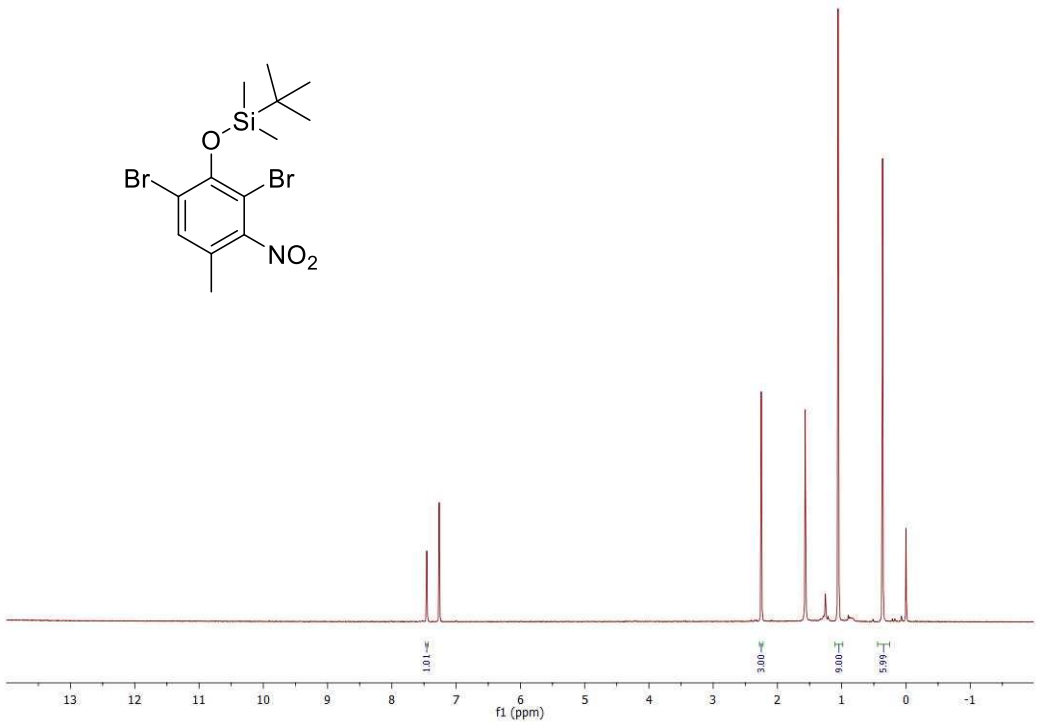

Figure A.20 ^{1}H NMR ($CDCl_3$) spectrum of *meta*-nitro-TBS-2,6-dibromo-4-methylphenol

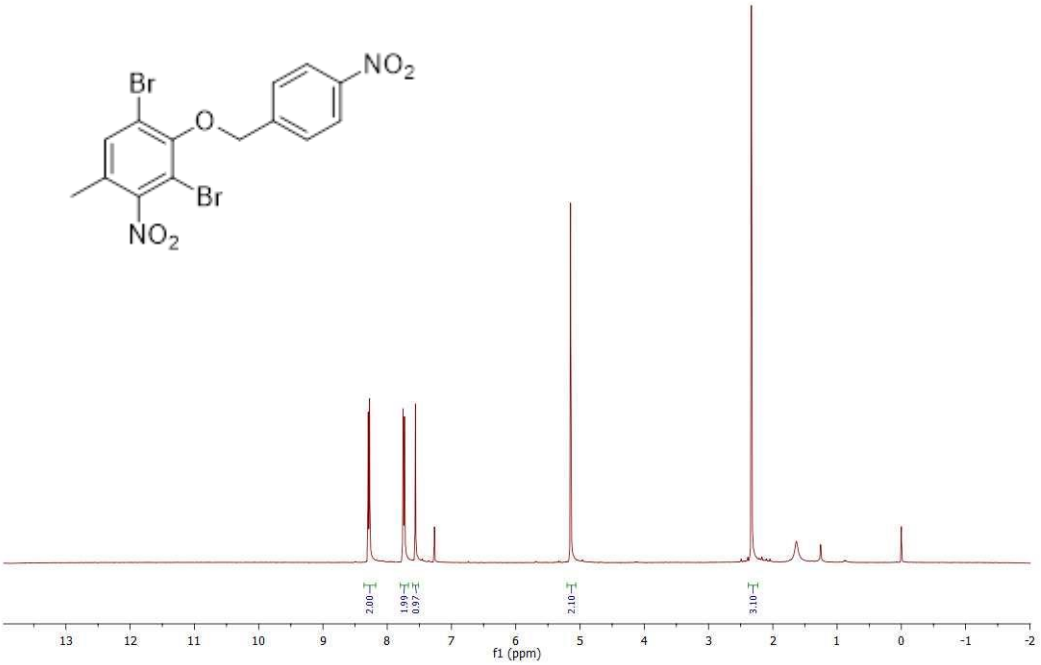

Figure A.21 ^{1}H NMR ($CDCl_3$) spectrum of **compound 8a**

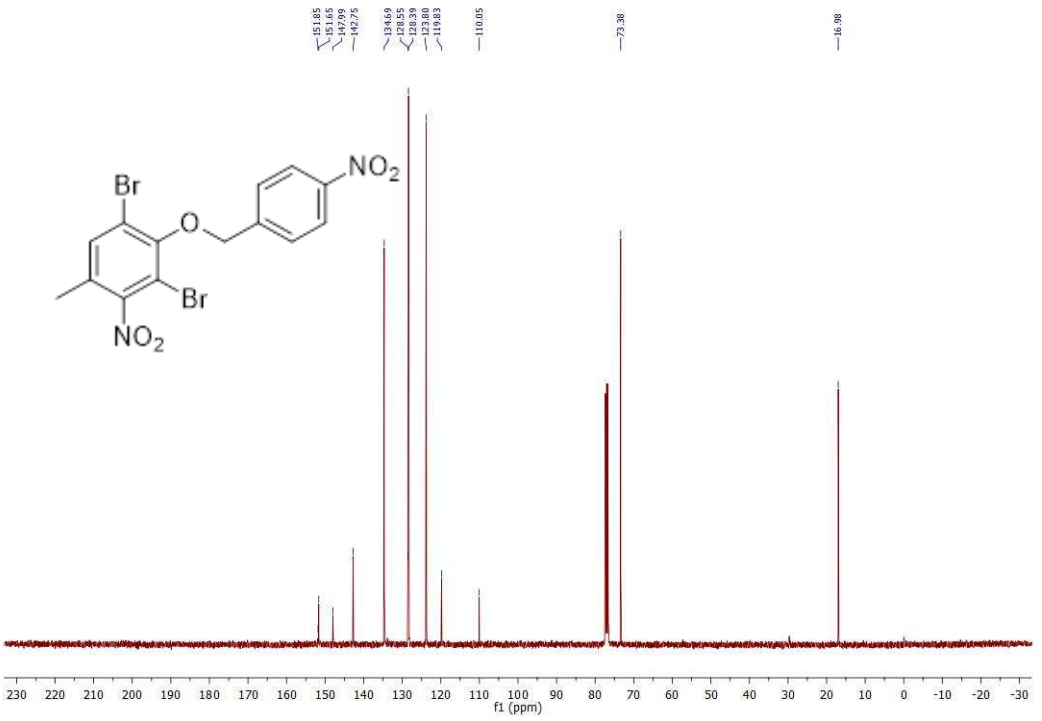

Figure A.22 ^{13}C NMR ($CDCl_3$) spectrum of **compound 8**

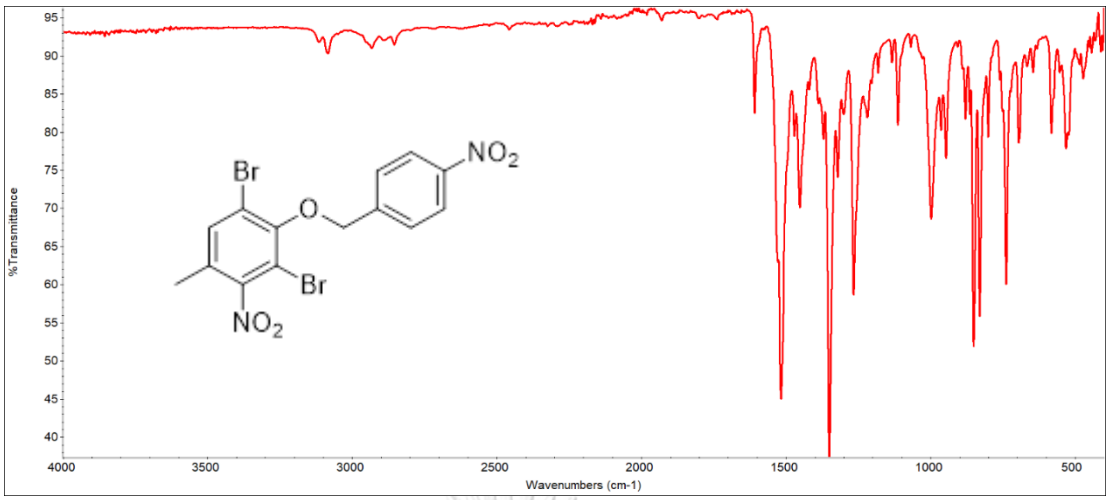

Figure A.23 IR spectrum of **compound 8a**

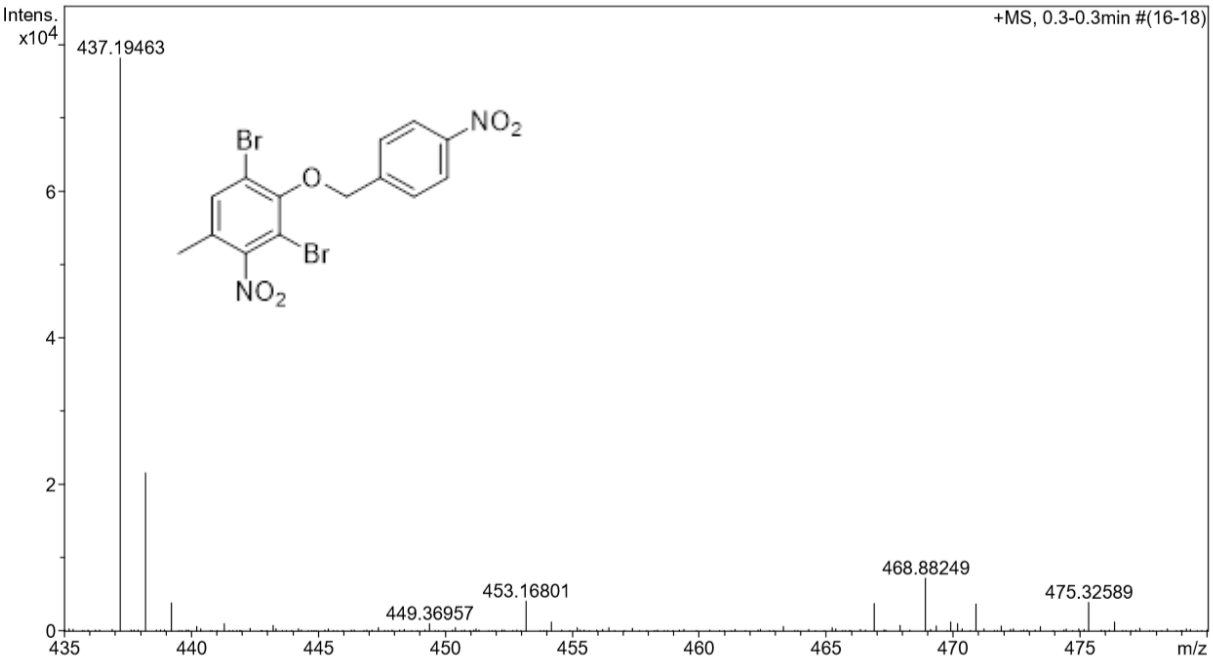

Figure A.24 Mass spectrum of **compound 8a**

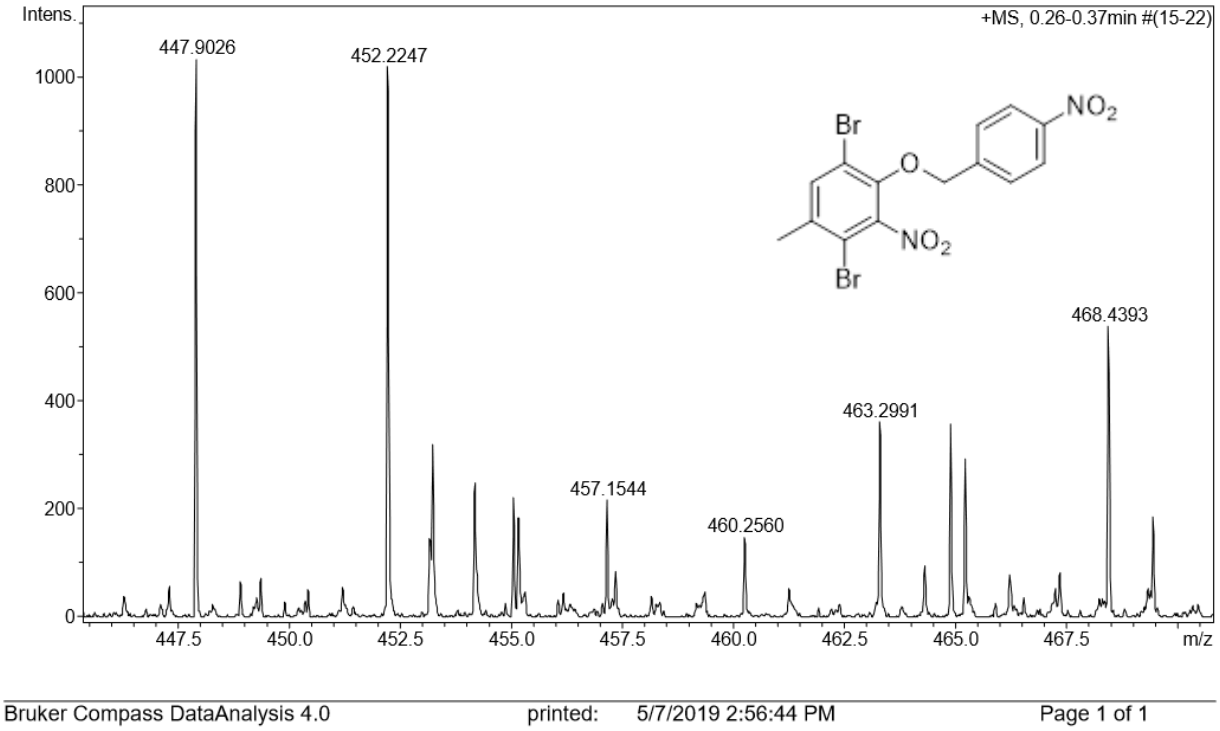

Figure A.25 Mass spectrum of **compound 8b**

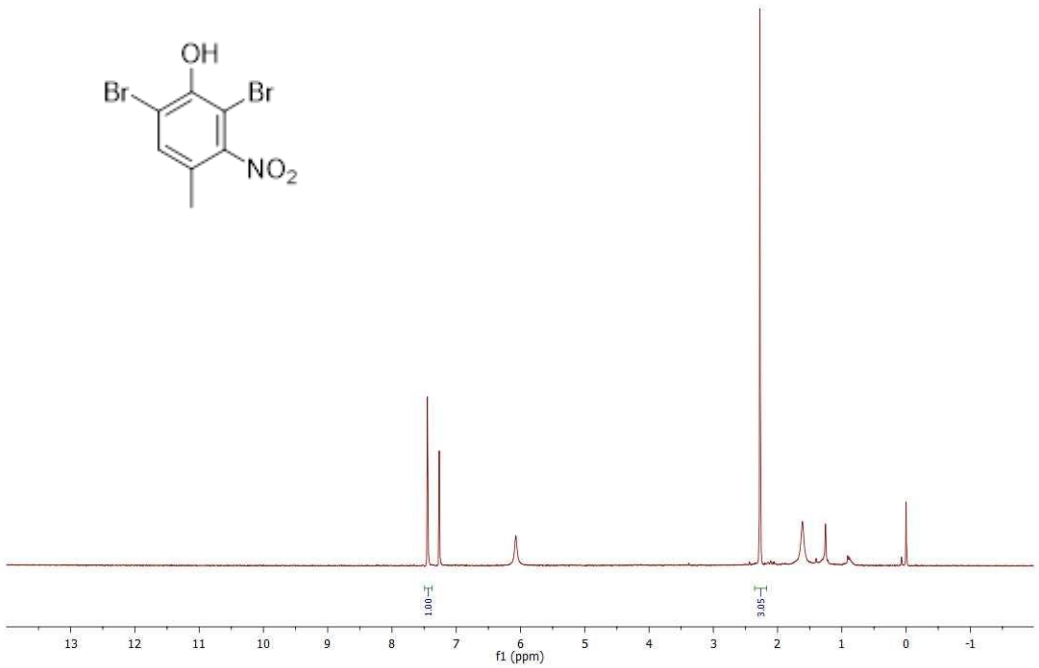

Figure A.26 ^{1}H NMR ($CDCl_3$) spectrum of **compound 9a**

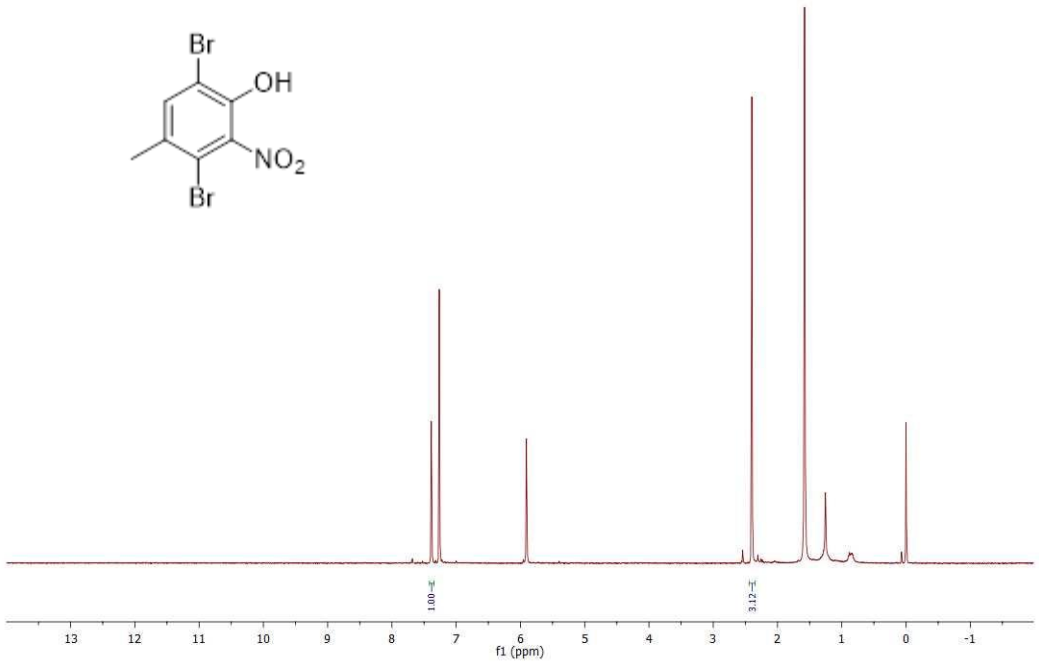

Figure A.27 ^{1}H NMR ($CDCl_3$) spectrum of **compound 9b**

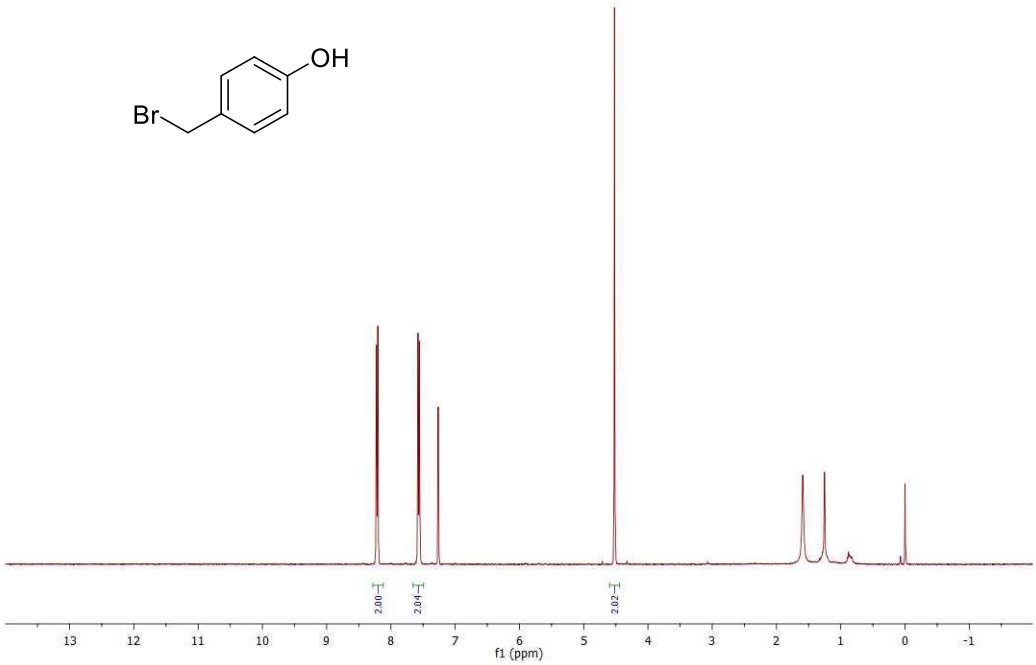

Figure A.28 ^{1}H NMR ($CDCl_3$) spectrum of **Nitro benzyl bromine**

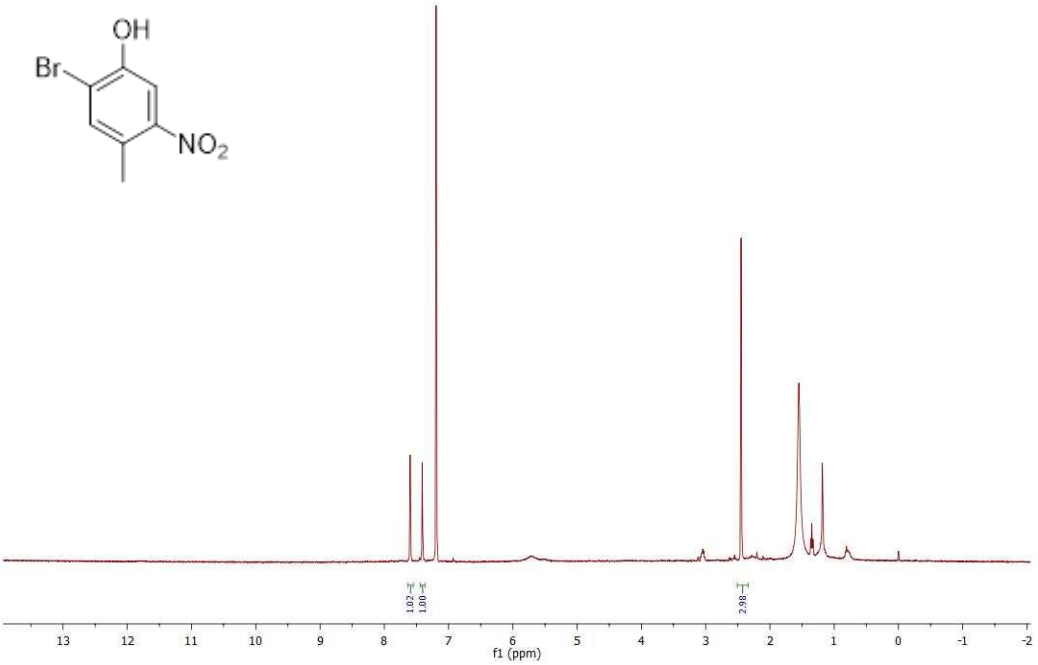

Figure A.29 ^{1}H NMR ($CDCl_3$) spectrum of **compound 10**

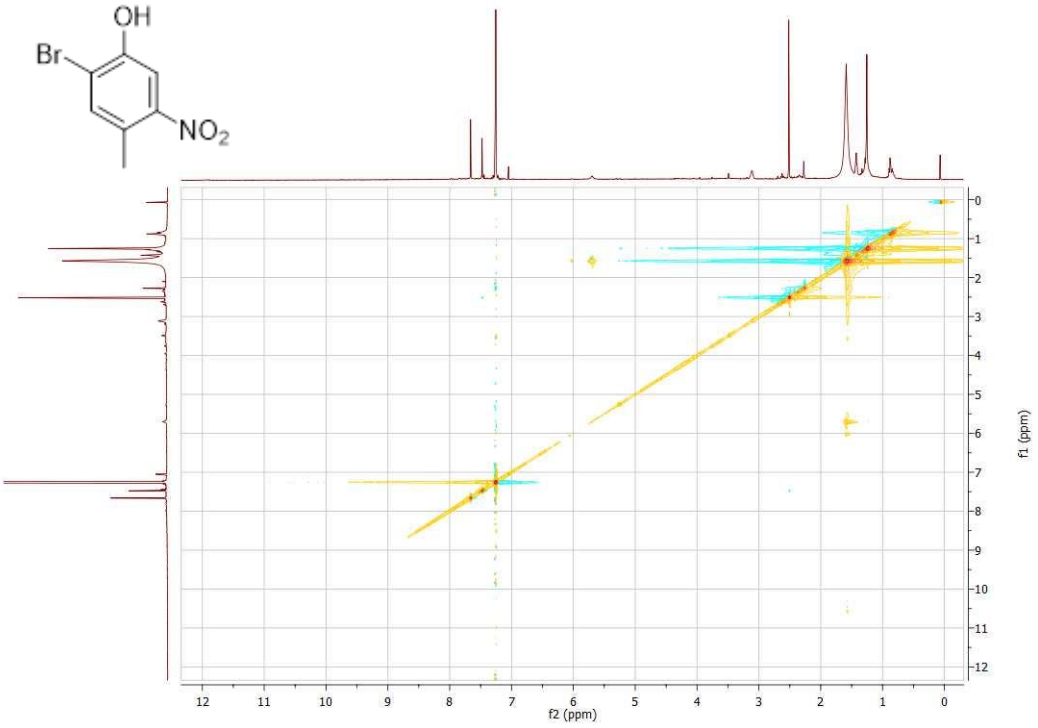

Figure A.30 ^{1}H-^{1}H NOESY NMR spectrum ($CDCl_3$) of compound **10**

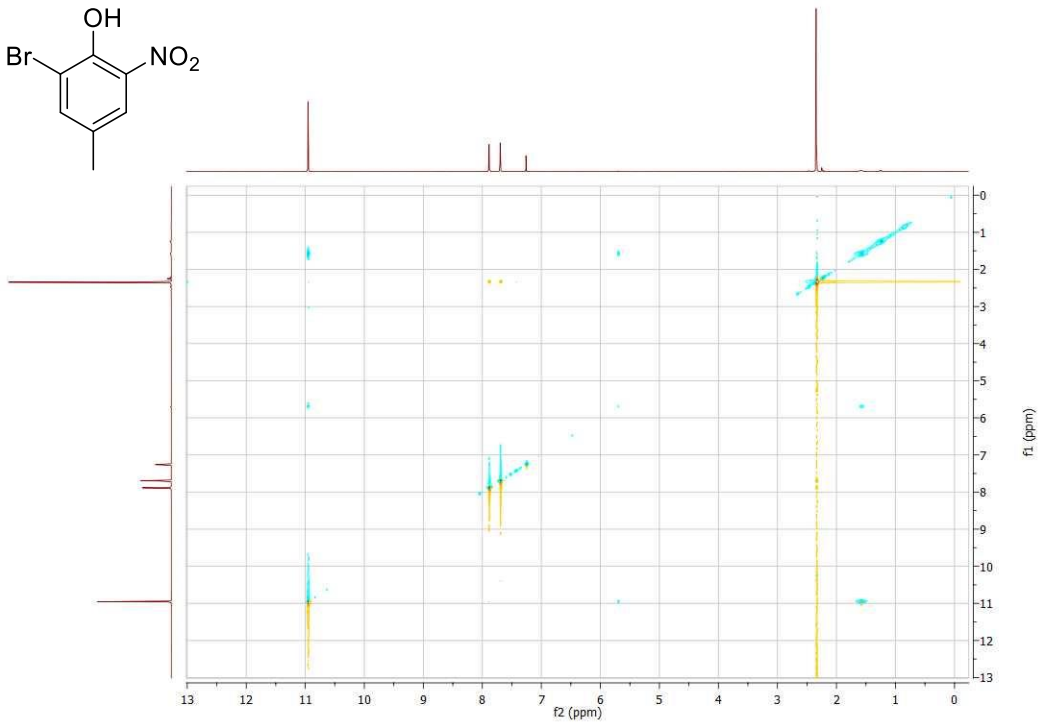

Figure A.31 ^{1}H-^{1}H NOESY NMR spectrum ($CDCl_3$) of compound **3**

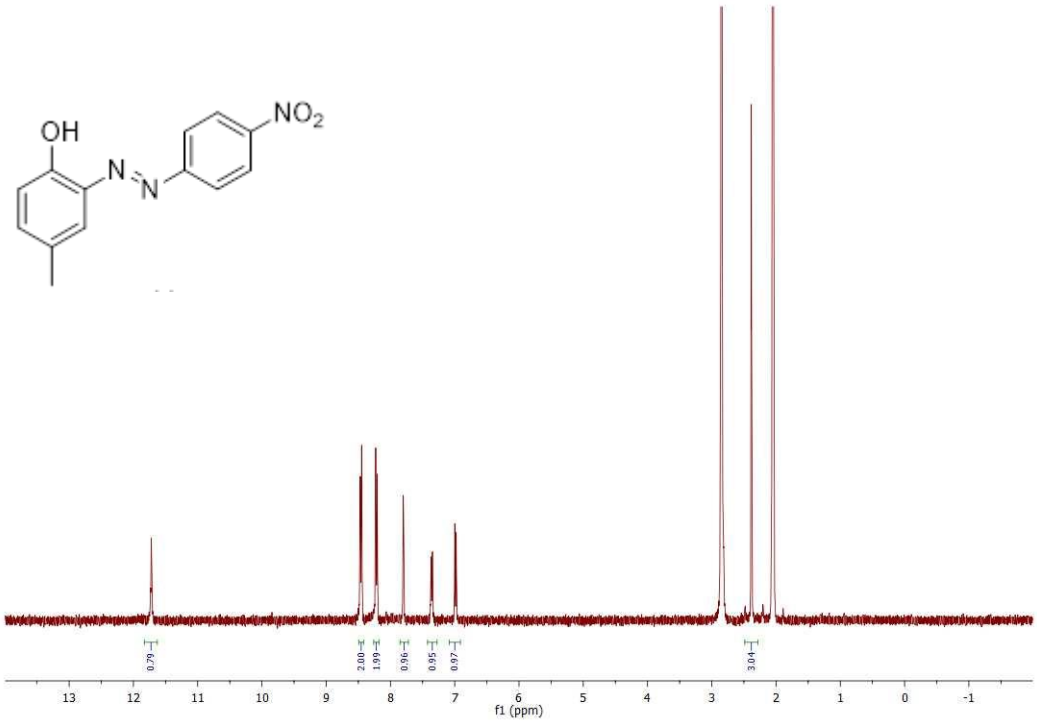

Figure A.32 ^{1}H NMR (acetone-d) spectrum of **compound 11**

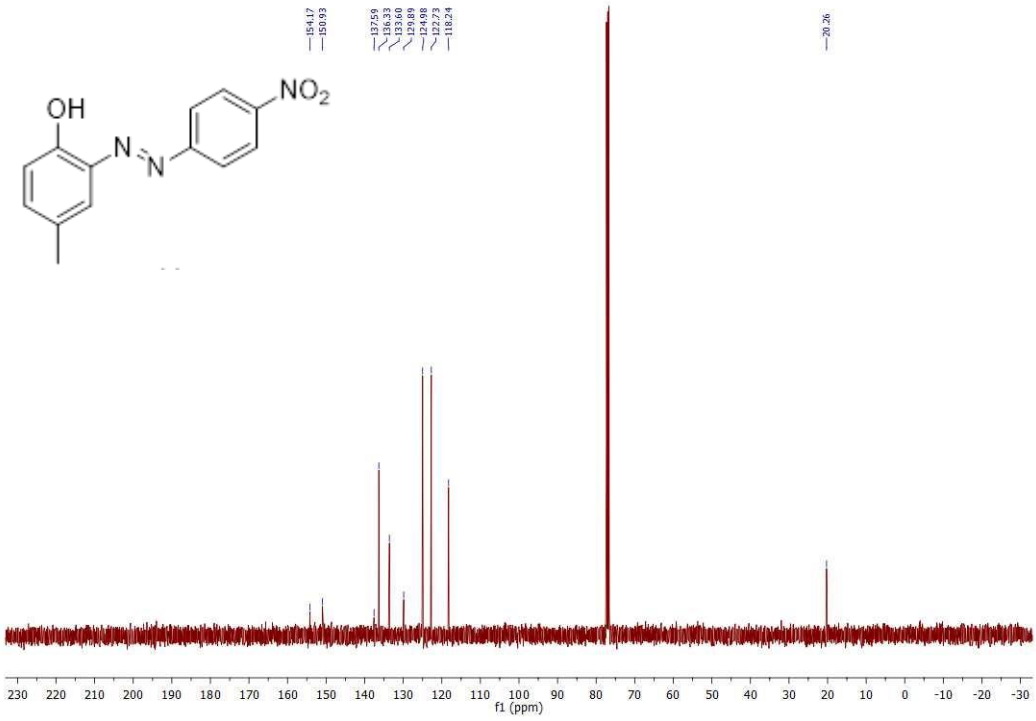

Figure A.33 ^{13}C NMR ($CDCl_3$) spectrum of **compound 11**

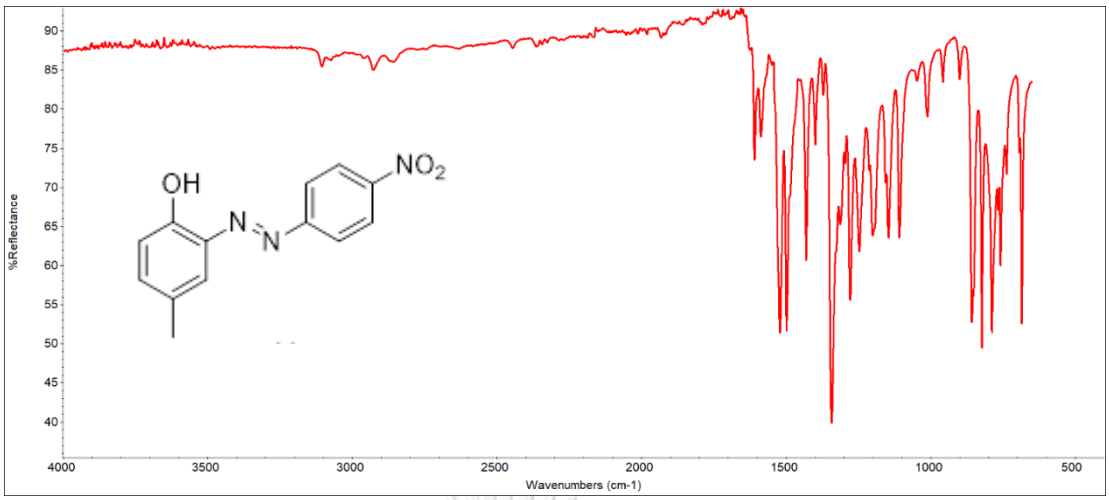

Figure A.34 IR spectrum of **compound 11**

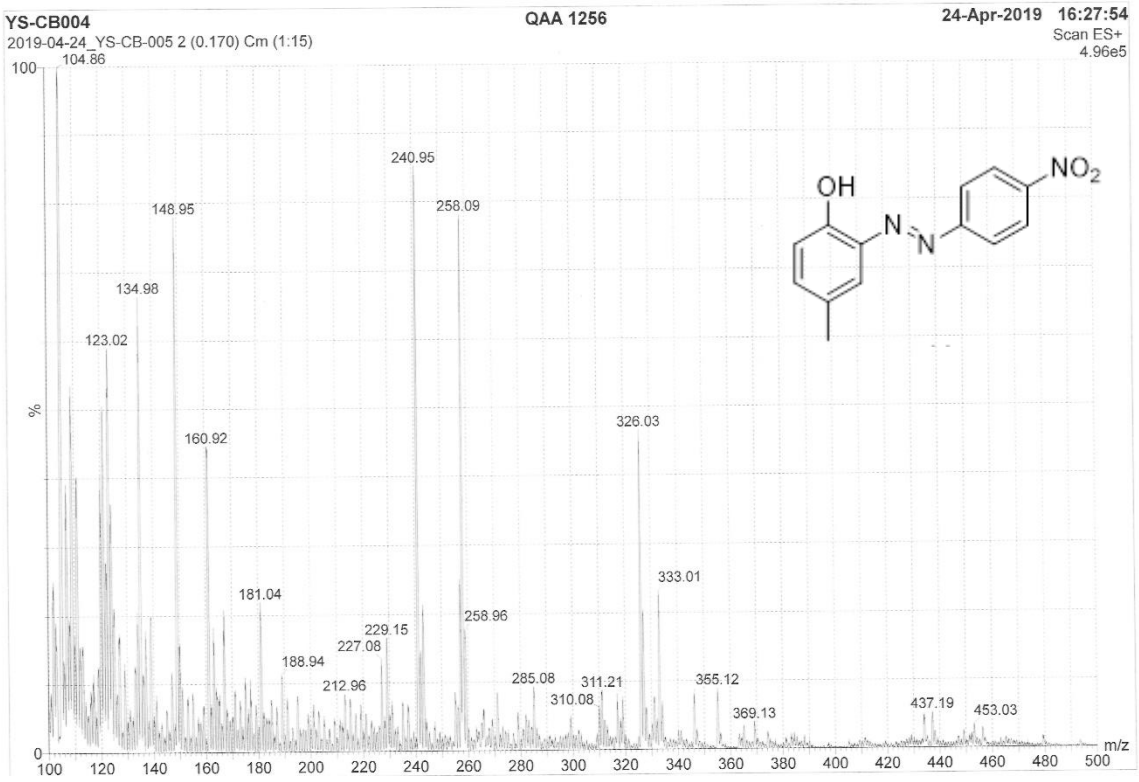

Figure A.35 Mass spectrum of **compound 11**

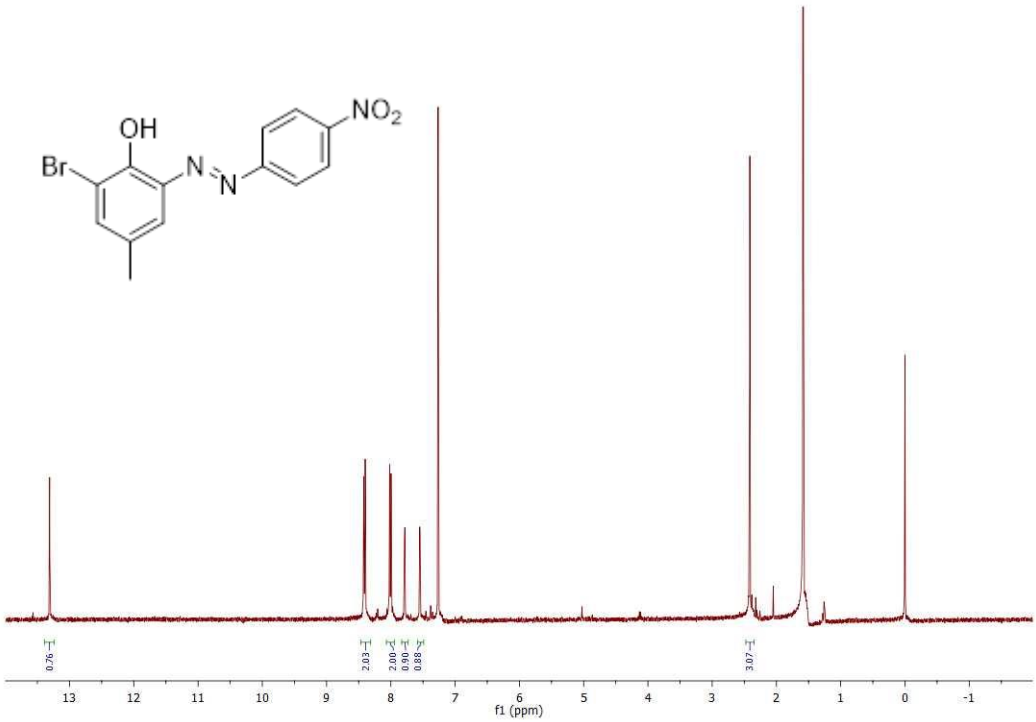

Figure A.36 ^{1}H NMR ($CDCl_3$) spectrum of **compound 12**

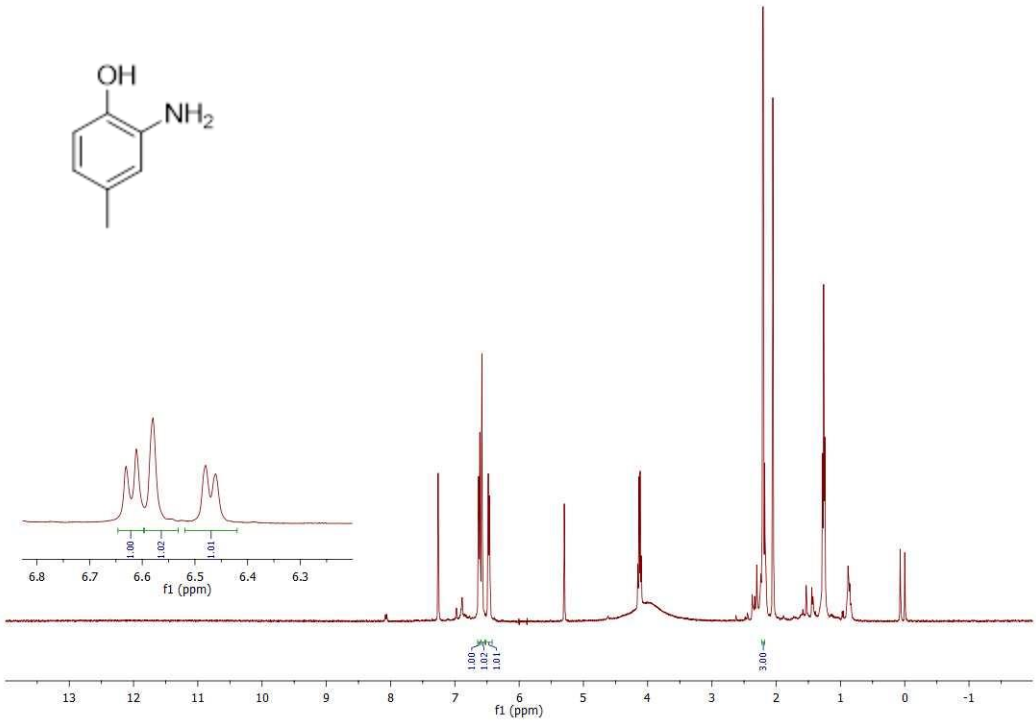

Figure A.37 ^{1}H NMR ($CDCl_3$) spectrum of **compound 13**

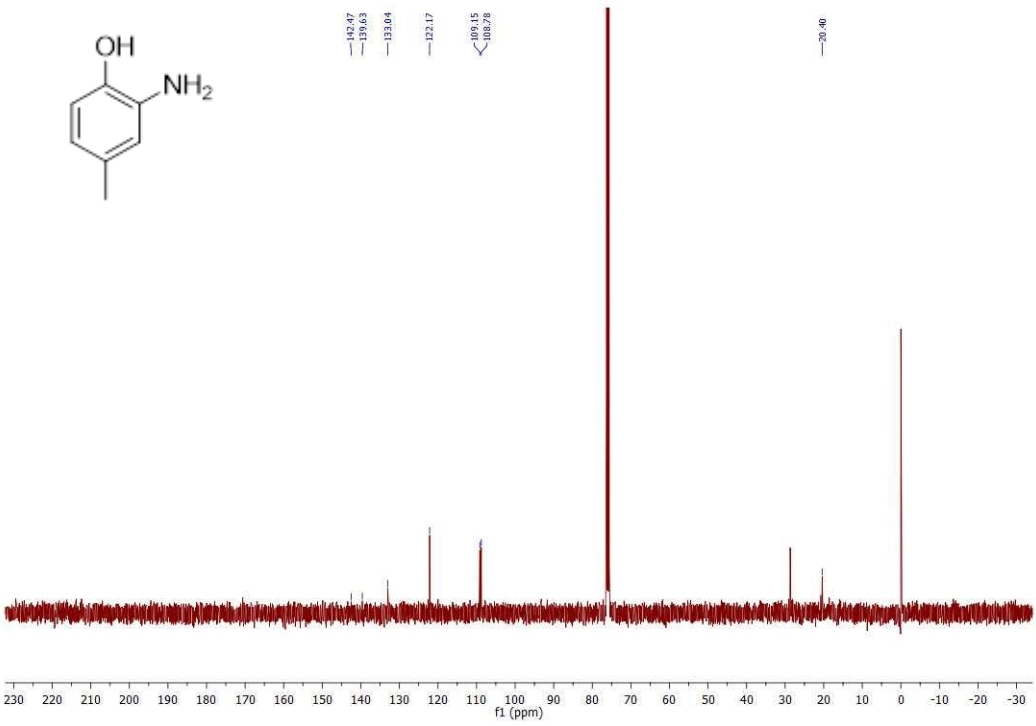

Figure A.38 ^{13}C NMR ($CDCl_3$) spectrum of **compound 13**

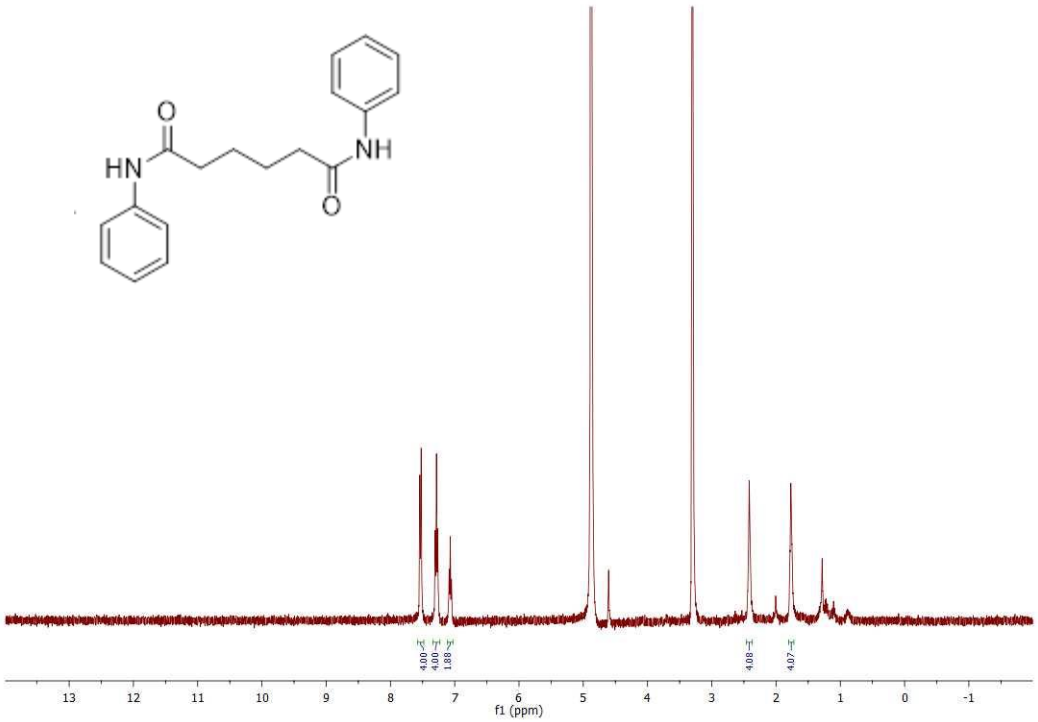

Figure A.39 ^{1}H NMR (CD_3OD) spectrum of **14**

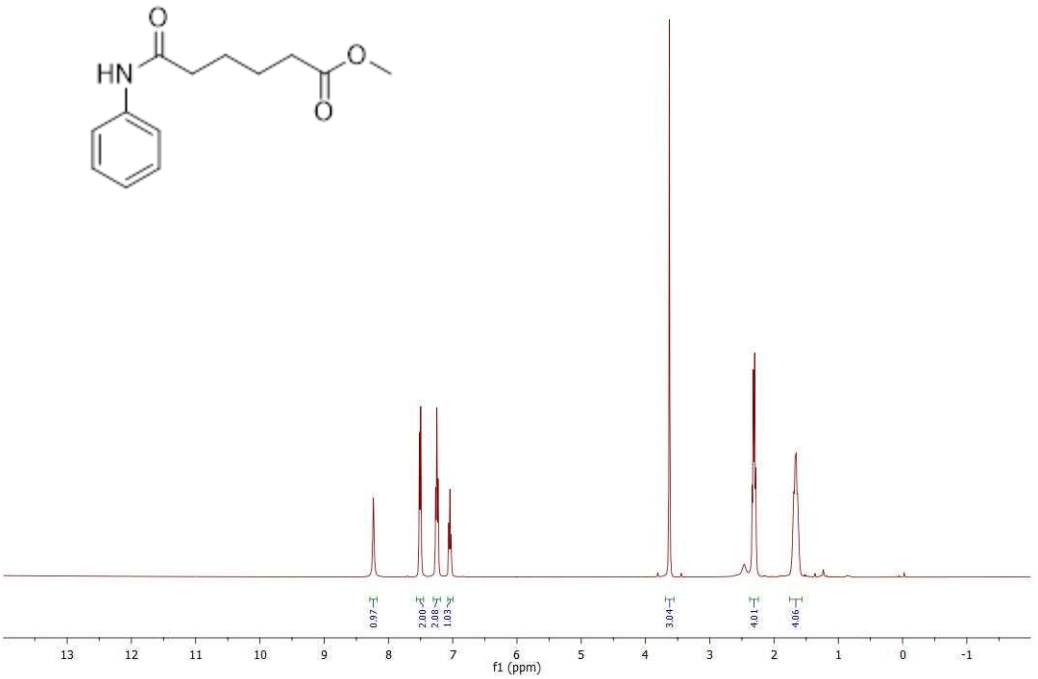

Figure A.40 ^{1}H NMR ($CDCl_3$) spectrum of **compound 15**

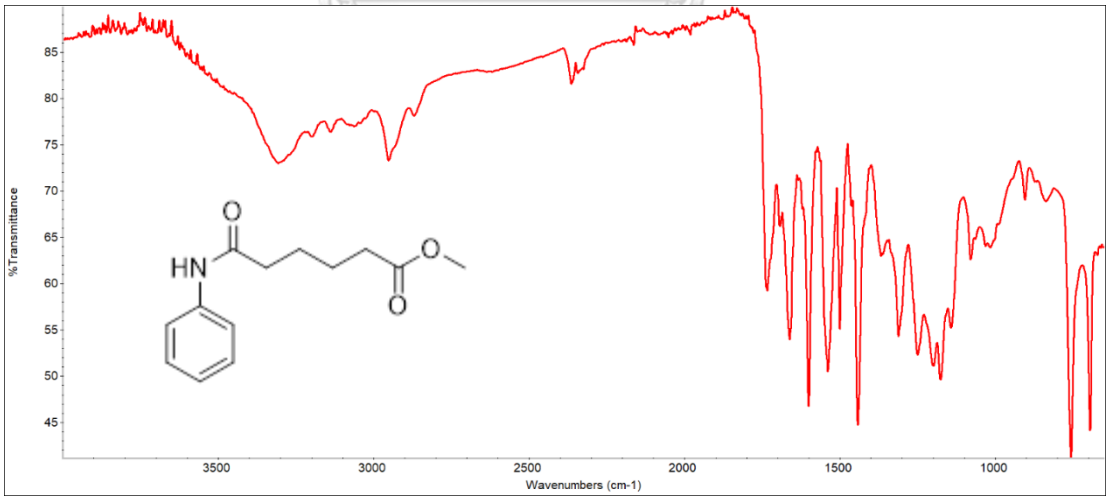

Figure A.41 IR spectrum of **compound 15**

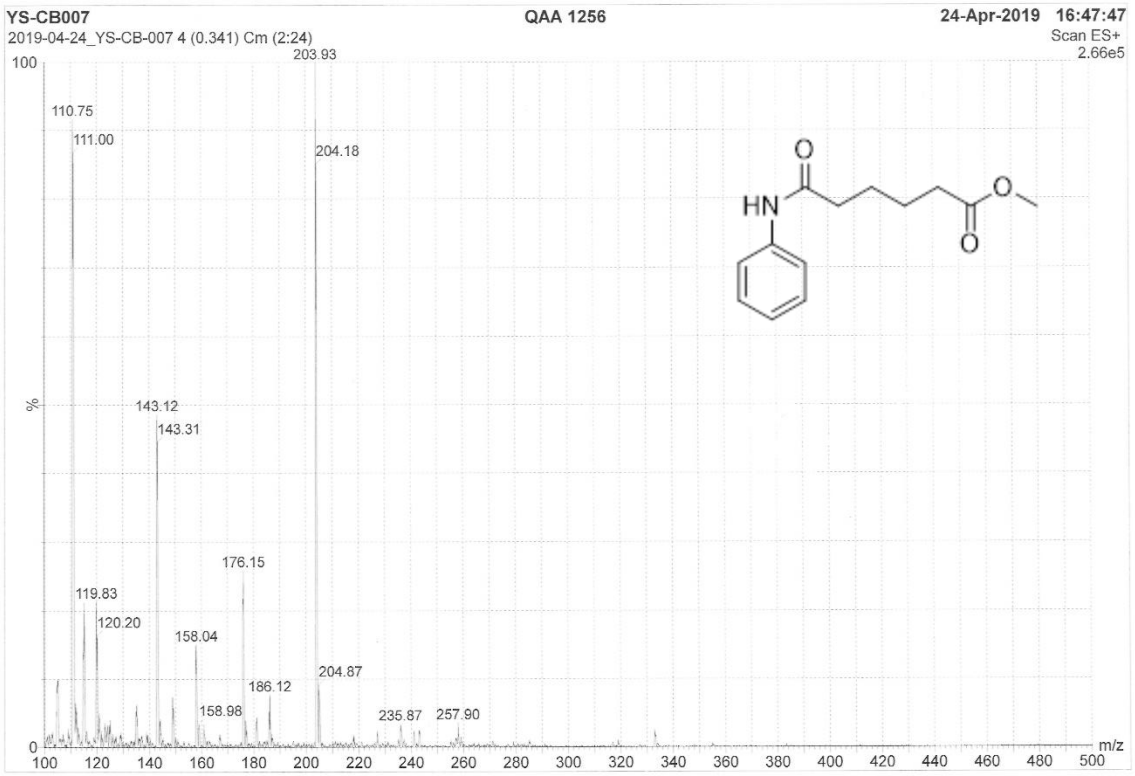

Figure A.42 Mass spectrum of **compound 15**

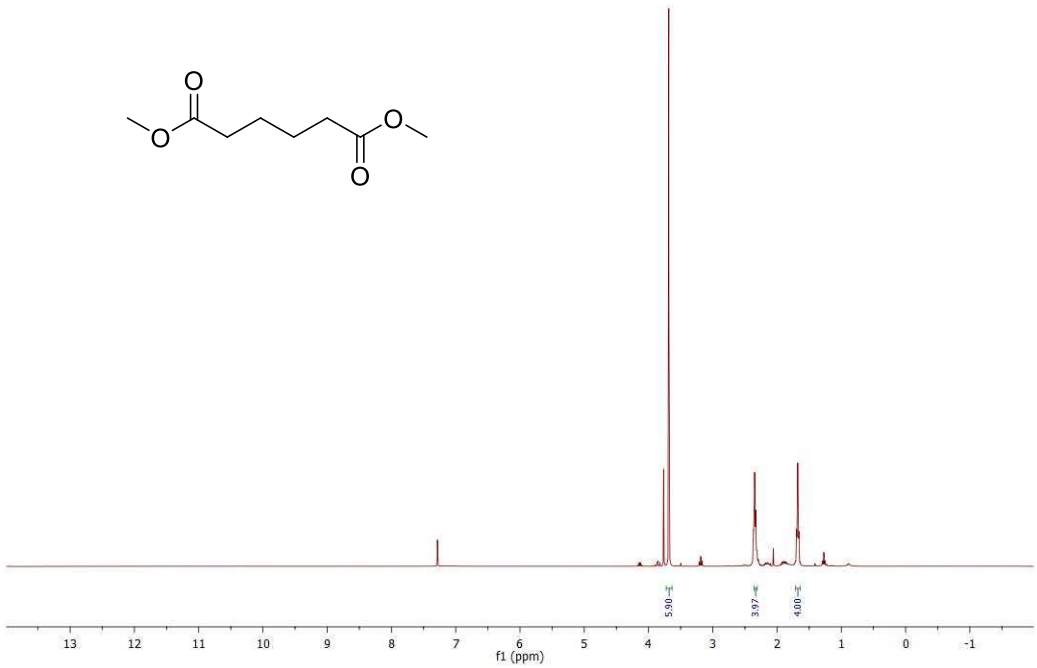

Figure A.43 ^{1}H NMR ($CDCl_3$) diester compound

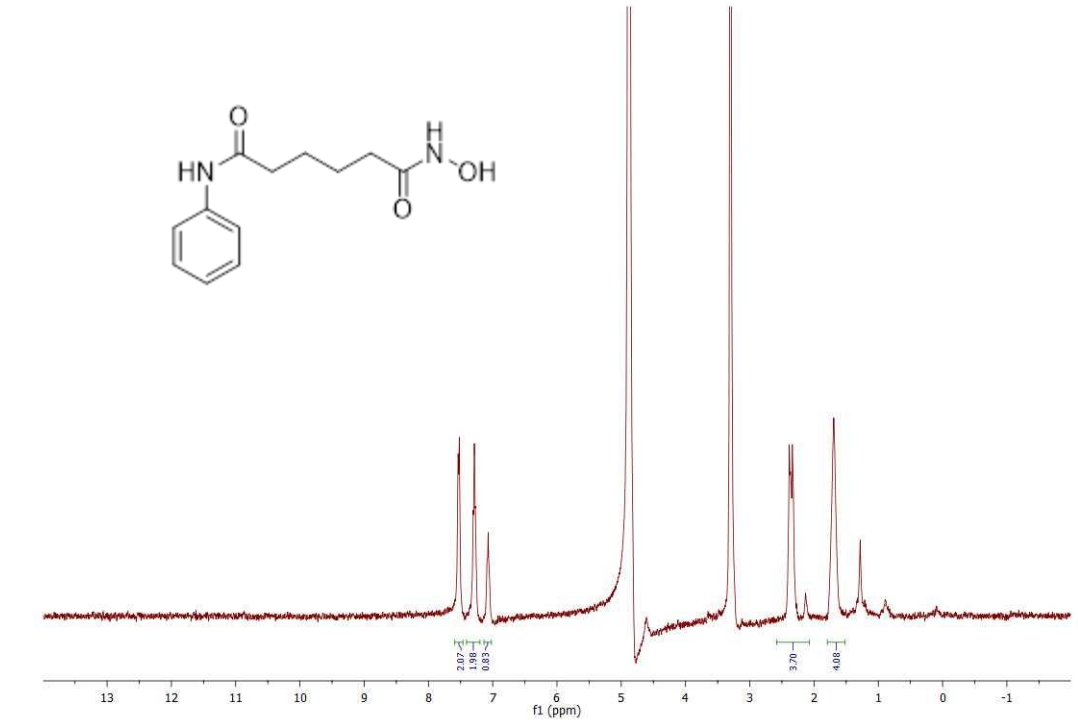

Figure A.44 ^{1}H NMR (CD_3OD) spectrum of **compound 16**

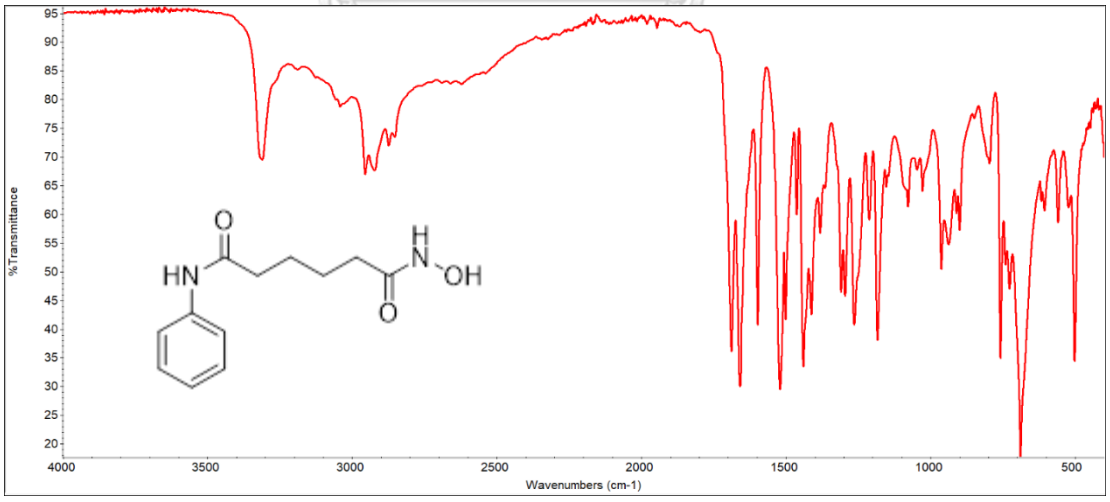

Figure A.45 IR spectrum of **compound 16**

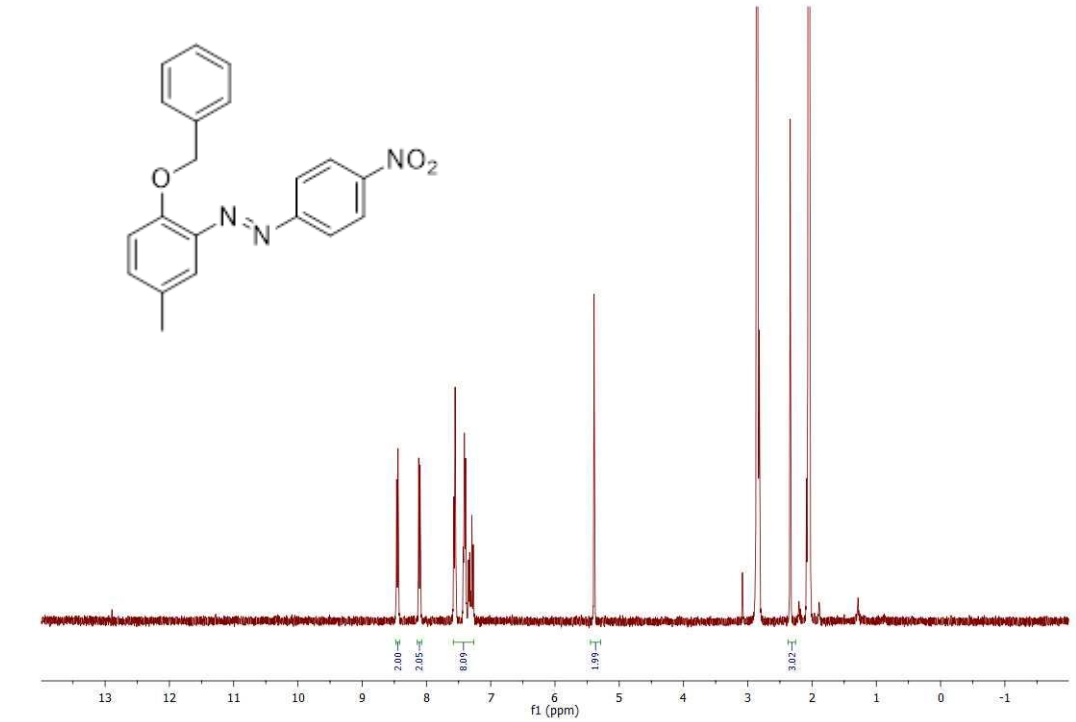

Figure A.46 ^{1}H NMR (acetone-d) spectrum of **compound 17**

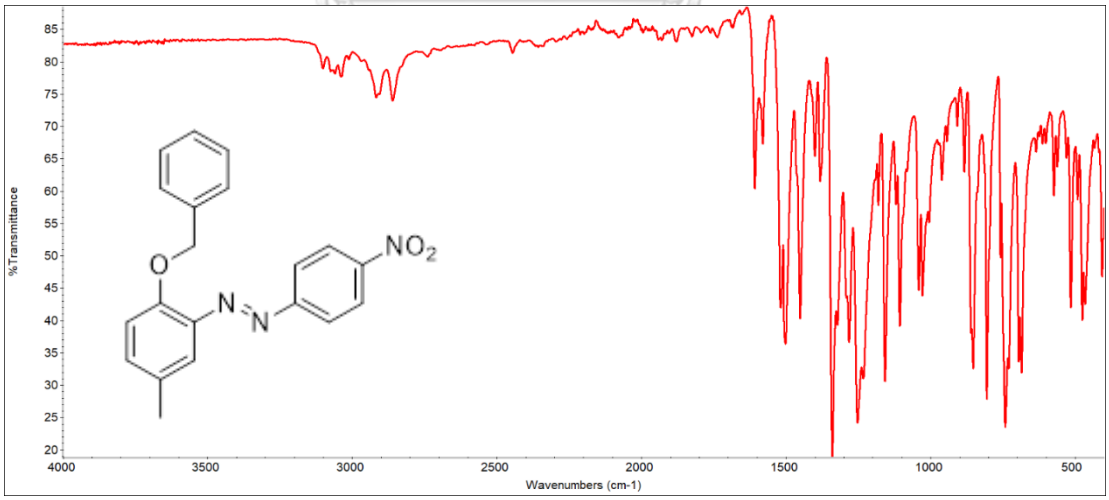

Figure A.47 IR spectrum of **compound 17**

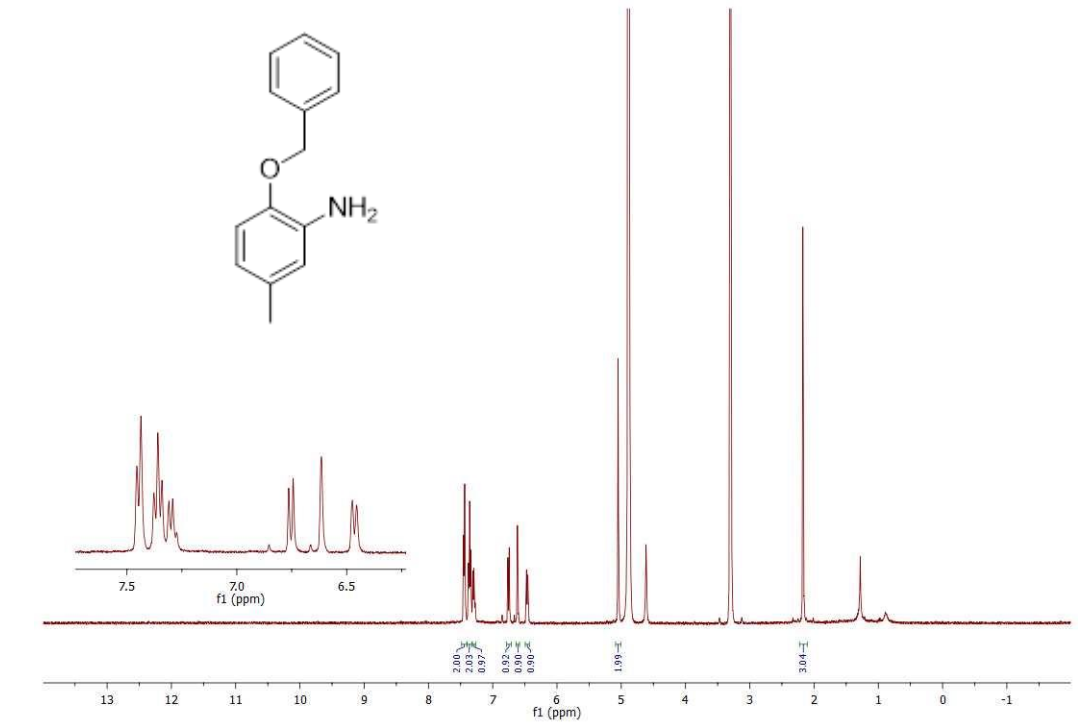

Figure A.48 ^{1}H NMR (CD_3OD) spectrum of **compound 18**

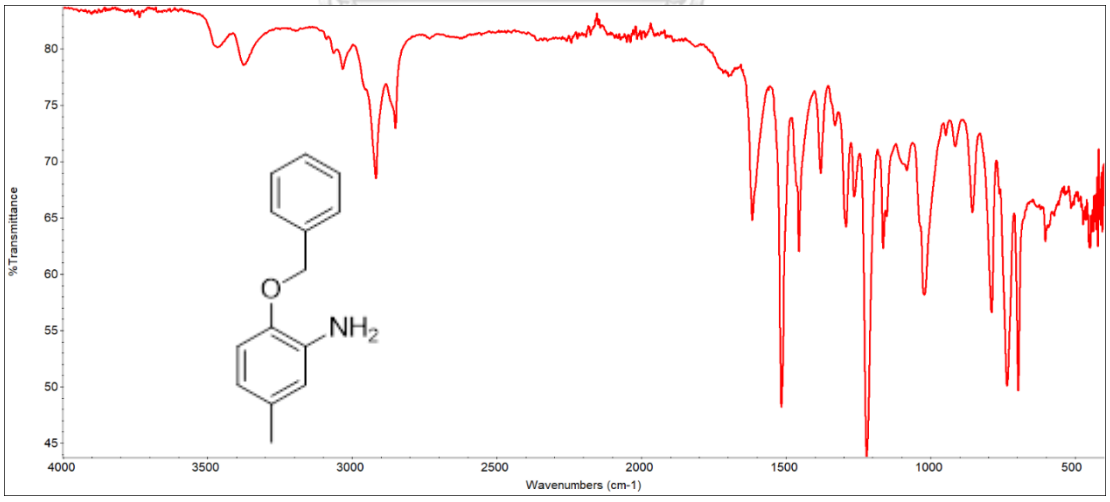

Figure A.49 IR spectrum of **compound 18**

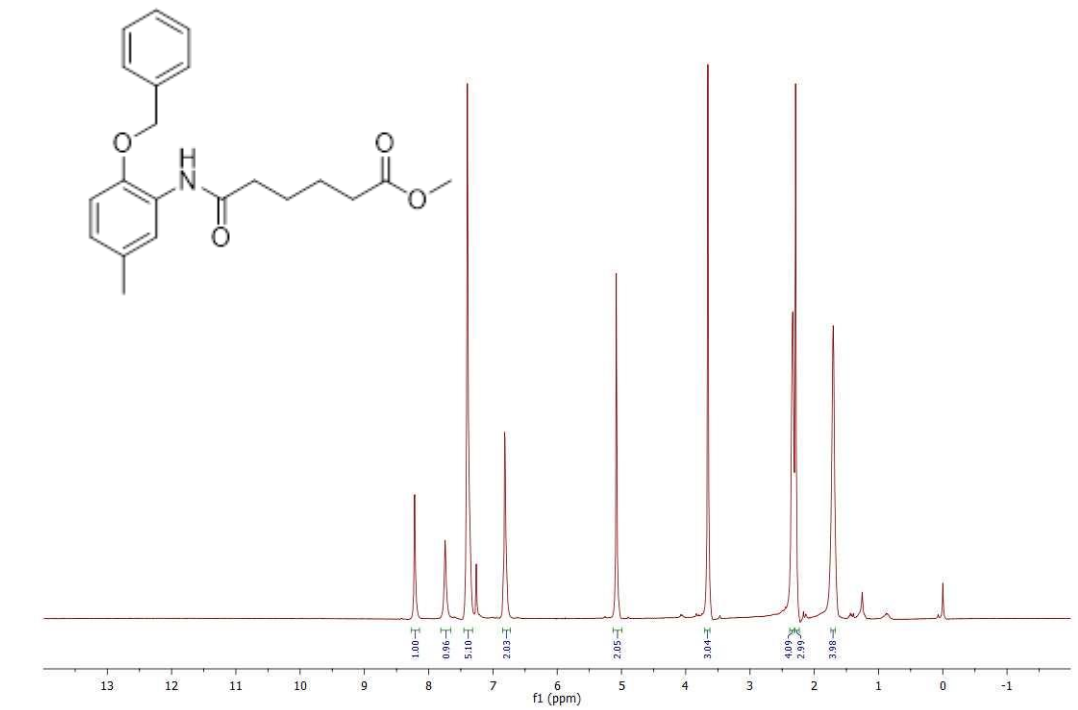

Figure A.50 ^{1}H NMR ($CDCl_3$) spectrum of **compound 19**

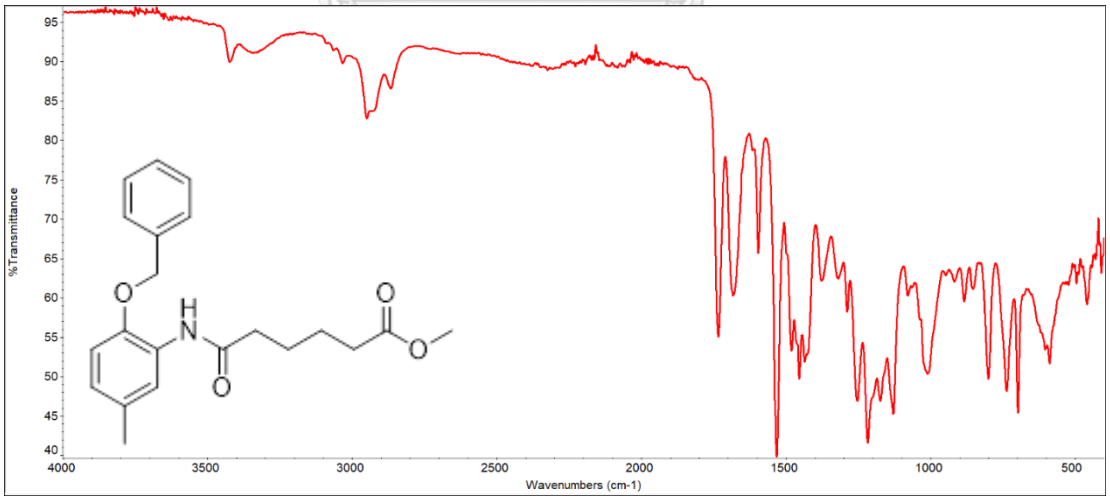

Figure A.51 IR spectrum of **compound 19**

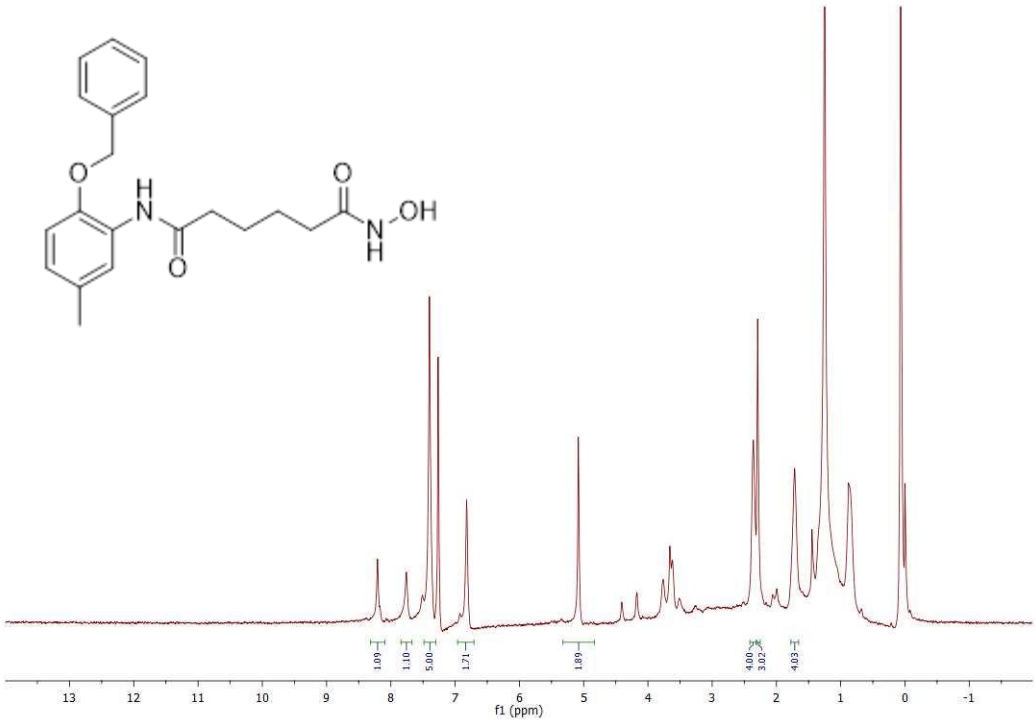

Figure A.52 ^{1}H NMR ($CDCl_3$) spectrum of **compound 20**

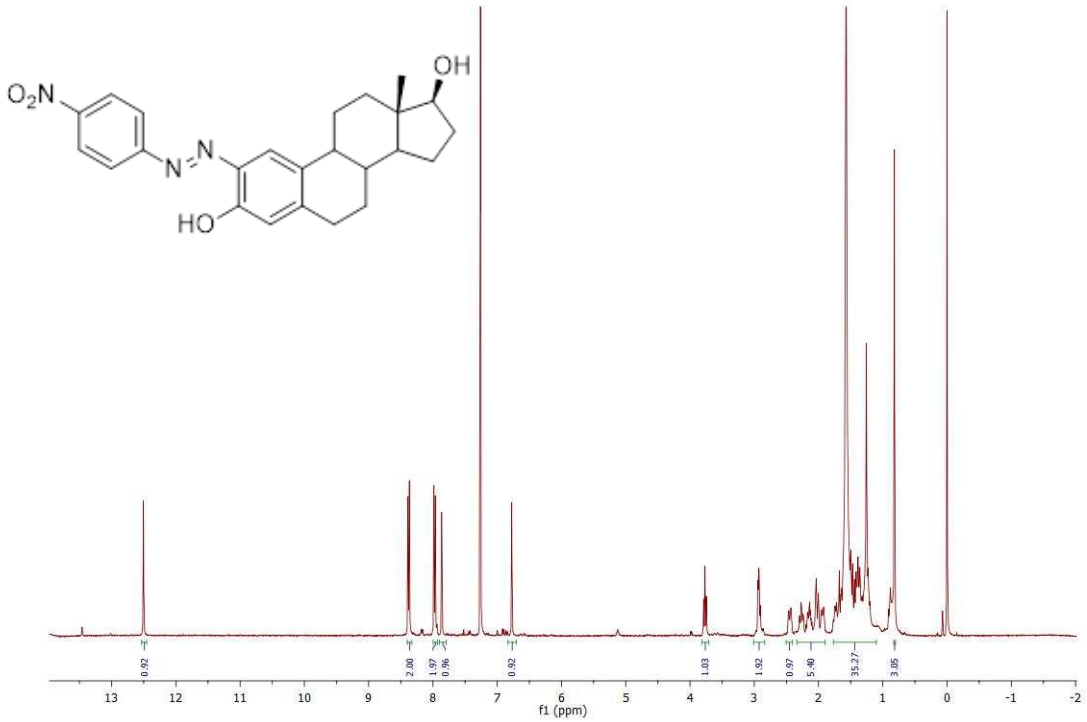

Figure A.53 ^{1}H NMR ($CDCl_3$) spectrum of **compound 21a**

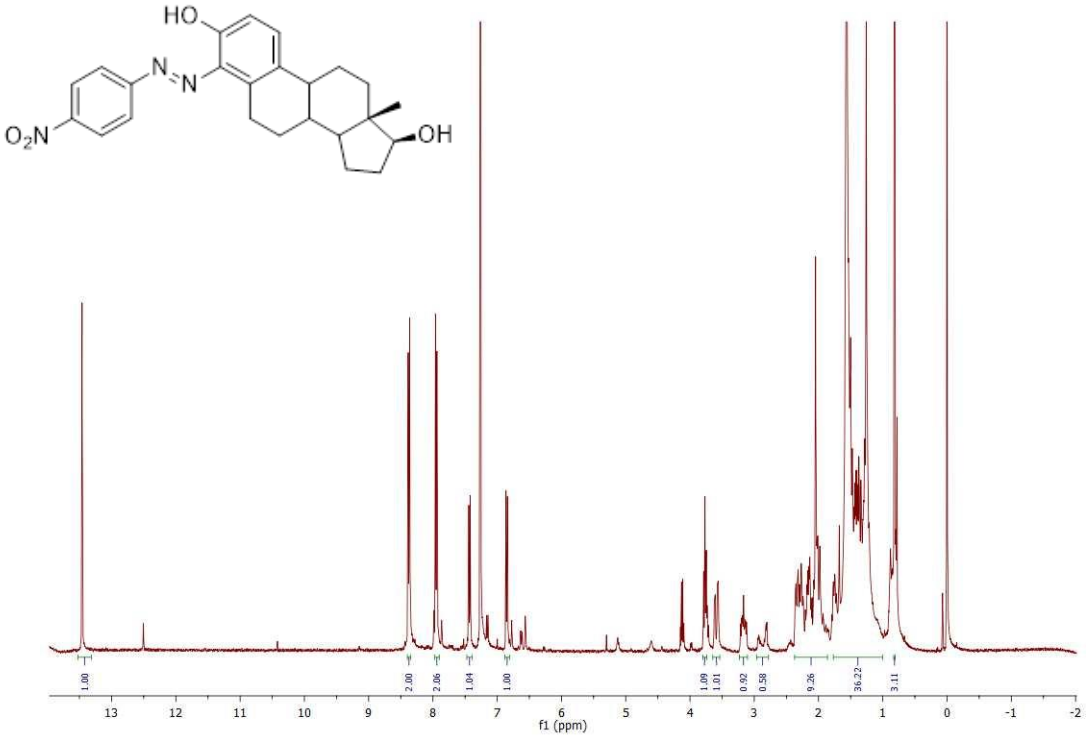

Figure A.54 ^{1}H NMR ($CDCl_3$) spectrum of **compound 21b**

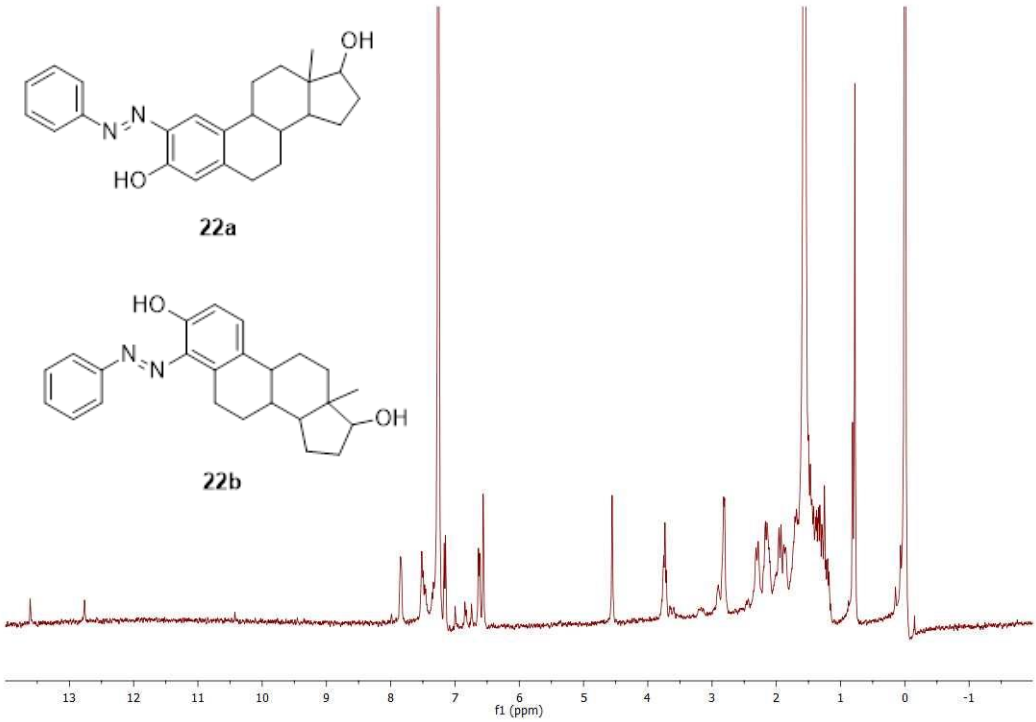

Figure A.55 ^{1}H NMR ($CDCl_3$) spectrum of **mixture 22a and 22b**

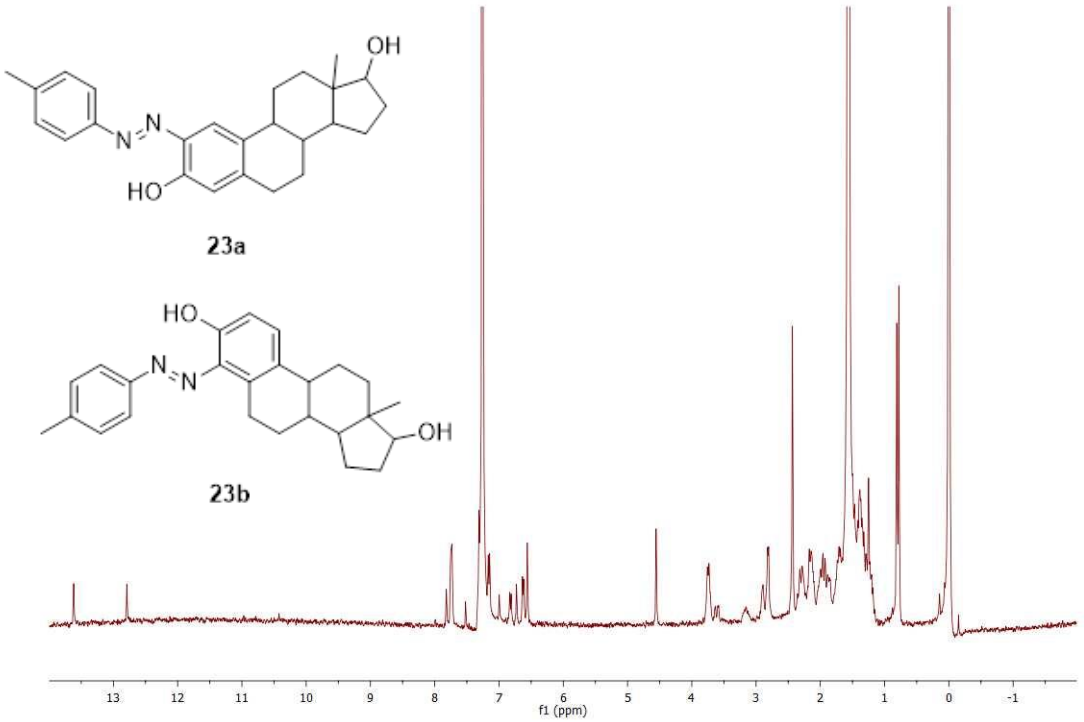

Figure A.56 ^{1}H NMR ($CDCl_3$) spectrum of **mixture 23a and 23b**

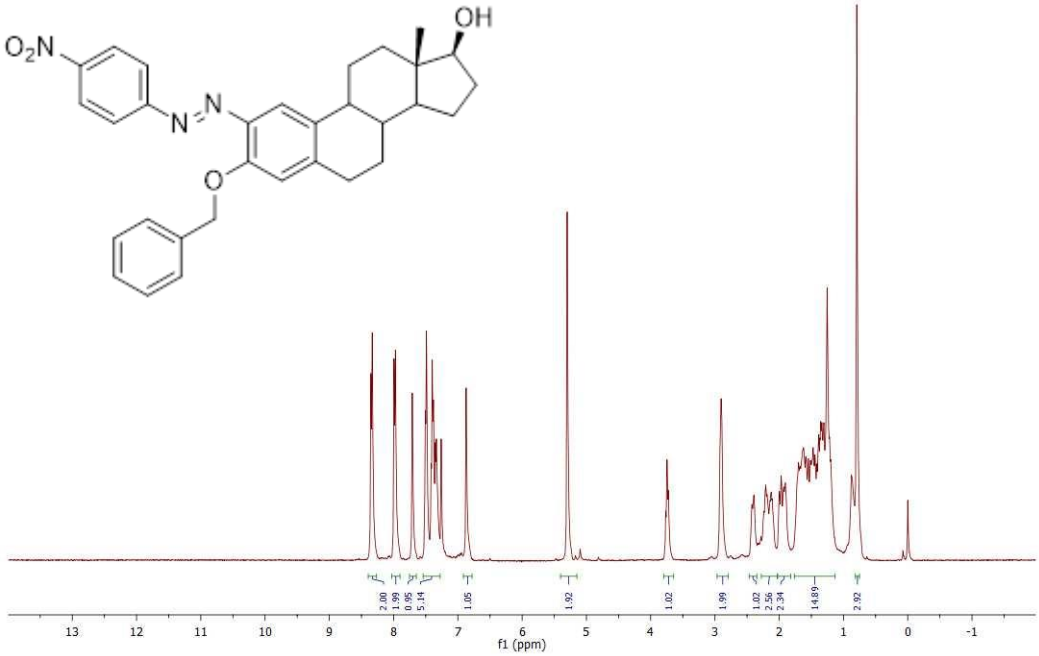

Figure A.57 ^{1}H NMR ($CDCl_3$) spectrum of **compound 24**

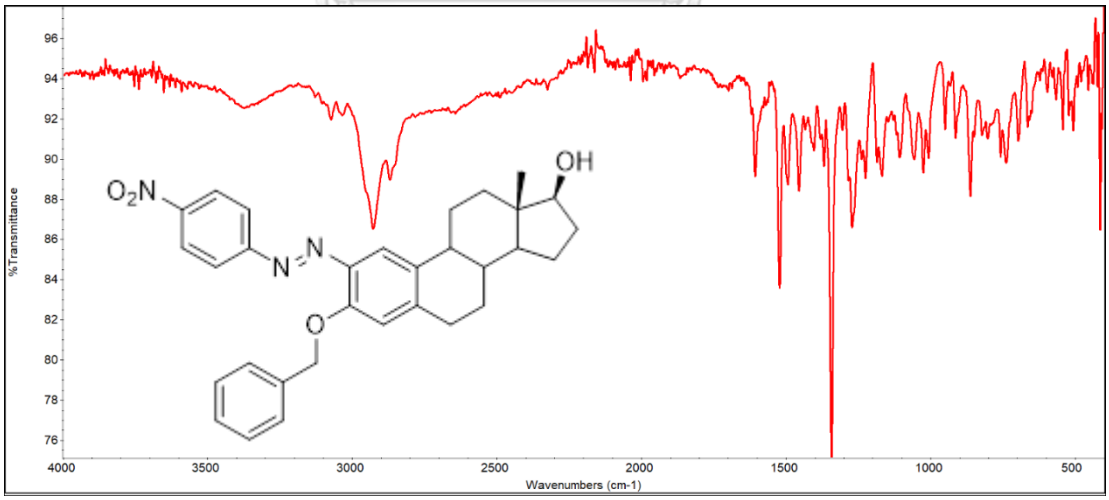

Figure A.58 IR spectrum of **compound 24**

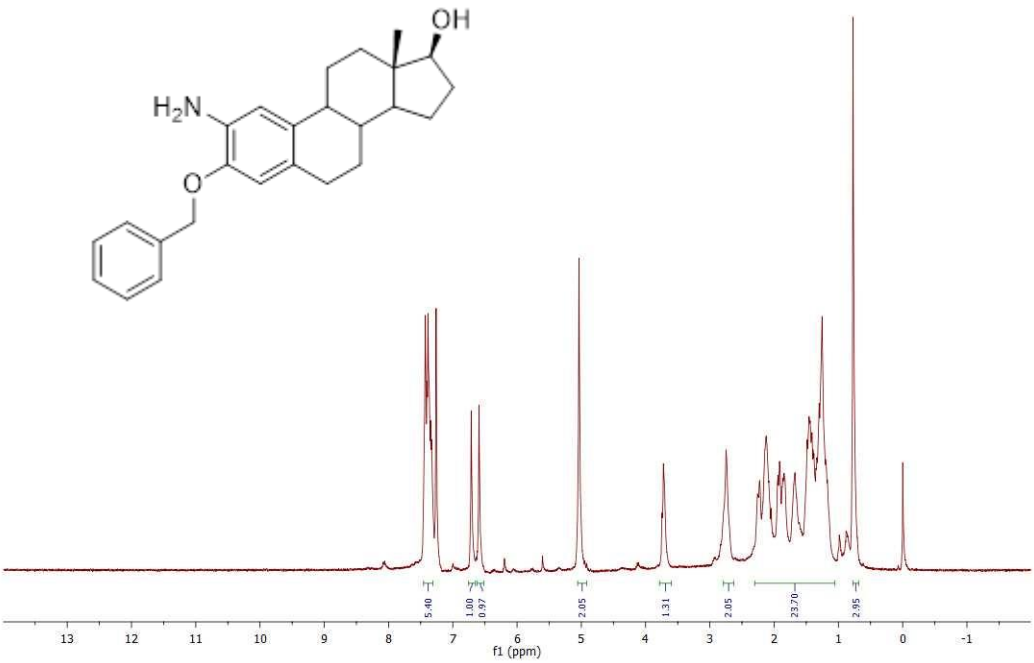

Figure A.59 ^{1}H NMR ($CDCl_3$) spectrum of **compound 25**

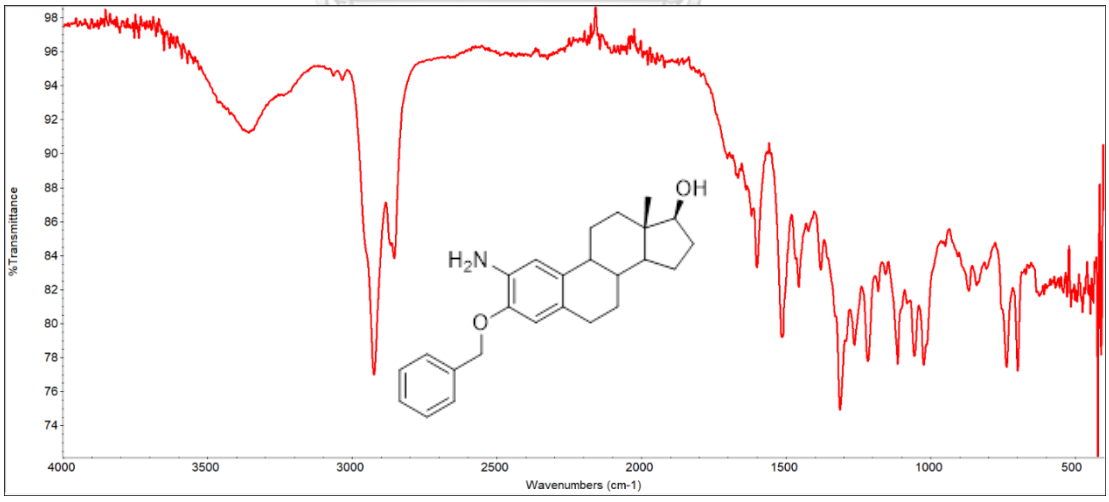

Figure A.60 IR spectrum of **compound 25**

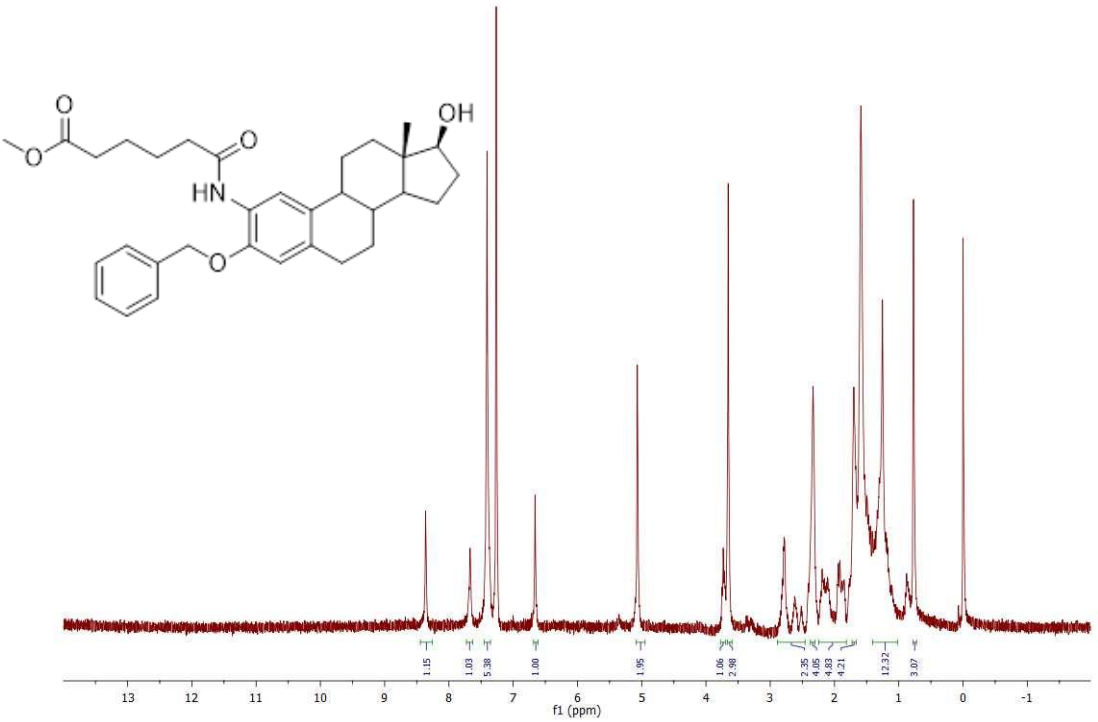

Figure A.61 ^{1}H NMR ($CDCl_3$) spectrum of **compound 26**

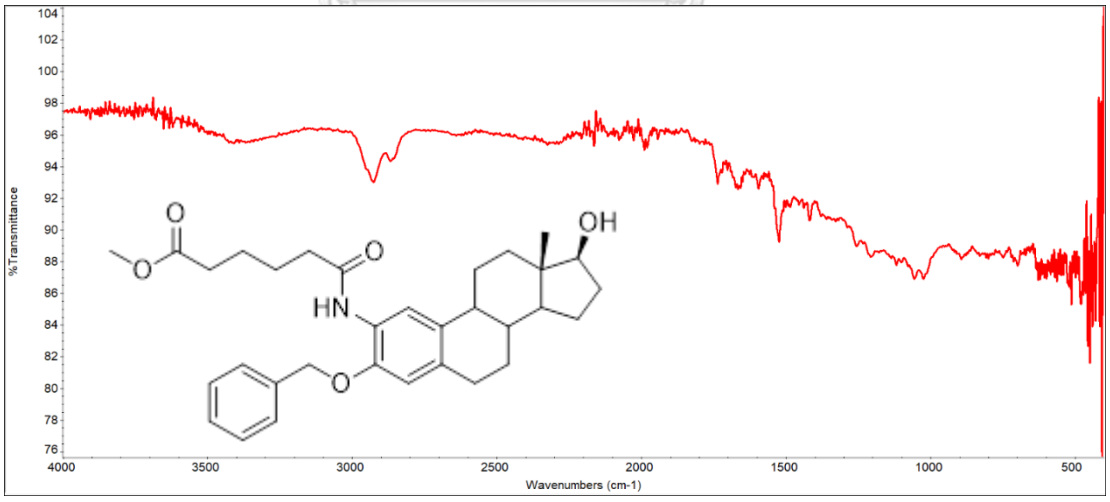

Figure A.62 IR spectrum of **compound 26**

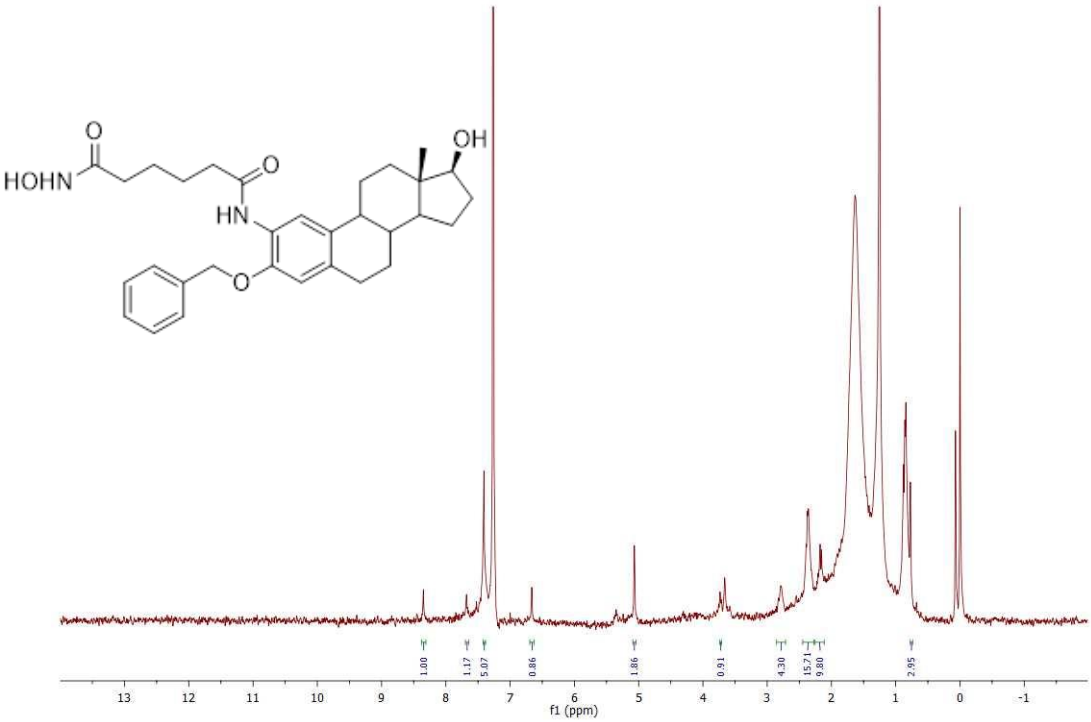

Figure A.63 ^{1}H NMR ($CDCl_3$) spectrum of **compound 27**

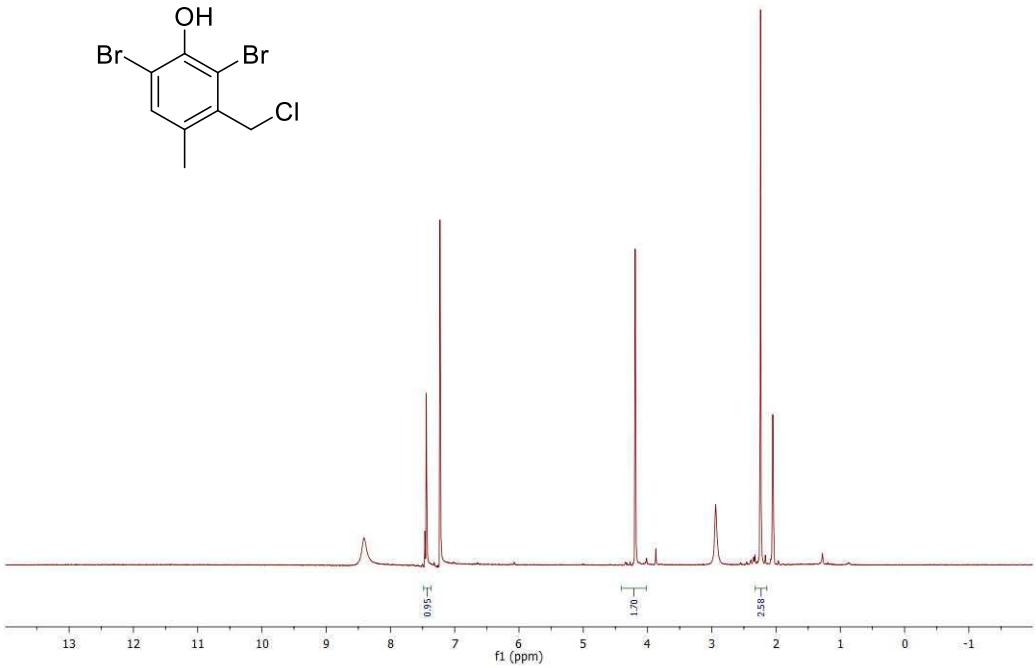

Figure A.64 ^{1}H NMR ($CDCl_3$) spectrum of **compound 28**

VITA

NAME	Chanoknun Boonyaratsewee
DATE OF BIRTH	4 September 1993
PLACE OF BIRTH	Bangkok
INSTITUTIONS ATTENDED	Bachelor's Degree of Science in Chemistry from Kasetsart University in 2016
HOME ADDRESS	11 Soi Thaiyanon 8 Sanumbinnum Road, Thasai Sub-district, Muang district, Nonthaburi Province.